Slovak University of Technology in Bratislava

Faculty of Civil Engineering

Department of Concrete Structures and Bridges

Annual Report

2013

Radlinského 11, 813 68 Bratislava, Slovakia
Tel.:++421-2-52 494 275 Fax ++421-2-52 926 213
www.svf.stuba.sk/sk/katedry/katedra-betonovych-konstrukcii-a-mostov

ANNUAL REPORT 2013
Department of Concrete Structures and Bridges
Faculty of Civil Engineering
Slovak University of Technology in Bratislava
Editor: Eng. Katarína Gajdošová, PhD.
Layout: Eng. Róbert Sonnenschein
Language corrections: Eng. Mária Bellová, PhD.
Edition: March 2014, Bratislava

CONTENT

PREFACE

In preface of Annual Report 2011, I stated that price cannot be the sole criterion in public procurement contracts. Incorrectly set system along with the crisis and downward pressure on prices meant that results of construction activities can have disastrous consequences. The influence of these factors was the reason for progressive collapse of several structures also in Slovakia (Trinity building, silos in Leopoldov, Kurimany Bridge, etc.).

And here it is! After a long time of waiting for good news from Brussels, the new EU rules on public procurement and concession contracts approved on January 2014 will ensure better quality and value for money when public authorities buy or lease works, goods or services.

Thanks to the new criterion of the "most economically advantageous tender" (MEAT) in the award procedure, public authorities will be able to put **more emphasis on quality**, environmental considerations, social aspects or innovation while still taking into account the price and life-cycle-costs of what is procured. “The new criteria” will put an end to the dictatorship of the lowest price and once again make quality the central issue.

The bidding procedure for companies will be simpler, with a standard "European Single Procurement Document" based on self-declarations. Only the winning bidder will have to provide original documentation. This should reduce the administrative burden on companies by over 80%, the Commission estimates. The new rules also encourage the division of contracts into lots to make it easier for smaller firms to bid.

To fight social dumping and ensure that workers' rights are respected, the new laws will include **rules on subcontracting** and tougher provisions on "abnormally low bids". Contractors that do not abide by EU labour laws may be excluded from bidding.

The directives will enter into force 20 days after publication in the Official Journal of the European Union. After this date, member states will have 24 months to implement the provisions of the new rules into national law.

In recent years the durability problem, poor performance, and most of all concrete repair failures have affected the image of concrete. The repair failures and endless ‘‘repair of repairs’’ made a substantial contribution to the current perceptions of concrete.

On the contrary to the amount of work spent on building new structures, the market of repair and protection has grown considerably as the age of the existing infrastructure is increasing. The extensive development of new methods and materials for the repair and protection of concrete structures has led to the need of standards for such works and products. At least four years, the European Standard EN 1504 on protection and repair of concrete structures is available. It was assumed that the standard will have a significant impact on the **quality of repair works**. Is it really so? The answer is not unambiguous. While most academic institutes and manufacturers of repair materials apply the principles and methods of the mentioned standard, most designers did not yet registered the standard. This is one of the important lessons from the seminar Repair of concrete structures, which took place at the end of 2013 in Smolenice (see page 16).

Juraj Bilčík

Department of Concrete Structures and Bridges

Head of the Department:
Juraj Bilčík
+421 2 59274 546
juraj.bilcik@stuba.sk

Professors

Vladimír Benko
+421 2 59274 554
vladimir.benko@stuba.sk

Ľudovít Fillo
+421 2 59274 508
ludovit.fillo@stuba.sk

Jaroslav Halvoník
+421 2 59274 555
jaroslav.halvonik@stuba.sk

Igor Hudoba
+421 2 59274 547
igor.hudoba@stuba.sk

Associate Professors

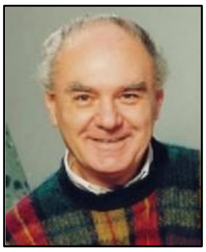

Ľubomír Bolha
+421 2 59274 387
lubomir.bolha@stuba.sk

Milan Čabrák
+421 2 59274 544
milan.cabrak@stuba.sk

Štefan Gramblička
+421 2 59274 552
stefan.gramblicka@stuba.sk

Ivan Harvan
+421 2 59274 557
ivan.harvan@stuba.sk

Július Šoltész
+421 2 59274 384
julius.soltesz@stuba.sk

Senior Lecturers

Iyad Abrahoim
+421 2 59274 551
iyad.abrahoim@stuba.sk

Andrej Bartók
+421 2 59274 540
andrej.bartok@stuba.sk

Mária Bellová
+421 2 59274 541
maria.bellova@stuba.sk

Viktor Borzovič
+421 2 59274 542
viktor.borzovic@stuba.sk

Jakub Brondoš
+421 2 59274 380
jakub.brondos@stuba.sk

Katarína Gajdošová
+421 2 59274 382
katarina.gajdosova@stuba.sk

Daniel Kóňa
+421 2 59274 385
daniel.kona@stuba.sk

Peter Paulík
+421 2 59274 350
peter.paulik@stuba.sk

OTHER MEMBERS

Doctoral Students		
Frólo Juraj	+421 2 59274 386	juraj.frolo@stuba.sk
Halabrínová Andrea	+421 2 59274 386	andrea.halabrinova@stuba.sk
Hanzel Ján	+421 2 59274 503	jan.hanzel@stuba.sk
Hollý Ivan	+421 2 59274 295	ivan.holly@stuba.sk
Ignačák Miroslav	+421 2 59274 549	miroslav.ignacak@stuba.sk
Kendický Peter	+421 2 59274 503	peter.kendicky@stuba.sk
Kišac Marian	+421 2 59274 381	marian.kisac@stuba.sk
Laco Ján	+421 2 59274 295	jan.laco@stuba.sk
Majtánová Lucia	+421 2 59274 503	lucia.majtanova@stuba.sk
Mikuš Ján	+421 2 59274 380	jan.mikus@stuba.sk
Pažma Peter	+421 2 59274 386	peter.pazma@stuba.sk
Sonnenschein Róbert	+421 2 59274 549	robert.sonnenschein@stuba.sk
Technical Staff		
Benedikovičová Helena	+421 2 59274 705	helena.benedikovicova@stuba.sk
Gábrišová Anna	+421 2 59274 505	anna.gabrisova@stuba.sk

I. NEW AT DeCoSaB

I.1 Defenses of the Doctoral Theses

BRONDOŠ, J.: CFRP Materials for Strengthening Concrete Members under an Impact Load
Supervisor: Bilčík, J.

ČUHÁK, M.: Nonlinear Analysis of Concrete Structures. Biaxial Bending with Axial Force
Supervisor: Fillo, Ľ.

DOLNÁK, J.: Application of High-Performance Concrete in Precast Bridge Structures
Supervisor: Halvoník, J.

KOVAČOVIC, M.: Shear Resistance between Concrete-Concrete Surfaces
Supervisor: Halvoník, J.

LELKES, A.: Theoretical Analysis of the Design of Composite Steel-Concrete Columns
Supervisor: Gramblička, Š.

PORUBSKÝ, T.: Nonlinear Analysis of Concrete Columns
Supervisor: Fillo, Ľ.

ROZLOŽNÍK, P.: Analysis of Reinforced Concrete Beams with Consideration of Redistribution and Plasticity
Supervisor: Fillo, Ľ.

VERÓNY, P.: Reinforcing of Concrete Columns - Analysis of the Influence of Transverse Reinforcement
Supervisor: Gramblička, Š.

II. RESEARCH TARGETS

The research activities of the Department are focused on new design methods for reinforced, prestressed and composite structures, ultimate limit design of concrete structures for durability, methods of repair and strengthening of building structures and bridges and utilization of high-performance and fiber concrete for concrete structures and precast elements.

III. RESEARCH PROJECTS

1.) VEGA 1/0857/11, Resistance Analysis of Concrete, Masonry and Composite Steel-Concrete Structures (2011-2013, FILLO, Ľ.),

2.) VEGA 1/0458/11, Factors Affecting the Effectiveness of the Utilization of High-Strength Concrete in Load-Bearing Elements and Structures (2011-2013, HUDOBA, I.),

3.) VEGA /0784/12, Holistic Design of Concrete Constructions (2012-2014, BILČÍK, J.)

4.) VEGA 1/0690/13, Diagnosis of Oldest Reinforced Concrete Bridges in Slovakia (2013-2015, HALVONÍK, J.)

5.) APVV 0442-12, Historical Experience and Current Requirements for the Design of Concrete Bridges and Knowledge Transfer of Information Acquired in Technical Practice, (2013-2016, HALVONÍK, J.)

IV. EVENTS

Excursion of Our Students

BUSINESS CENTER, Bratislava, Slovakia
2-nd May, 2013

The excursion is included into compulsory subjects for Structures of Buildings and Structural and Transportation Engineering fields of study. Excursion was organised to RC office block under construction. This building with reinforced concrete load-bearing structure is situated in Bratislava - Petržalka.

Night of the Researchers

Egg Protection Device Competition on the Night of the Researchers

At the end of September 2013, our department participated in the Science Festival, which is held every year under the title: Night of the researchers. This event serves mainly to popularize the science in the eyes of the general public. The activity, we have presented, was the student competition: "Egg protection device", which consists in the design of reinforced concrete frame according to pre- specified criteria. Then the egg is placed under the frame and the puncher of a given weight is being released on it from an increasing height. The winner frame is the one, which can withstand the impact from the greatest height ..., plainly, this structure could best protect the egg placed underneath the frame. Candidates could guess which design is best suited for this purpose. The frames varied in shapes and in the amount of reinforcement as well as in its arrangement. Those who finally made the best guess won small prizes. The activity took the attention especially of the children, who watched in awe the impacts of the puncher and were happy when the frame succeeded in protecting the egg. By this simple way we were able to point out that even the concrete structures could be an interesting topic of a study or research. The activity was even declared as one of the most interesting, despite various other well prepared activities and experiments presented by other departments, universities and research institutes. We believe that our participation was not the last. Test testing equipment and the tested frames were made by: Ing. Peter Paulík, PhD. and Ing. Peter Pažma.

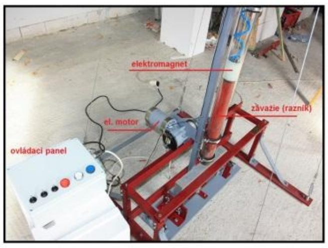

Conferences we visited

Concrete Technology 2013, Jihlava, Czech Republic, 18-th April, 2013

Concrete Technology 2013 was its content traditionally representative sectional conferences dedicated to the latest developments of concrete technology and the implementation of concrete structures.

Tel Aviv 22-24-th April, 2013

The symposium theme, "Engineering a Concrete Future: Technology, Modelling and Construction", encompassed innovative aspects of concrete engineering in its various stages, including topics in several distinct areas of interest.
The Tel Aviv symposium was a great opportunity to gain state-of-the-art knowledge on recent developments, technologies and interesting current projects, share and discuss information and ideas with experts, form international networks, as well as renew old acquaintances.

Concrete and Concrete Structures, Terchová, Slovakia, 23-25-th October, 2013

Based on the great success of Conference "Concrete and Concrete Structures 2009", the conference brought this year again to academics, researchers and practitioners from Central Europe the review of recent achievements, share the latest developments and discuss present as well as future challenges in concrete and concrete structures.

Czech Concrete Days, Hradec Kralove, Czech Republic, 27-28-th November, 2013

The 20th Czech concrete days organised by Czech concrete society offered a comprehensive overview of current developments in the construction sector. Czech concrete days are a communication and innovation platform for experts in the field of concrete and construction technology.


KONEČNÁ POZVÁNKA
CBS
11. konference
TECHNOLOGIE BETONU
2013

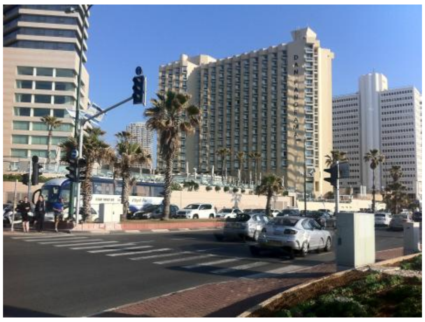

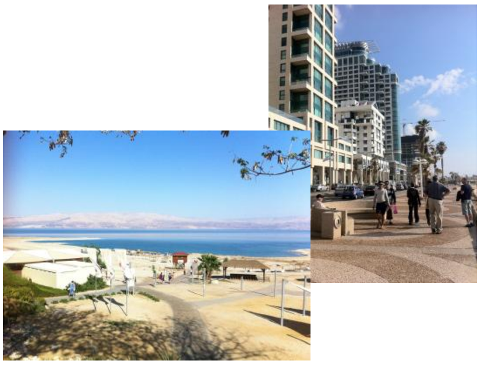

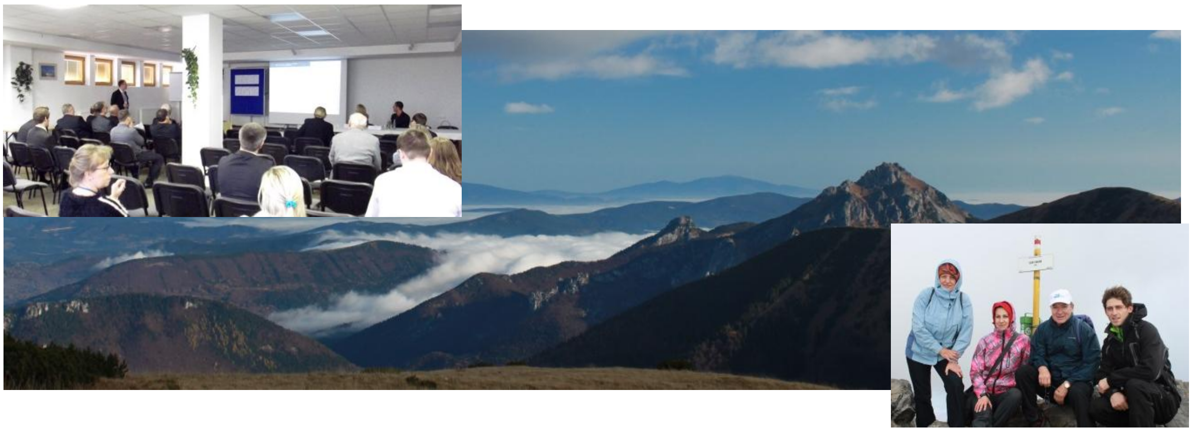


KONEČNÁ POZVÁNKA
Jubilejní
20. BETONÁŘSKÉ DNY 2013
spojené s výstavou
BETON 2013

Repair of Concrete Structures 2013

The Eighth Seminar

On the 3rd and 4th December 2013 the eighth Seminar Repair of Concrete Structures was organized by the DeCoSaB under the guidance of prof. Bilcik and other representatives of the department in cooperation with Association for Repair of Concrete Structures. The intention of the seminar was to allow for a meeting of a wide technical community focused on the field of diagnostics and repair of concrete and masonry structures. Experts, professionals and academic staff members presented the reasons for failures of concrete and masonry structures. New methods and materials for protection and repair according EN 1504 was presented. Many designed and executed repairs and strengthening's of buildings, bridges, towers were demonstrated. Important and rich discussion provided a big space for sharing of information and experiences. The personal interaction among seminar participants during breaks and the evening event was an important and valuable detail of the meeting. The seminar was held the third time at the Congress Centre Smolenice of Slovak Academy of Sciences – in Smolenice Castle. Total of 60 active participants took their places in a five technical sessions, learn new facts available for their work in the field of diagnostics, repair and strengthening of concrete and masonry structures and established many new partnerships. Participants agreed on the finding that the seminar had a good professional and social level. Seminar is organized each two years and we are even now looking forward to meet again in December 2015.

Official seminar opening by Professor Bilčík

Seminar venue was the Smolenice cas-

Railway concrete arch bridge in Nové Zámky before/after strengthening and repair (paper Dobosz et. al)

Tunnel Horelica (paper Kucharik)

Vertical cracks in the secondary lining in tunnel Horelica (paper Kucharik)

Abrasion erosion of concrete due to water flow (paper Koniar)

CT axonometric view of steel fibers in a concrete cube (paper Hobst et al)

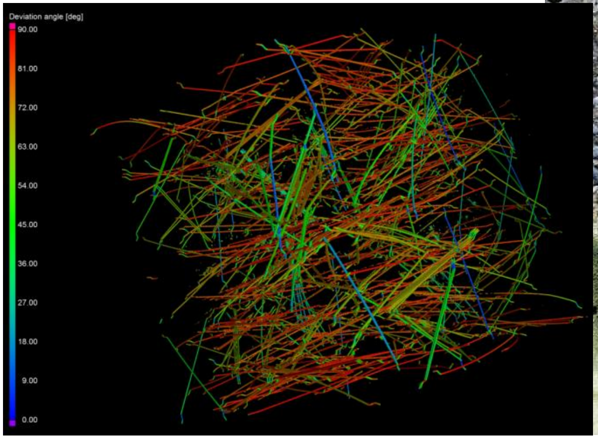

Saying goodbye to year 2013

Christmas session

At the end of year 2013, the members of our department as traditionally met all together around a small Christmas tree just few days before Christmas. Once again, we spend one afternoon together. Talking about every event and memory we spent with colleagues.

At the beginning, the head of the department, professor Bilcik, gave a speech on Christmas time and the importance of family and loved ones. Many times, we spend more time with colleagues than the family, and that is the question – are they not our family?

V. COOPERATION

V.1 International Cooperation

1.) Klokner Institute ČVUT Prague, Czech Republic
2.) ETH - Laboratory for Building Materials, ETH Zurich, Switzerland
3.) Institut für Baustatik und Konstruktion, ETH Zurich, Switzerland
4.) Baustoffinstitut, TU Munich, Germany
5.) Department of Civil and Materials Engineering, University of Illinois at Chicago, USA
6.) RIB Bausoftware, Stuttgart, Germany
7.) Betosan, s.r.o., Prague, Czech Republic
8.) European Commission, DG Research, Brussels, Belgium
9.) Imperial College for Science, Technology and Medicine, London, U.K.
10.) St. Paul University, Brussels, Belgium
11.) Fachhochschule Braunschweig – Wolfenbütel, Germany
12.) Institut für Massivbau, TU Darmstadt, Germany
13.) Fachhochschule Coburg, Germany

V.2 Membership in International Professional Organizations

1.) BENKO, V.: Austrian Standard Institut. Member of Standard Commitees – ON-AG 01301, ON-AG 1011 01, ON-AG 010 01, ON-AG 176 02. ON-K 176, ON-K 010
2.) BENKO, V.: ECEC European Council of Engineers Chamber – Delegate
3.) BENKO, V.: ECCE European Council of Civil Engineers – Delegate
4.) BENKO,V.: ASCE American Society of Civil Engineers
5.) BILČÍK, J.: American Concrete Institute
6.) FILLO, Ľ.: Representative of the Slovak Republic in CEN TC 250 – SC2 Eurocodes – Design of Concrete Structures
7.) FILLO, Ľ.: Member of Task Group *fib* TG 1.1 Design Application
8.) FILLO, Ľ.: Honorary Member of Czech Concrete Society, Hradec Králové, Czech Republic, 25.11.2009
9.) HALVONÍK, J: Representative of the Slovak Republic on CEN TC 250 – SC1 Eurocodes – Actions on Structures
10.) HALVONÍK, J: Representative of the Slovak Republic on CEN TC 250 Eurocodes

VI. ACTIVITIES

Commercial Activities for Firms and Institutions

1.) BELLOVÁ, M.: Determination of Time for Fire Resistance Classification of Masonry Walls Made from Moulded Masonry Units of LIAS Vintířov Company

2.) BILČÍK, J.: Expert Opinion on the CBC Building III, IV and V Verification on Karadzic Street in Bratislava with Regard to Safety, Serviceability and Durability Limit States

3.) BILČÍK, J.: Repair Proposal of Cylindrical Tanks SO 17.1 and 17.2 with External Prestressing and Technological Process of Rehabilitation

4.) ČABRÁK, M.: Translation of European Standards from English to Slovak

5.) FILLO, Ľ.: Forensic Assessment of Structures in Buildings CBC3,CBC4 and CBC5 for Seismic Design Situations and Control of Flat Slabs for Serviceability Limit States (SLS) – Deflection, 2013

6.) GAJDOŠOVÁ, K.: Translation of FprEN 1337-1:2012 Structural Bearings. Part 1: General

7.) GRAMBLIČKA, Š.: Statically Assessment of Structural System of Trinity Multifunctional Complex of Buildings Trinity in Bratislava

VII. PUBLICATIONS

VII.1 Books and Textbooks

Textbooks

1.) HARVAN, I.: Prestressed Concrete: Design According to Common European Standards. 2nd edition, Slovak University of Technology in Bratislava, 2013, ISBN 978-80-227-4057-9, 262 pp. (in Slovak)

VII.2 Journals

Scientific Papers Abroad

1.) BILČÍK, J. – HALAŠA, I.: Requirements for Watertight Parts of Concrete Buildings Structures. In: Beton: Technologie - Konstrukce – Sanace, ISSN 1213-3116, Vol. 13, No. 1 (2013), pp. 80-83 (in Slovak)
2.) GAJDOŠOVÁ, K. – BILČÍK, J.: Full-Scale Testing of CFRP-Strengthened Slender Reinforced Concrete Columns. In: Journal of Composites for Construction, ISSN 1090-0268, Vol. 17, No. 2 (2013), pp. 239-248 (in English)
3.) GRAMBLIČKA, Š.: Errors and Failures of Load-Bearing Structures of Buildings. In: Stavebnictví, ISSN 1802-2030, Vol. 7, No. 5 (2013), pp. 50-54 (in Slovak)
4.) GRAMBLIČKA, Š.: The 18th Conference of Structural Engineers in Piešťany: Statics of Buildings 2013. In: Stavebnictví, ISSN 1802-2030, Vol. 7, No. 5 (2013), p. 68 (in Slovak)
5.) GRAMBLIČKA, Š. – VERÓNY, P.: Transverse Reinforcement in Reinforced Concrete Columns. In: SSP - Journal of Civil Engineering, ISSN 1336-9024, Vol. 8, Issue 2 (2013), pp. 41-50 (in English)
6.) HARVAN, I.: Shear Resistance of Girderless Concrete Slabs Using Eurocode 2. In: Stavebnictví, ISSN 1802-2030, Vol. 7, No. 11-12 (2013), pp. 52-57 (in Slovak)

Scientific papers in Slovak Journals

1.) BELLOVÁ, M.: Design of Masonry Structures According to EUROCODE 6. EUROSTAV, ISSN 1335-1249, Vol. 19, Nos. 11-12 (2013), pp. 68-71 (in Slovak)
2.) GAJDOŠOVÁ, K.: Series: The Most Interesting Bridges in Slovakia. 2nd Part: "Krajinský Bridge in Piešťany". In: Inžinierske stavby, ISSN 1335-0846, Vol. 61, No. 3 (2013), pp. 60-61 (in Slovak)
3.) HALAŠA, I. – BILČÍK, J.: Concrete for Watertight Concrete Structures. In: Stavebné hmoty, ISSN 1336-6041, Vol. 9, No. 1 (2013), pp. 30-32 (in Slovak)
4.) HANZEL, J. – GAJDOŠOVÁ, K.: Series: The Most Interesting Bridges in Slovakia. 5th Part: Peterský Bridge in Liptovský Hrádok. In: Inžinierske stavby, ISSN 1335-0846, Vol. 61, No. 5 (2013), pp. 46-47 (in Slovak)

5.) HUDOBA, I. – MIKUŠ, J. – DOVÁL, M.: Possibilities of the Utilization of a New Generation of Concrete in Concrete Elements and Structures. In: Stavebné materiály, ISSN 1336-7617, Vol. 9, No. 2 (2013), pp. 24-26 (in Slovak)

6.) IGNAČÁK, M. – ŠOLTÉSZ, J.: Influence of Hydration Heat on Base Slabs in Early Stages. In: Stavebné materiály, ISSN 1336-7617, Vol. 9, No. 1 (2013), pp. 24-25 (in Slovak)

7.) MAJTÁNOVÁ, L. – BORZOVIČ, V.: Uľanka Railway Bridge. In: Inžinierske stavby, ISSN 1335-0846, Vol. 61, No. 5 (2013), pp. 44-45 (in Slovak)

8.) PAULÍKOVÁ, V. – BORZOVIČ, V.: Kopráš Viaduct. In: Inžinierske stavby, ISSN 1335-0846. - Vol. 61, No. 4 (2013), pp. 46-47 (in Slovak)

VII.3 Conferences

Contributions to Proceedings Abroad

1.) ABRAHOIM, I.: Anchorage Regions of Pre-Tensioned Concrete Members According to STN EN 1992-1-1. In: Proceedings of 20th Concrete Days 2013 Conference, Hradec Králové, Czech Republic, 27.-28.11.2013, ISBN 978-80-87158-34-0, pp. 390-395 (in Slovak)

2.) ABRAHOIM, I.: Verification of Cracking of Post-Tensioned Concrete Members According to STN EN 1992-1-1. In: Proceedings of 20th Concrete Days 2013 Conference, Hradec Králové, Czech Republic, 27.-28.11.2013, ISBN 978-80-87158-34-0, pp. 384-389 (in Slovak)

3.) BILČÍK, J.: Rehabilitation of a Concrete Granulation Tower. In: Proceedings of 23rd International Symposium on Repair of Concrete Structures 2013, Brno, Czech Republic, 15.-17.5.2013, ISBN 978-80-905471-0-0, pp. 56-59 (in Slovak)

4.) BILČÍK, J. – GAJDOŠOVÁ, K. – BRONDOŠ, J.: Strengthening of Concrete Columns by FRP Materials. In: Proceedings of 23rd International Symposium on Repair of Concrete Structures 2013, Brno, Czech Republic, 15.-17.5.2013, ISBN 978-80-905471-0-0, pp. 30-35 (in Slovak)

5.) BRONDOŠ, J. – BILČÍK, J.: Testing of Concrete Members Strengthened With CFRP Materials Under Impact Load. In: Proceedings of Conference on Investigation and Quality in Civil Engineering 2013, Brno, Czech Republic, 1.-2.10.2013, ISBN 978-80-214-4777-6, pp. 25-32 (in Slovak)

6.) DOLNÁK, J.: Comparison of the Rheology Properties of Experimental Concrete. In: Proceedings of 15th Technical International PhD Study Conference Juniorstav 2013, Brno, Czech Republic, 7.2.2013, ISBN 978-80-214-4670-0 (in Slovak)

7.) FILLO, Ľ.: Decreased Reliability of Axially Loaded Columns. In: Proceedings of 20th Concrete Days 2013 Conference, Hradec Králové, Czech Republic, 27.-28.11.2013, ISBN 978-80-87158-34-0, pp. 329-332 (in English)

8.) FILLO, Ľ. – HALVONÍK, J.: Punching of Concrete Flat Slabs and Footings. In: Proceedings of Scientific Conference on Modelling in Structural Mechanics 2013, Ostrava, Czech Republic, 22.-23.5.2013, ISBN 978-80-248-2985-2 (in Slovak)

9.) FILLO, Ľ. – HALVONÍK, J.: Resistance Restriction of Flat Slabs. In: Proceedings of 20th Concrete Days 2013 Conference, Hradec Králové, Czech Republic, 27.-28.11.2013, ISBN 978-80-87158-34-0, pp. 234-239 (in English)

10.) GAJDOŠOVÁ, K. – BRONDOŠ, J.: The Effect of Load Type on the Action of CFRP Laminates in Strengthened Cross-Section. In: Proceedings of 20th Concrete Days 2013 Conference, Hradec Králové, Czech Republic, 27.-28.11.2013, ISBN 978-80-87158-34-0, pp. 377-380 (in English)

11.) GRAMBLIČKA, Š. – VERÓNY, P.: Reinforced Concrete Columns-Analyses of Transverse Reinforcement. In: Proceedings 13th International Scientific Conference on VSU´2013, Volume 2, Sofia, Bulgaria, 6.-7.6.2013, pp. 271-276 (in English)

12.) GRAMBLIČKA, Š. – LELKES, A.: Slender Composite Steel-Reinforced Concrete Columns. In: Proceedings 13th International Scientific Conference on VSU´2013, Volume 2, Sofia, Bulgaria, 6.-7.6.2013, pp. 277-282 (in English)

13.) HALVONÍK, J. – DOLNÁK, J.: Prestress Losses in Pretensioned Beams Cast from Highperformance Concrete. In: Proceedings of 20th Concrete Days 2013 Conference, Hradec Králové, Czech Republic, 27.-28.11.2013, ISBN 978-80-87158-34-0, pp. 252-257 (in English)

14.) HALVONÍK, J. – FILLO, Ľ.: Punching-The Reasons of Failure in a Complex Trinity. In: Proceedings of Scientific Conference on Modelling in Structural Mechanics 2013, Ostrava, Czech Republic, 22.-23.5.2013, ISBN 978-80-248-2985-2 (in Slovak)

15.) CHANDOGA, M. – HALVONÍK, J. – PRÍTULA, A.: Short and Long Time Deflection of Pre- and Post-Tensioned Bridge Beams. In: Proceedings of fib Symposium on Engineering a Concrete Future: Technology, Modeling & Construction, Tel-Aviv, Israel, 22.-24.4.2013, ISBN 978-965-92039-0-1, pp. 487-490 (in English)

16.) IGNAČÁK, M.: Measuring of the Development of the Temperature of a Base in Early Stages. In: Proceedings of 15th Technical International PhD Study Conference Juniorstav 2013, Brno, Czech Republic, 7.2.2013, ISBN 978-80-214-4670-0 (in Slovak)

17.) IGNAČÁK, M. – PRCÚCH, I. – ŠOLTÉSZ, J.: Thermal Analysis of Base Slabs in Early Stages. In: Proceedings of 11th Conference on Technology of Concrete 2013, Jihlava, Czech Republic, 18.4.2013, ISBN 978-80-87158-33-3, pp. 116-122 (in Slovak)

18.) KIŠAC, M.: Resistance of Slender Armoured Concrete Columns. In: Proceedings of 15th Technical International PhD Study Conference Juniorstav 2013, Brno, Czech Republic, 7.2.2013, ISBN 978-80-214-4670-0 (in Slovak)

19.) LACO, J.: Bond of Post-Tensioned Prestressing Units Coated with Emulsifiable Oil. In: Proceedings of 15th Technical International PhD Study Conference Juniorstav 2013, Brno, Czech Republic, 7.2.2013, ISBN 978-80-214-4670-0 (in Slovak)

20.) LACO, J. – BORZOVIČ, V.: Bond of Strands Coated with Different Anticorrosion Agents. In: Proceedings of 20th Concrete Days 2013 Conference, Hradec Králové, Czech Republic, 27.-28.11.2013, ISBN 978-80-87158-34-0, pp. 173-178 (in English)

21.) MIKUŠ, J: Possibilities of the Applications of Ultra High-Performance Concrete. In: Proceedings of 15th Technical International PhD Study Conference Juniorstav 2013, Brno, Czech Republic, 7.2.2013, ISBN 978-80-214-4670-0 (in Slovak)

22.) PAULÍK, P. – HUDOBA, I.: Influence of Aggressive Chemical Environment on Behaviour of HPFRC in Conditions of Long-Term Bending Performance. In: Proceedings of fib Symposium on Engineering a Concrete Future: Technology, Modeling & Construction, Tel-Aviv, Israel, 22.-24.4.2013, ISBN 978-965-92039-0-1, pp. 73-76 (in English)

23.) PRCÚCH, I. – IGNAČÁK, M. – ŠOLTÉSZ, J.: Temperature Field Analysis of Selected Structures in Their Early Stage. In: Proceedings of Scientific Conference on Modelling in Structural Mechanics 2013, Ostrava, Czech Republic, 22.-23.5.2013, ISBN 978-80-248-2985-2 (in Slovak)

24.) ŠOLTÉSZ, J. – IGNAČÁK, M.: Computation of HCLPF Parameters for 3D Shell Modelled RC Structures-Seismic Certificate. In: CESB 13 Prague, Central Europe towards Sustainable Building 2013, Prague, Czech Republic, 26th - 28th June 2013, Grada Publishing, ISBN 978-80-247-5015-6, pp. 469-472 (in English)

Contributions to Proceedings in Slovak Republic

1.) BAJZA, A. – BILČÍK, J.: Urea Granulation Tower at Duslo Šaľa. In: Proceedings of 8th Seminar on Repair of Concrete Structures, Smolenice, Slovak Republic, 3.-4.12.2013, ISBN 978-80-8076-109-7, pp. 39-44 (in Slovak)

2.) BARTÓK, A. – ŠOLTÉSZ, J. – IGNAČÁK, M.: Causes of Steel Silo Collapse at Leopoldov, Strengthening of Intact Silos. In: Proceedings of 18th Conference on Statics of Buildings 2013, Piešťany, Slovak Republic, 14.-15.03.2013, ISBN 978-80-89655-00-7, pp. 237-246 (in Slovak)

3.) BELLOVÁ, M.: Design of Fire Walls as Barriers Against a Fire Spreading. In: Proceedings of 8th Seminar on Repair of Concrete Structures, Smolenice, Slovak Republic, 3.-4.12.2013, ISBN 978-80-8076-109-7, pp. 103-108 (in Slovak)

4.) BELLOVÁ, M.: Eurocodes: Structural Fire Design. In: Procedia Engineering, Vol. 65: Concrete and Concrete Structures 2013, Terchová, Slovak Republic, 23.-25.10.2013, ISSN 1877-7058, pp. 382-386 (in English)

5.) BELLOVÁ, M.: Choice of Masonry Wall Materials from the Point of Their Fire Resistance. In: Proceedings of 18th Conference on Statics of Buildings 2013, Piešťany, Slovak Republic, 14.-15.03.2013, ISBN 978-80-89655-00-7, pp. 181-189 (in Slovak)

6.) BELLOVÁ, M.: Some Remarks Towards Surface Reinforcement Used in Concrete Members. In: Procedia Engineering, Vol. 65: Concrete and Concrete Structures 2013, Terchová, Slovak Republic, 23.-25.10.2013, ISSN 1877-7058, pp. 370-375 (in English)

7.) BENKO, V. – VYSKOČ, A. – ĎURAČKA, J. – PERLA, J.: Rehabilitation and Strengthening of Activation Tanks for Sewage Treatment, In: Proceedings of 18th Conference on Statics of Buildings 2013, Piešťany, Slovak Republic, 14.-15.03.2013, ISBN 978-80-89655-00-7, pp. 291-294 (in Slovak)

8.) BILČÍK, J. – GAJDOŠOVÁ, K. – BOLHA, Ľ.: Analysis of Separating Cracks Development in Concrete Tanks. In: Procedia Engineering, Vol. 65: Concrete and Concrete Structures 2013, Terchová, Slovak Republic, 23.-25.10.2013, ISSN 1877-7058, pp. 75-80 (in English)

9.) BILČÍK, J. – HOLLÝ, I.: Effect of Reinforcement Corrosion on Bond Behaviour. In: Procedia Engineering. Vol. 65: Concrete and Concrete Structures 2013, Terchová, Slovak Republic, 23.-25.10.2013, ISSN 1877-7058, pp. 248-253 (in English)

10.) BILČÍK, J.: Punching Shear Strengthening of Flat Slabs. In: Proceedings of 8th Seminar on Repair of Concrete Structures, Smolenice, Slovakia, 3.-4.12.2013, ISBN 978-80-8076-109-7, pp. 155-158 (in Slovak)

11.) BORZOVIČ, V.: Bond Stress of Prestressing Units in Post-Tensioned Concrete Bridges. In: Procedia Engineering, Vol. 65: Concrete and Concrete Structures 2013, Terchová, Slovak Republic, 23.-25.10.2013, ISSN 1877-7058, pp. 143-148 (in English)

12.) ČUHÁK, M. – BOHUNICKÝ, B.: Failure of Structure: Experiment in Real Conditions. In: Proceedings of 18th Conference on Statics of Buildings 2013, Piešťany, Slovak Republic, 14.-15.03.2013, ISBN 978-80-89655-00-7, pp. 63-68 (in Slovak)

13.) FILLO, Ľ. – ČUHÁK, M. – PORUBSKÝ, T.: Reliability of Asymmetrically Reinforced Columns. In: Procedia Engineering, Vol. 65: Concrete and Concrete Structures 2013, Terchová, Slovak Republic, 23.-25.10.2013, ISSN 1877-7058, pp. 387-392 (in English)

14.) GAJDOŠOVÁ, K. – BRONDOŠ, J.: CFRP Laminate Strips Action in RC Cross-Section. In: Procedia Engineering, Vol. 65: Concrete and Concrete Structures 2013, Terchová, Slovak Republic, 23.-25.10.2013, ISSN 1877-7058, pp. 341-345 (in English)

15.) GAJDOŠOVÁ, K. – BRONDOŠ, J.: The Utilization of CFRP Laminates in Reinforced Concrete Cross-Section. In: Proceedings of 8th Seminar on Repair of Concrete Structures, Smolenice, Slovakia, 3.-4.12.2013, ISBN 978-80-8076-109-7, pp. 131-136 (in Slovak)

16.) GRAMBLIČKA, Š.: Defects of Reinforced Concrete Structures in the Design Activity. In: Proceedings of 18th Conference on Statics of Buildings 2013, Piešťany, Slovak Republic, 14.-15.03.2013, ISBN 978-80-89655-00-7, pp. 171-176 (in Slovak)

17.) GRAMBLIČKA, Š.: Failures of Bearing Structures Due to Defects and Deficiencies in the Design Activity. In: Proceedings of 18th Conference on Statics of Buildings 2013, Piešťany, Slovak Republic, 14.-15.03.2013, ISBN 978-80-89655-00-7, pp. 5-10. (in Slovak)

18.) HALVONÍK, J. – DOLNÁK, J. – BORZOVIČ, V.: Long-Term Losses of Prestress in Precast Members Cast from HPC. In: Procedia Engineering, Vol. 65: Concrete and Concrete Structures 2013, Terchová, Slovak Republic, 23.-25.10.2013, ISSN 1877-7058, pp. 81-86 (in English)

19.) HALVONÍK, J. – FILLO, Ľ.: The Maximum Punching Shear Resistance of Flat Slabs. In: Procedia Engineering, Vol. 65: Concrete and Concrete Structures 2013, Terchová, Slovak Republic, 23.-25.10.2013, ISSN 1877-7058, pp. 376-381 (in English)

20.) HARVAN, I.: Comments on the Design of the Flexural Reinforcement of Concrete Flat Slabs by the Application of European Standards. In: Proceedings of 18th Conference on Statics of Buildings 2013, Piešťany, Slovak Republic, 14.-15.03.2013, ISBN 978-80-89655-00-7, pp. 153-158 (in Slovak)

21.) HARVAN, I.: Some Details of the Solution of Shear Resistance in the Punching of Concrete Flat Slabs by the Application of European Standards. In: Proceedings of 18th Conference on Statics of Buildings 2013, Piešťany, Slovak Republic, 14.-15.03.2013, ISBN 978-80-89655-00-7, pp. 159-170 (in Slovak)

22.) HOLLÝ, I. – BILČÍK, J.: Corrosion of RC Balcony and Ramp. In: Proceedings of 8th Seminar on Repair of Concrete Structures, Smolenice, Slovakia, 3.-4.12.2013, ISBN 978-80-8076-109-7, pp. 45-50 (in Slovak)

23.) HUDOBA, I. – DOVAĽ, M. – MIKUŠ, J.: Experience with Ultra High Performance Concrete and Possibilities of Its Application in Slovakia. In: Proceedings of National Conference (with international participation) on Concrete 2013, Štrbské Pleso, SR, 2.-4.10.2013, ISBN 978-80-970210-9-2, pp. 94-99 (in Slovak)

24.) HUDOBA, I. – MIKUŠ, J.: The Application of UHSC for Load-Bearing Composite Elements and Structures. In: Procedia Engineering, Vol. 65: Concrete and Concrete Structures 2013, Terchová, Slovak Republic, 23.-25.10.2013, ISSN 1877-7058, pp. 212-217 (in English)

25.) IGNAČÁK, M. – SONNENSCHEIN, R. – ŠOLTÉSZ, J.: Frequent Causes of "White Tanks" Defects. In: Proceedings of 18th Conference on Statics of Buildings 2013, Piešťany, Slovak Republic, 14.-15.03.2013, ISBN 978-80-89655-00-7, pp. 247-252 (in Slovak)

26.) IGNAČÁK, M. – ŠOLTÉSZ, J. – PRCÚCH, I.: Thermal and Strength Analysis of Foundation Slabs. Industrial Floors and Cement Covers of Road Pavements in the Early Stages. In: Procedia Engineering, Vol. 65: Concrete and Concrete Structures 2013, Terchová, Slovak Republic, 23.-25.10.2013, ISSN 1877-7058, pp. 94-99 (in English)

27.) KIŠAC, M.: Effect of Slenderness on the Resistance of Columns Mode of Various Concrete Classes. In: 23rd Annual PhD Student Conference on Advances in Architectural, Civil and Environmental Engineering, Bratislava, Slovak Republic, 30.10.2013, ISBN 978-80-227-4102-6, pp. 432-438 (in Slovak)

28.) LELKES, A. – GRAMBLIČKA, Š.: Theoretical and Experimental Studies on Composite Steel-Concrete Columns. In: Procedia Engineering, Vol. 65: Concrete and Concrete Structures 2013, Terchová, Slovak Republic, 23.-25.10.2013, ISSN 1877-7058, pp. 405-410 (in English)

29.) PAULÍK, P.: The Effect of Curing Conditions /in Situ vs. Laboratory/ on Compressive Strength Development of High Strength Concrete. In: Procedia Engineering, Vol. 65: Concrete and Concrete Structures 2013, Terchová, Slovak Republic, 23.-25.10.2013, ISSN 1877-7058, pp. 113-119 (in English)

30.) PAULÍK, P.: The Effect of Curing Conditions on the Development of the Compressive Strength Development of High-Strength Concrete. In: Proceedings of 8th Seminar on Repair of Concrete Structures, Smolenice, Slovakia, 3.-4.12.2013, ISBN 978-80-8076-109-7, pp. 71-78 (in Slovak)

31.) SONNENSCHEIN, R. – ŠOLTÉSZ, J. – IGNAČÁK, M.: Causes of Formation of Separating Cracks. In: Proceedings of 8th Seminar on Repair of Concrete Structures, Smolenice, Slovakia, 3.-4.12.2013, ISBN 978-80-8076-109-7, pp. 21-26 (in Slovak)

32.) ŠOLTÉSZ, J. – SEDLÁK, J. – MAKOVIČKA, D. – TENGLER, M.: Upgrade of Seismic Capacity of the Prefabricated Structure of a Fire Station Building. In: Proceedings of 8th Seminar on Repair of Concrete Structures, Smolenice, Slovakia, 3.-4.12.2013, ISBN 978-80-8076-109-7, pp. 149-154 (in Slovak)

Eng. Juraj Frólo

Design of Composite Steel-Concrete Columns with Inner Massive Steel Core Profile

1 INTRODUCTION

At present high-resistance columns with high slenderness are demanded increasingly in building structures. In sector of composite structures would be possible to design these columns with required properties as composite steel-concrete columns with steel massive inner core. For higher resistance high strength materials could be used. Current standard STN EN 1994-1-1 offers design-steel concrete structures of steel up to S460 and concrete up to C50/60. Design of composite columns of high performance concrete according STN EN 1994-1-1 is not possible because of insufficient test data for high strength concrete in composite structures. It has been known about residual stresses in steel cross-sections for last 30 years. Due to limited information about the effect of residual stresses in massive inner profiles, standards don´t cover the use of these profiles.

2 RESIDUAL STRESSES IN STEEL PROFILE, INFLUENCE OF CREEP AND SHRINCAGE OF CONCRETE

At present high-resistance columns with residual stresses in massive steel bars arise during the cooling process of steel production due to uneven temperature distribution. Residual stresses cause reduction flexural stiffness and ultimate load and have significant influence for ultimate resistance of composite column. Determination of residual stresses in massive steel section can be approximately defined according Figure 1 [Roik, Bergmann, 1987].Creep and shrinkage of concrete in composite members cause redistribution internal forces from the concrete to the structural steel. For composite columns loaded under axial force and bending moment it means decrease of flexural stiffness of column. Decrease of flexural stiffness is more significant in composite columns made of high performance concrete.

3 PROPOSALS FOR DESIGN ACCORDING STN EN 1994-1-1

Based on experimental and numerical analysis are presented following recommendations for design mentioned composite columns [Hanswille, Lipes, 2008]. Internal forces have to be determined by second order theory with effective flexural stiffness $(EI)_{eff,II}$ taking into account creep and shrinkage of concrete. Bending resistance have to be reduced by correction factor a_M for non-linear resistance (Figure 2). Maximum value of equivalent bow imperfection w_0 is given in Figure 3.

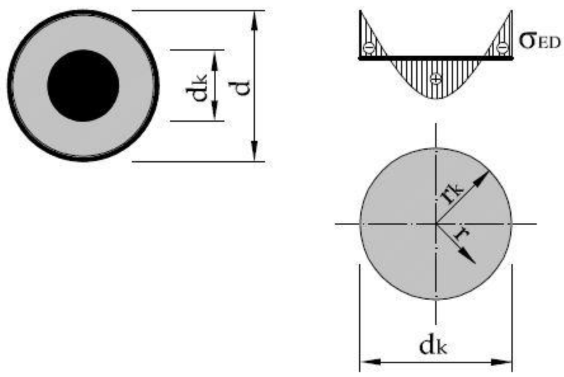

$$\sigma_{ED} = \sigma_{ED,0} \cdot \frac{d_k}{200}$$

$$\sigma_{ED,0} = -125 MPa$$

$$\sigma_E(r) = \sigma_{ED} \cdot \left[1 - \frac{2r^2}{r_k^{\,2}}\right]$$

σ_{ED} – stress at the surface of steel profile [MPa]
$\sigma_{ED}(r)$ – stress in radius r of steel profile [MPa]
d_k – diameter of steel profile [mm]
r_k – radius of steel profile [mm]
r – selected radius from center of steel profile [mm]

Fig. 1: Approximate calculation of residual stresses of circular massive steel profile

$$\alpha_M = \alpha_{M0} - \alpha_N \frac{N_{Ed}}{N_{pl,Rd}}$$

N_{Ed} - design value of axial force [kN]
$N_{pl,Rd}$ - design value of plastic axial resistance [kN]

Steel grade of the core section	$f_{yd,core}$ [MPa]	Concrete grade	f_{cd} [MPa]	$d_k/d = 0$		$d_k/d = 0.75$	
				α_{M0}	α_N	α_{M0}	α_N
S235	218	C30/37	20	0.90	0.10	0.85	0.15
		C60/75	40	0.90	0.25	0.80	0.15
		C100/115	60	0.90	0.40	0.75	0.15
S460	418	C30/37	20	0.85	0.25	0.70	0.20
		C60/75	40	0.85	0.35	0.60	0.20
		C100/115	60	0.85	0.45	0.50	0.20

Fig. 2: Correction factor a_M for non-linear bending resistance

$$\frac{L}{w_0} = 400 \cdot k_1 \cdot k_2 \cdot k_3$$

L/w_0 – equivalent bow imperfection [-]
k_1 – influence of steel grade of massive steel profile [-]
k_2 – influence of the diameter of massive steel profile [-]
k_3 – influence of related slenderness of composite column [-]

	Steel grade	S355	$k_1 = 1,0$
		S460	$k_1 = 1,25$
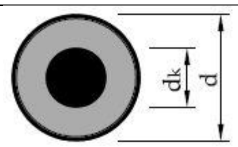	Diameter d_k of steel profile	$\leq 200\,mm$	$k_2 = 1 + \frac{d_k[mm]}{400}$
		$> 200\,mm$	$k_2 = 2 - \frac{d_k[mm]}{400}$
$\bar{\lambda}_{rel} = \sqrt{\frac{N_{pl,k}}{N_{cr}}}$	Related slenderness of column	$\bar{\lambda}_{rel} \leq 0,5$	$k_3 = 0,8$
		$\bar{\lambda}_{rel} > 0,5$	$k_3 = 0,7 + 0,2 \cdot \bar{\lambda}_{rel}$

Fig. 3: Geometrical bow imperfection for composite columns with inner massive steel core

Eng. Andrea Halabrínová

Longitudinal Shear Resistance of Composite Slabs

1 INTRODUCTION

A composite flooring system consists of a profiled steel sheeting and a concrete slab. The use of composite slabs arises from the significant advantages that are offered by this system. First the steel sheeting acts as permanent shutting for the in-situ cast concrete slab, so there is no need to remove formwork. Secondly, the steel sheeting can be effectively use as the tensile reinforcement. Thirdly, there can be a significant reduction of concrete filled for a floor. Fourth, the steel sheeting is very light, so it can be transported, placed and handled by the workers easily. Finally, the cellular geometry of the sheeting permits the formation of ducting cells within the floor, so that service can be incorporated and distributed within the floor depth. This all makes composite slabs fast to build, less laborious and more effective. The durability of the composite system depends on the composite action between the steel sheeting and concrete slab which can be ensured by several forms of interlocking devices – mechanical interlock provided by deformations of profiled steel sheeting, frictional interlock for profiles shaped in a re-entrant form or end anchorage. The possible modes of failure for this type of construction are categorized: flexure – negative (II.) and positive (I.) bending moment, vertical shear (III.) or longitudinal shear (IV.). In many cases the capacity of composite slab with profiled steel sheeting depends on the longitudinal shear resistance at the steel-concrete interface. The effectiveness of shear connection is studied by means of leading tests on simply supported composite full-scale slabs. *(Fig. 1)*

2 M-K METHOD

The m-k method is based on establishing the gradient and intercept of a linear relationship by plotting the results from the composite slab tests in terms of the vertical shear against shear bond. The shear bond characteristic is rated by two empirical parameters m for the mechanical interlocking between steel and concrete and k for friction between them. Using these parameters design vertical shear resistance is calculated. This must exceed the vertical shear at an end support while longitudinal shear failure. *(Fig. 2)*

3 PARTIAL SHEAR CONNECTION METHOD

In this method the degree of partial shear connection of ductile behaviour composite slab is calculated. Before reaching the maximum load, there is complete redistribution of longitudinal shear stress at the interface, so a value for the mean ultimate shear stress τ_u can be calculated. *(Fig. 3)*

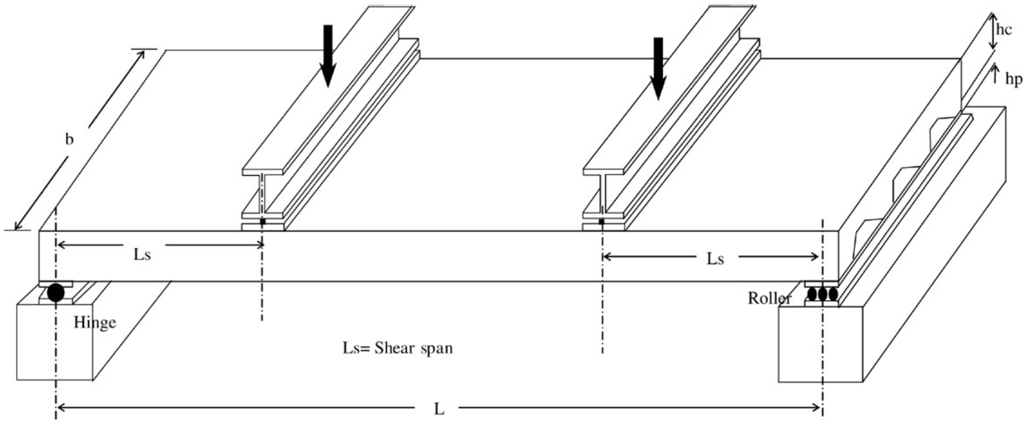

Fig. 1: Test set-up from EN 1994-1-1, Annex B

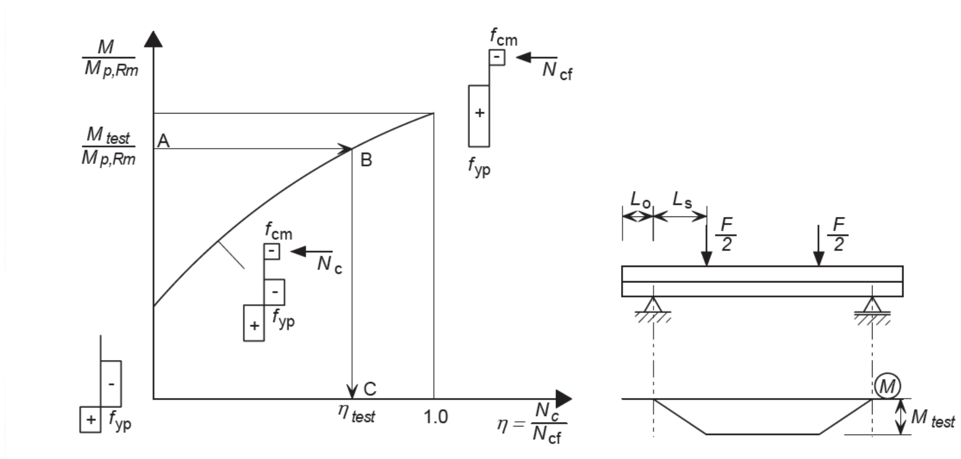

Mean value for the ultimate shear stress:

$$\tau_u = \frac{\eta_{test} N_{cf}}{b(L_s + L_o)}$$

Mean value for the ultimate shear stress with additional longitudinal shear resistance caused by the support reaction:

$$\tau_u = \frac{\eta_{test} N_{cf} - \mu V_t}{b(L_s + L_o)}$$

Fig. 2: m-k method

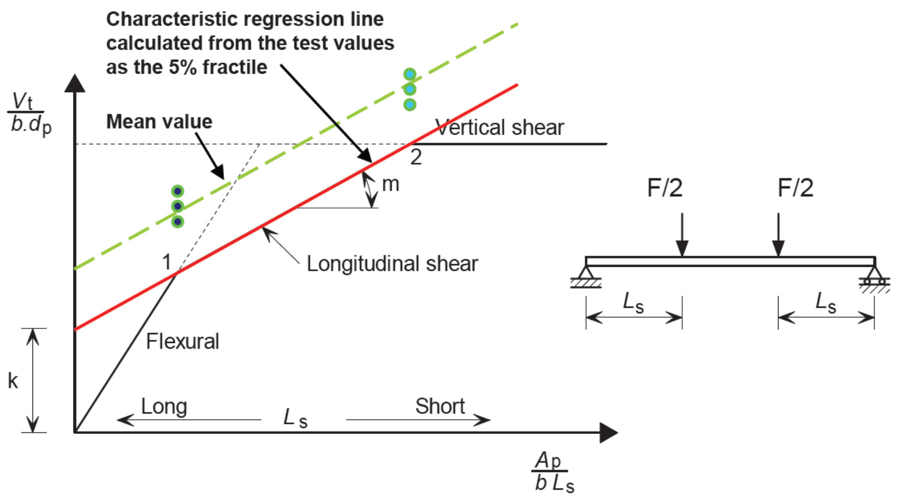

Design shear resistance $V_{l,Rd} = \frac{b d_p}{\gamma_{VS}} \left(\frac{m A_p}{b L_s} + k \right)$

Fig. 3: Partial shear connection method

Eng. Marian Kišac

Experimental Investigation of Slender Columns

1 INTRODUCTION

The most usual stress path of concrete columns is the loading by an axial compressive force at a given eccentricity, which we also call the basic eccentricity e_0. In very slender columns, a bigger columns deformation occurs. In the critical cross-section the critical normal force N_{cr} is reached. At this value of force the column loses its stability before the strength of cross-section is reached. At this point, without increasing the load, the strain increases and thus the bending moment increases to the moment when the cross-section fails in strength. For recording this effect we prepare an experimental investigation on slender columns with slenderness λ=88.

In upcoming experiment, columns are rectangular in cross-section with dimensions 240x150 mm. Total length of columns including helping steel plates is 3840 mm. Steel plates of thickness of 20 mm are mounted on both ends. The plates are monolithically joined to reinforcement cage of reinforced concrete columns. Their purpose is to prevent the local failure at the point of loading force acting during testing, which could forego the loss of stability of column.

Columns are reinforced with four longitudinal reinforcing bars of diameter of Ø14 mm. At critical areas on both ends of columns, additional longitudinal reinforcing bars of diameter of Ø14 mm with the length of 600 mm are placed and welded to steel plates. Transverse reinforcement is made of two-branched links of diameter of Ø6 mm, because of additional reinforcement in critical places four-branched links were designed to increase in confinement effect.

To achieve column failure inside the interaction diagram, that means the loss of its stability before the strength failure of cross-section, we have chosen the basic eccentricity e_0=40mm. Force will be carried in into the column linearly - by a steel cylinder. To predict the general behaviour and the failure mode of columns, software Atena and Stab2NL were used.

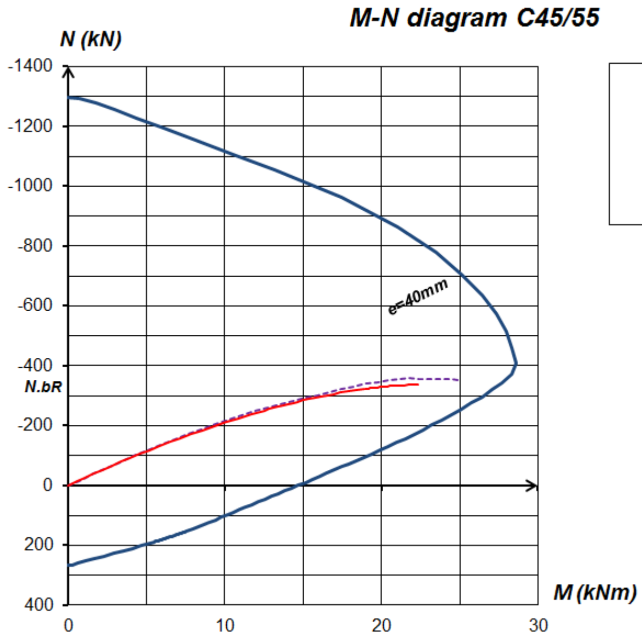

Fig. 1: Interaction diagram

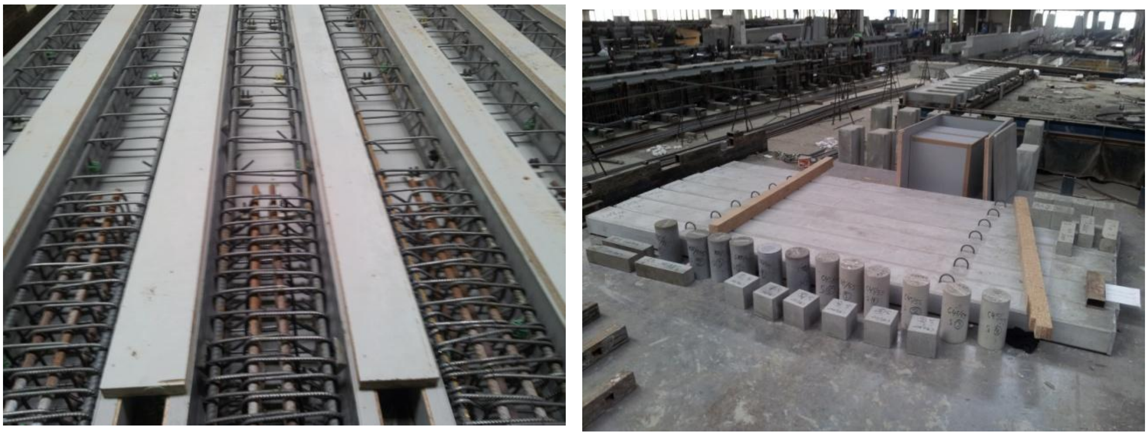

Fig. 2: Specimens preparation

Eng. Peter Pažma

Analysis of Secondary Effects on Statically Indeterminate Structures due to Prestressing

1 INTRODUCTION

In this article I focused on the analysis of prestressing effects on statically indeterminate structures. I defined differences between statically determinate and statically indeterminate structures. The participation and scale of these secondary effects caused by prestressing and their impact on the overall stress-state of the structure are presented. Furthermore, I deal with the influence of the secondary effects of prestressing after development of plastic hinge in structural element.

2 PRIMARY EFFECT OF PRESTRESSING

Prestressing is method of amplification of concrete structures when steel strands directly cause compressive stress. Effect of the prestressed depends on the position of the strands in cross-section. The most effective position is when steel strand are designed out of the centre of gravity of the cross-section. In addition to the basic influences of power P on cross-section area A, there are present also tensions caused by eccentricity of the power P from centre of gravity (Fig.1). For base structural types, like statically determinate structures, we define prestress effects as the primary effect (PE). On the other hand, we know difficult construction – e.g. statically indeterminate structures – where the statically indeterminate support restrains of the free deformation due to prestressing. This reaction, which occurs in place of statically indeterminate support, causes next tension changes which are called secondary effects (SE).

3 SECONDARY EFFECT OF PRESTRESSING

As you can see on Fig.2, secondary effects of prestressing have non-negligible effect on the overall stress-state. Due to increasing external load, occurs to creation of plastic hinge in place of statically indeterminate support. This leads to a partition of the originally statically indeterminate structure on more basic statically determinate structures. Position of the prestressing strands is same for both structures.

As we know, secondary effects occur especially on statically indeterminate structures. This leads to several questions: How are the secondary effects redistributed to the basic structures after creation of plastic hinge or whether these effects disappear completely?

4 RESEARCH PHASE

In my dissertation thesis I focus this issue and I will compare theoretical results with the experimental model. My model is 10,5m long two span continuous beam with dimensions 400x250mm in the cross-section area.

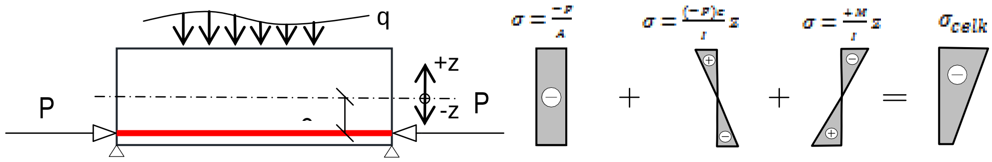

Fig. 1: Prestressing force outside centre of gravity of cross-section

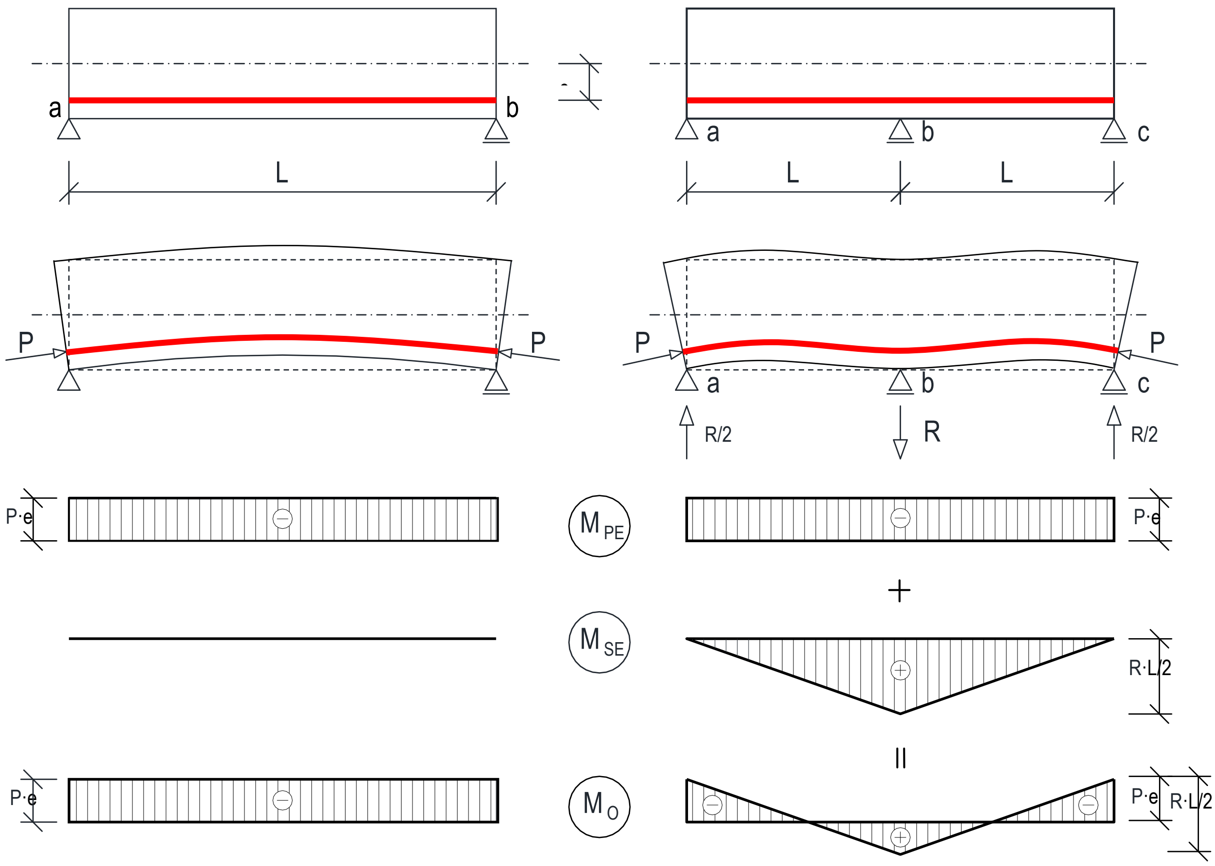

Fig. 2: Resulting diagrams comparing statically determinate and indeterminate structure

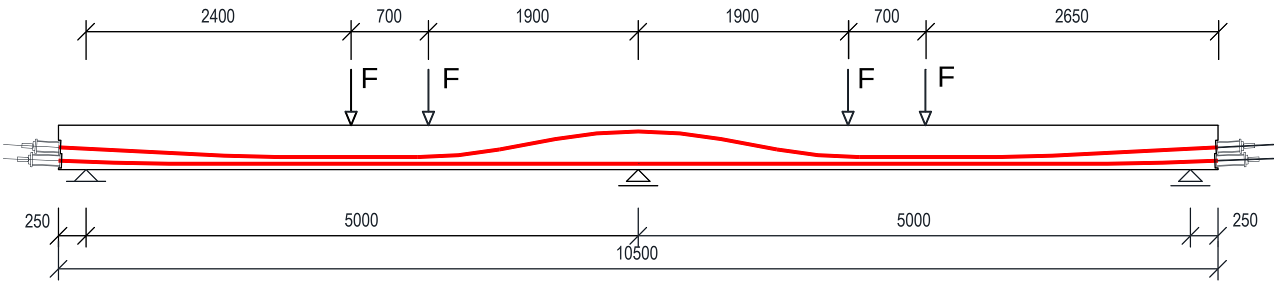

Fig. 3: Cable geometry in two span continuous beam

Eng. Róbert Sonnenschein

Refinement of the Internal Tension Parameter "*k*" for Cross-Section Thicknesses Between 0,3 m and 0,8 m

1 INTRODUCTION

The specified in DIN 1045-1 function curve for internal Tension Parameter *k*, which is needed to determine the minimum reinforcement for the load case centric forced from outflowing heat of hydration, supplies mechanically incorrect results for component thicknesses between 0.30 m and 0.80 m. Remedy the presented two variants of the approach for the coefficient which allows for the effect of non-uniform self-equilibrating stresses.

$$\begin{aligned} h &\le 0{,}30m \quad k = 0{,}80 \\ h &\ge 0{,}80m \quad k = 0{,}50 \end{aligned} \tag{1}$$

2 DEVELOPMENT CURVE k ACCORDING TO DIN 1045-1

In the following chapter, the curves for the minimum reinforcement as a function of the component thickness are analyzed. Is treated in this paper, the load case "inner compulsion" in which the internal Tension Parameter *k* according to Eq. (1) varies. The inner compulsion to be set by the flow of the heat of hydration and therefore reclaim the approach tensile strength of the concrete according to DIN 1045-1, paragraph 11.2.2 (5) mitigated. Not all common rod diameters for reasons of clarity in the further evaluated, but it is limited to the diameter of 10, 12, 14, 16 and 20 mm (Fig.1). The following sizes are reported for the other parameters:

Concrete C25/30 – $f_{ct,eff}$ =1,5MPa; element width – b =1m; concrete cover – c =30mm; crack width – $w_{k,max}$ =0,3mm, module of elasticity of steel– E_s =200GPa.

3 APPROACH OF THE TRANSITION ZONE BY TWO PARABOLAS

The transition region of the internal Tension Parameter *k* should be replaced by two quadratic parabolas when specifying suitable boundary conditions. Functions parabolas are:

$$\left.\begin{aligned} P_1(h) &= \frac{1}{10}\cdot(-16\cdot h^2 + 8\cdot h + 7) \\ P_2(h) &= \frac{1}{10}\cdot(8\cdot h^2 - 16\cdot h + 13) \end{aligned}\right\} = k(h)...h(m)$$

Parabolic Equation 1 is valid in the range *0.25 < h ≤ 0.50*, parabolic equation 2 is in the range *0.50 < h ≤ 1.00*.

3 USING AN EXPONENTIALLY DECAYING FUNCTION

With h as the thickness of the internal Tension Parameter *k* as can be exponentially decreasing function for option 2 to specify:

$$k(h) = \frac{1}{2} + \frac{3}{10}\cdot\frac{1}{1 + 2\cdot h^3 + 2\cdot h^4} \qquad h\ (\mathrm{m})$$

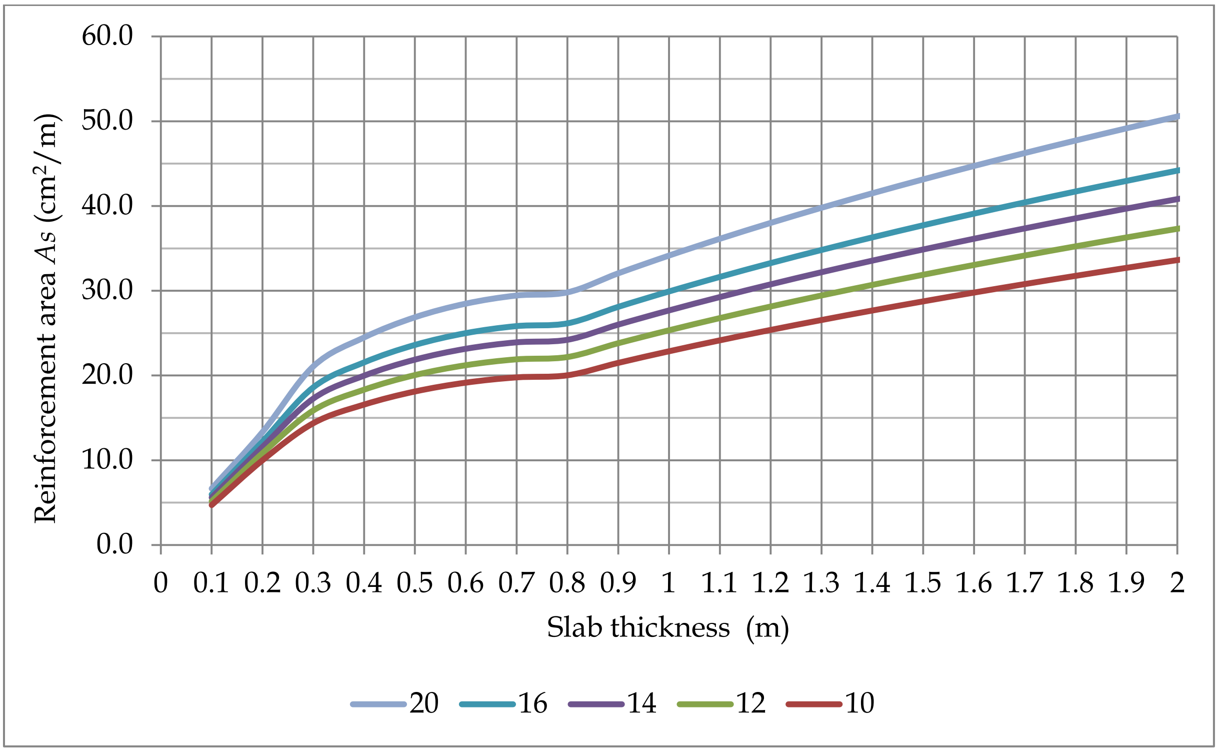

Fig. 1: Necessary minimum reinforcement with „k“ according to DIN 1045-1

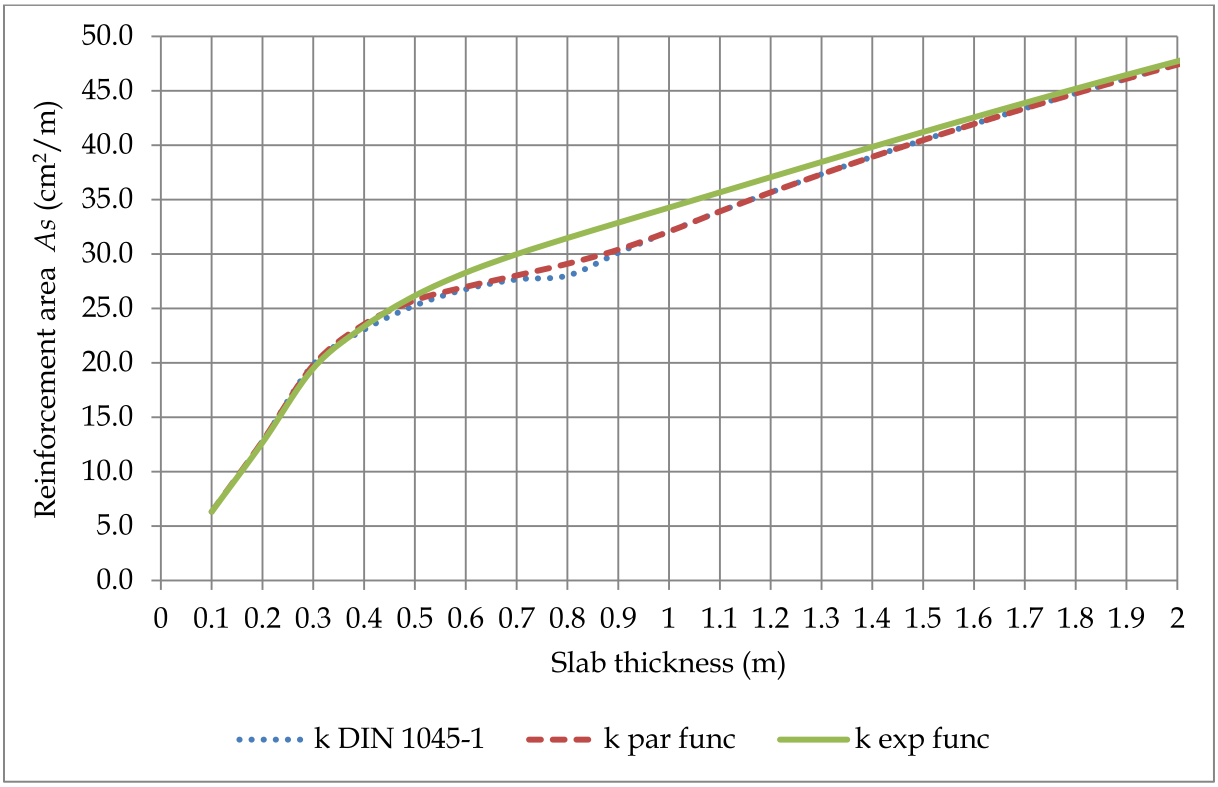

Fig. 2: Comparison of the minimum reinforcement for the introduced alternatives of parameter „k“ in case of steel bar diameter 16 mm

Full-Scale Testing of CFRP-Strengthened Slender Reinforced Concrete Columns

Katarina Gajdosova, Ph.D.[1]; and Juraj Bilcik[2]

Abstract: The paper presents an investigation into the performance of slender rectangular reinforced concrete columns strengthened with carbon fiber-reinforced polymers (CFRPs) in two manners. The first approach is a well-known form of CFRP sheet jacketing with the effect demonstrated in many studies, and a second one is a relatively new retrofit method of near surface mounted (NSM) CFRP strips. A total of eight full-scale specimens with rectangular cross sections (210 × 150 mm) were tested to failure under eccentric compressive loading. The total length of the specimens was 4,100 mm. The results of this study demonstrate a significant difference in slender and short column strengthening in accordance with the predominant stress manner. It was confirmed that the effect of CFRP wraps on the increase in column strength is proportionally greater for short RC columns subjected to predominant compression. The longitudinal fibers in CFRP strips bonded into grooves in concrete cover are more effective in enhancing the flexural load-carrying capacity of slender reinforced concrete columns subjected to eccentric loading. The most effective approach to flexural capacity enhancement was demonstrated by a synergistic effect of NSM CFRP reinforcement ensured by CFRP sheet wrapping. **DOI: 10.1061/(ASCE)CC.1943-5614.0000329.** © *2013 American Society of Civil Engineers.*

CE Database subject headings: Concrete columns; Fiber reinforced polymer; Slenderness ratio; Eccentric loads; Full-scale tests.

Author keywords: Concrete rectangular column; Carbon fiber-reinforced polymer; Slenderness ratio; Eccentric loads.

Introduction

Strengthening of concrete structures with the use of traditional materials (concrete, reinforcement) as used in the past not only increases the load-carrying capacity, but also the dimensions of the cross section. In the last few decades, new progressive composite materials for strengthening have been recognized. The most widely known and used are carbon fiber-reinforced polymers (CFRPs) because of their properties, especially their resistance to corrosion, high strength to weight ratio, and easy handling and installation. The field of application of FRPs in the strengthening of concrete structures is extended to each type of stress. This paper focuses on the strengthening of slender concrete columns, in which compression and bending stresses are applicable. The load-carrying capacity and ductility enhancement effect of FRP sheet wrapping on axially loaded short concrete columns was demonstrated with a number of tests.

In comparison with the large database of publications dealing with confined short columns, the investigation of eccentrically loaded slender columns is insufficient. The extension of this method of application is restricted because there are apparent differences between the behavior of short and slender columns.

Research in this field was started by Mirmiran et al. (2001), who investigated concrete—filled fiber-reinforced polymer tubes (CFFT) and found a significant decrease in column load-carrying capacity with an increase in slenderness ratio. Tested CFFT columns tended to be more susceptible to slenderness effects because the glass FRP materials used have a higher strength and lower stiffness than steel. In addition, Pan et al. (2007) proved that the strengthening effect decreases with an increase in the slenderness ratio and that the effect of the slenderness ratio on the load-carrying capacity of FRP-wrapped concrete columns is more significant than that of ordinary reinforced concrete columns because confinement enhances the strength instead of bending stiffness. The impact of increasing load eccentricity and column slenderness on the decreasing effect of the CFRP confinement on the enhancement of the column load-carrying capacity was confirmed by Tao and Han (2007). The results of tests on concrete confined specimens of Tamuzs et al. (2007) showed that a tangential wrapping increases the load-carrying capacity only for columns with slenderness λ less than 40.

The effect of unidirectional and bidirectional CFRP sheets laminated to the surface of a square column with a slenderness of approximately 70 was a point of experimental investigation for Tao and Yu (2008). The ultimate strength measured for columns strengthened only in the transverse direction is quite close to that of nonstrengthened ones. Higher increase in load-carrying capacity is achieved by additionally strengthening in the longitudinal direction. The longitudinal fibers become more effective when bending becomes dominant.

Fitzwilliam and Bisby (2010) verified the strengthening effects of lamination with two and four CFRP sheet layers in both the transverse and longitudinal directions on small-scale specimens (columns with circular cross sections and slenderness λ = 10–35). The more slender the column is, the lower the load-carrying capacity increase from confinement is. The increase in load-carrying capacity from transverse CFRP wraps was more significant for short columns, whereas longitudinal CFRP wraps can be used to improve the behavior of slender CFRP wrapped circular concrete columns and allow them to achieve higher strengths, similarly to the equivalent short CFRP-wrapped columns.

[1]University Teacher, Dept. of Concrete Structures and Bridges, Faculty of Civil Engineering, Slovak Univ. of Technology, 813 68 Bratislava, Slovakia (corresponding author). E-mail: katarina.gajdosova@stuba.sk

[2]Head, Dept. of Concrete Structures and Bridges, Faculty of Civil Engineering, Slovak Univ. of Technology, 813 68 Bratislava, Slovakia. E-mail: juraj.bilcik@stuba.sk

Note. This manuscript was submitted on March 30, 2012; approved on August 16, 2012; published online on March 15, 2013. Discussion period open until September 1, 2013; separate discussions must be submitted for individual papers. This paper is part of the ***Journal of Composites for Construction***, Vol. 17, No. 2, April 1, 2013. © ASCE, ISSN 1090-0268/2013/2-239-248/$25.00.

In the investigations of Tao and Yu (2008) and Fitzwilliam and Bisby (2010), only CFRP sheet wraps were used for strengthening in the longitudinal direction. Within the last three or four years, a limited number of studies dealing with NSM FRP reinforcement have appeared; see Barros et al. (2008) and Bournas and Triantafillou (2009). In these studies, small- or large-scale specimens with small slenderness ($\lambda = 17$ and 22) were tested. This is the first time that CFRP strips such as near surface mounted (NSM) reinforcement additionally secured with CFRP sheet jacketing are studied for strengthening of full-scale rectangular columns with considerable high slenderness ($\lambda = 95$).

This paper is focused on the investigation the effectiveness of CFRP strengthening for eccentrically loaded slender columns.

The majority of reinforced concrete columns in practice is constructed as slender columns with a rectangular cross section and is loaded eccentrically, so it is necessary to derive and verify the design procedures for including the strengthening effects of fiber-reinforced polymers. The purpose of this study is to verify the effectiveness of NSM CFRP reinforcement for flexural strengthening of slender reinforced concrete columns and provide a methodology for the calculations for practical design applications. Experimental and numerical investigations are described in the following sections.

Experimental Program

Testing was performed on eight full-scale slender rectangular reinforced concrete columns in four series. The series differed with respect to the method of strengthening. The first, a reference series, consisted of nonstrengthened columns, and the remaining series were strengthened by CFRPs, i.e., longitudinal NSM CFRP strips, transverse CFRP sheet wrapping, and a combination of these two methods. To achieve very slender columns that largely approximate load-bearing members in real structures, the specimens were designed as columns 4,100 mm long, with rectangular cross sections 210×150 mm, symmetrically reinforced with 2×4 $\phi 10$ mm longitudinal bars, and with hinged supports at both ends (Fig. 1). Four-shear stirrups of 6 mm diameter at a spacing of 150-mm centers were mounted lengthwise and reduced to 30-mm centers at the ends. At both column ends, 30-mm thick steel plates were set to assist in better load distribution. The corners of the cross section were beveled by embedding triangular laths (10×10 mm) in the formwork edges. For columns strengthened by confining, these corners were additionally chamfered to a radius of 20 mm.

First, two columns (C1 and C2) were tested as nonstrengthened columns. Two other columns (C3 and C4) were strengthened by the near surface mounted reinforcement method, i.e., in the form of CFRP strips (1.4×10 mm) mounted into grooves (three on each of the longer side of the cross section) in concrete cover [Fig. 2(a)]. The next two columns (C5 and C6) were strengthened by confinement of one layer of transverse CFRP sheet (300-mm width) in the form of stirrups at 50 mm centers [Fig. 2(b)]. The remaining two columns (C7 and C8) were strengthened with a combination of the previously noted methods.

Materials

For the purpose of the comparison of experimental and analytical modeling results, the material properties of the concrete and steel specimens were laboratory tested. The properties of the CFRP sheets and strips provided by the manufacturer (Table 1) were not verified, following a good agreement with the results of previous experimental tests carried out at our department during a former investigation.

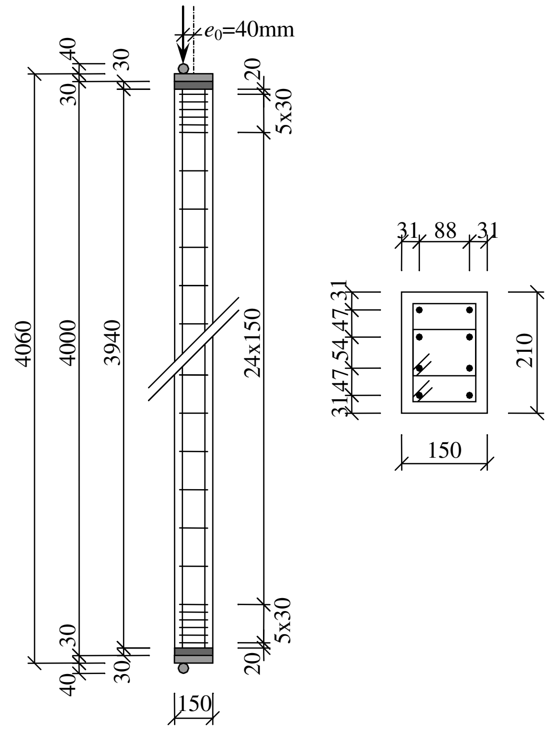

Fig. 1. Geometry of specimens (dimensions in mm)

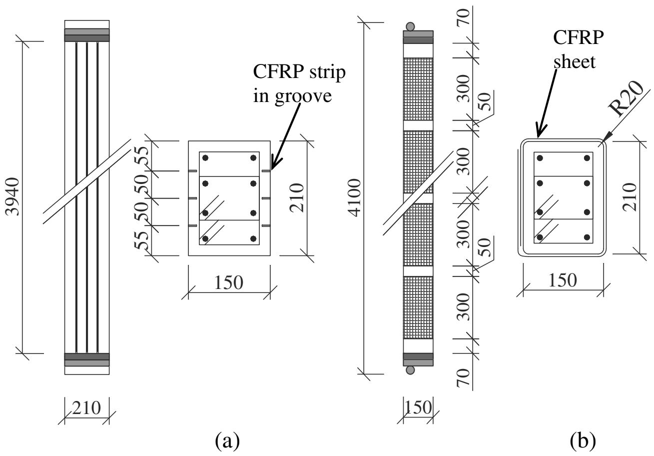

Fig. 2. Strengthening configuration: (a) C3, C4; (b) C5, C6 (dimensions in mm)

Table 1. Properties of CFRP Materials

Property	CFRP strip	CFRP sheet, weight of C-fiber in primary direction (300 g/m^2)
Tensile strength (MPa)	2,500	3,900
Modulus of elasticity (GPa)	168	240

The same concrete mix was used for all columns. During the concreting of the columns, cubic, cylindrical, and prismatic specimens were also prepared and tested after 28 days and immediately before the columns were tested. The results are summarized in Table 2. The average 28-day cylindrical concrete strength was

Table 2. Material Properties of Concrete

Property	28th day	316th day
Cube strength (MPa)	35.6	42.1
Cylindrical strength (MPa)	32.0	34.2
Static modulus of elasticity (GPa)	Not measured	36.8

32 MPa. Three bars of each diameter of the reinforcing steel were tested for their material properties, the results of which are shown in Table 3. The measured yield strength of longitudinal reinforcement was approximately 560 MPa.

Specimens

The columns were cast in a horizontal position in prepared formwork. After 14 days the columns were demolded, and after 28 days the columns were prepared for strengthening (Fig. 3). Along the entire length of columns C3, C4, C7, and C8, three grooves (3×15 mm) on each of the longer sides of the cross section were cut, cleaned, and filled with epoxy adhesive MBrace Epoxikleber 220, into which CFRP strips, MBrace S&P CFK 150/2000, were inserted [Fig. 3(a)].

The beveled corners of columns C5–C8 were chamfered, and columns were confined by one layer of CFRP sheet MBrace, S&P C-Sheet 240, with the help of MBrace epoxy resin, in the form of 300-mm wide stirrups anchored with an overlap of 170 mm on the longer side of the cross section [Fig. 3(b)].

Items of Investigation

All eight columns were tested in the same manner, i.e., by increasing the compression force applied at an initial eccentricity of 40 mm. This eccentricity was predefined by the position of a steel roller (welded to a top steel plate at column ends) placed between the steel angle section members (welded to a bottom steel plate) to ensure a hinged connection (Fig. 4).

The strains of the concrete, steel, and CFRP reinforcement, and the deflection from the increasing bending moment at midheight, were monitored during loading. The primary objective of the experimental study was the examination of the relationship between deflection at midheight and the eccentrically acting compression force. In total, three linear variable displacement transducers (LVDTs) were used as they are considered the most accurate measurement method for this purpose, one at midheight and two controls at the ends of column (Fig. 5). Indirect methods for checking the midheight deflection were based on deflection calculations from the curvature. This was determined from the strain in the steel and concrete or by geodetic surveying in a direction perpendicular to LVDTs. Strains of all materials were measured by strain gauges (T1–T4, steel; T5–T8, concrete; T9–T10, CFRP strips; T11–T12, CFRP sheet), and strains at concrete face in midheight crosssection were controlled with removable deformeters (D1–D4) at both sides (compressed, tensile). At column height, five geodetic points (G1–G5) were used to control the deformation of a column. Measure tapes 150-mm long were mounted at these points and the horizontal displacement of each point was measured by theodolite.

Parameters obtained during the testing were recorded by computer software. The test was stopped after cross-section failure, following achievement of buckling resistance, and a decrease in compression force (the descending branch was noted).

Table 3. Material Properties of Steel

Property	ϕ6 mm	ϕ10 mm
Yield strength (MPa)	605	562
Tensile strength (MPa)	625	637
Modulus of elasticity (GPa)	237	208
Ultimate tensile strain (%)	6.64	10.75

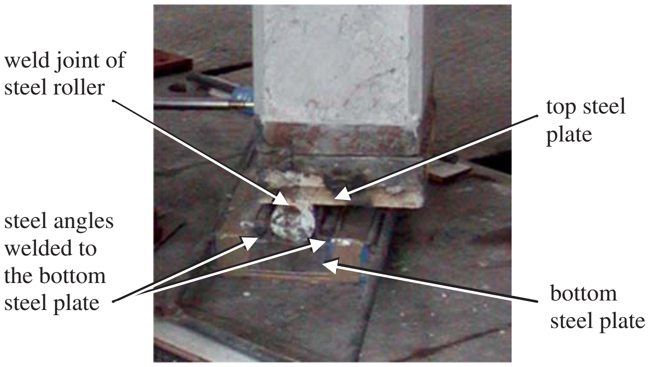

Fig. 4. Detail of hinged connection

Fig. 3. Strengthening of specimens: (a) NSM CFRP strips; (b) CFRP sheet confinement

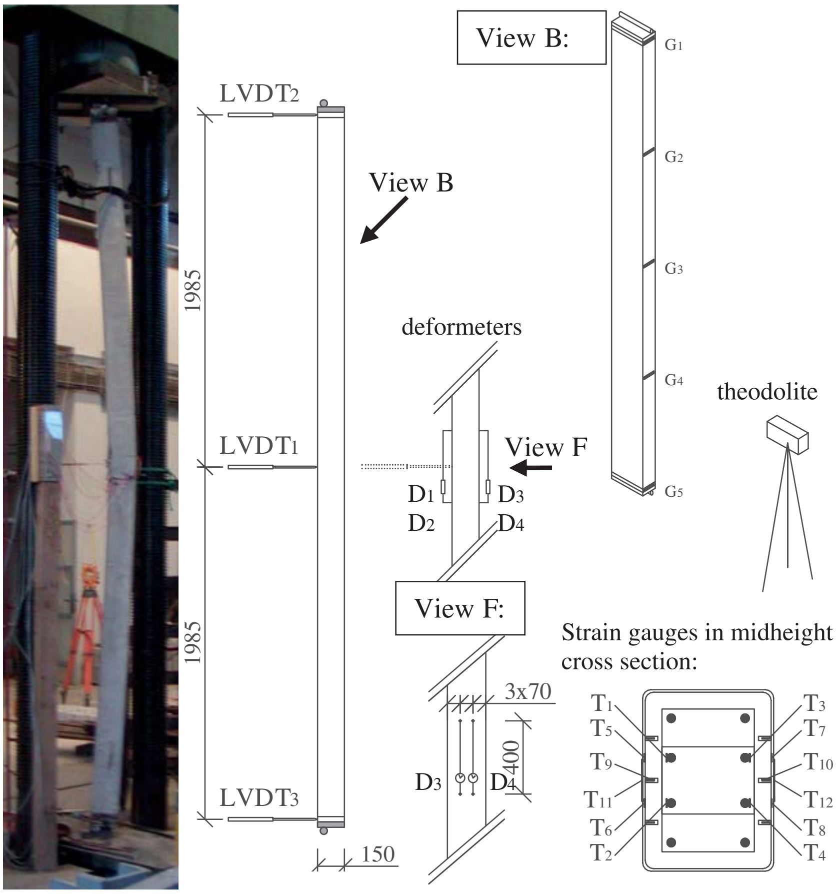

Fig. 5. Column during experimental testing

Test Results

General

The load–deflection curves were measured by LVDTs for all of the tested columns. The value of measured deflection is calculated as a difference between deflection at midheight (LVDT1) and the average of the top and bottom deflection (LVDT2 and LVDT3). Strains needed for the calculation of curvature and deflection were measured by strain gauges. When two gauges are mounted on the investigated side of a cross section, the average value is calculated and used. Checking methods (deformeters, theodolite) were only applied to the last step before peak load achievement, as after this point, the deflection increases without any force increase and the steps after peak load was achieved cannot be controlled without continuous computer measurement.

Load–moment curves are used for comparison of various measurements and for determination of increase in resistance attributable to strengthening. Bending moment acting in a midheight cross section is calculated from applied force and total deflection of an investigated cross section

$$M = N \cdot (e_{\text{measured}} + e_0) \cdots \text{[Nm]} \tag{1}$$

where e_{measured} = deflection in midheight cross section measured directly (LVDTs, geodetic surveying) or indirectly (strain gauges, deformeters); and e_0 = initial end eccentricity = 40 mm.

For indirect methods the deflection is calculated from a curvature following the strains

$$e_{\text{measured}} = k \cdot \frac{l^2}{10} \cdots \text{[m]} \tag{2}$$

where l = column length (4,100 mm); and k = curvature

$$k = \frac{\varepsilon_c - \varepsilon_t}{h_{c-t}} \cdots \text{[1/m]} \tag{3}$$

where ε_c = strain at compressed face of mid height cross section; ε_t = tensile strain at the face of cross section (by deformeters) or in steel reinforcement (by strain gauges); and h_{c-t} = distance between points with strains ε_c and ε_t.

A comparison of results from all measurement methods is shown in Fig. 6. Good agreement was obtained. Directly measured values from geodetic theodolites and indirectly calculated values from strains measured with strain gauges and deformeters show the deflections of the most stressed cross section at the middle of the column height close to the LVDT measurements.

Column Resistance

All columns tested in the experimental investigation failed in buckling. The increase in resistance attributable to strengthening can be expressed as an enhancement of maximum achieved compression force beside the nonstrengthened reinforced concrete column, i.e., 12.9% for columns strengthened by longitudinal NSM CFRP strips, 2.4% for columns strengthened by confining with one layer of transverse CFRP sheet, and 15.4% for columns strengthened by a combination of CFRP strips and CFRP sheet (Fig. 7).

J. Compos. Constr. 2013.17:239-248.

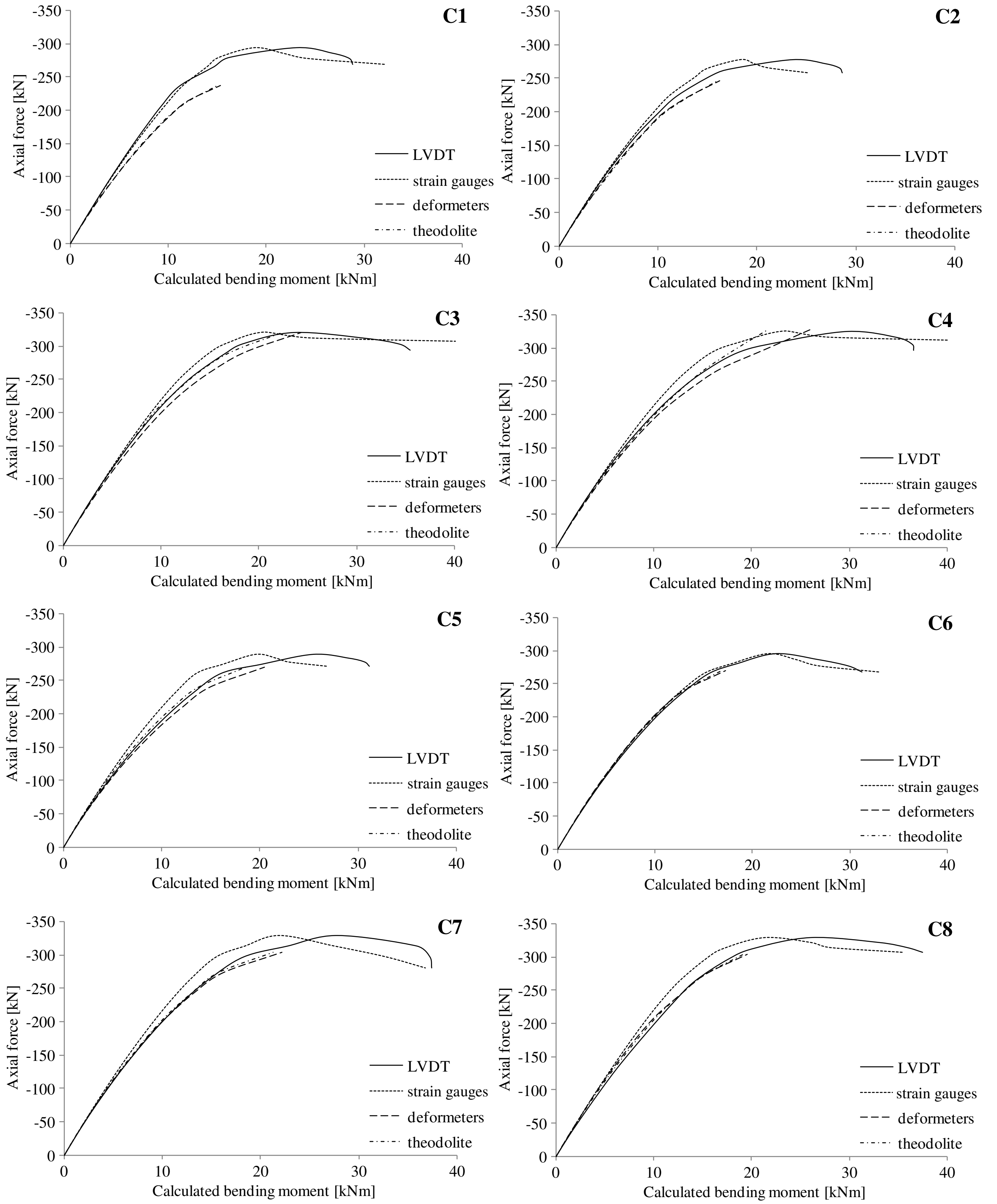

Fig. 6. Comparison of direct and indirect measurement methods

For confined columns, no significant variation in the behavior during loading was observed. More ductile postpeak behavior occurred at columns strengthened with longitudinal NSM CFRP strips. The difference between deflection at peak load and final deflection is 1.5 times greater for strengthened columns.

Failure Modes

Failure mode of all columns was specified by crushing and spalling of the concrete. At nonstrengthened columns, several bigger cracks were observed at the middle of the height of a column on the tensile side of a cross section [Figs. 8(a and b)].

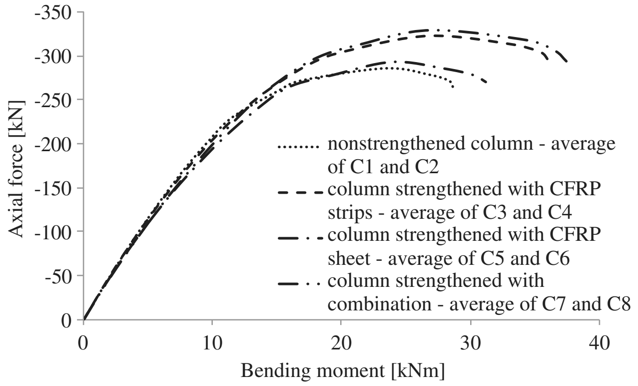

Fig. 7. Load-moment relationship measured with LVDT during experimental testing

Tensile cracks at columns strengthened with longitudinal NSM CFRP strips were not continuous over the entire side of cross section; they primarily appeared near the edges [Fig. 8(c)]. After falling off of a concrete layer, buckling of the longitudinal steel reinforcing bar and rupture of CFRP strips were observed [Fig. 8(d)]. At columns strengthened with transverse CFRP wrapping, the primary tensile crack appeared up or down the middle CFRP stirrup and several smaller cracks were found under the sheet after its removal [Figs. 8(e–g)]. The same cracking mechanism was achieved at columns strengthened with a combination of NSM CFRP strips and a CFRP sheet jacket [Fig. 8(h)]. To prevent the cracking over or below the middle CFRP stirrup, it is recommended to wrap a specimen continuously or with covering of particular stirrups in the middle segment of a column for further investigation.

Relative Strains

Strains of all used materials at the column midheight were observed. The strains of CFRP materials served the purpose of evaluating their capacity utilization.

The rupture of the NSM longitudinal CFRP strips was observed at ultimate strains of 0.25–0.28%. Similar values were measured by Olivova (2007); see Fig. 9. Ultimate strains from tension tests were five times higher. This decrease can be caused by different stress paths, as there is a large curvature at the midheight cross section and the CFRP strips are stressed in the direct and bending stress manner rather than pure tension during the tension test, so the strain capacity utilization of the CFRP strips is limited.

Measured compression strains of CFRP strips during failure were lower by 40% in comparison with tensile strains. No significant buckling of strips in compression was observed. In specimens with CFRP wraps there was no difference in the behavior of CFRP strips in tension and compression; compared with specimens without wraps, the failure strains were higher by 15% for CFRP strips at both sides.

The confinement effect of transverse CFRP sheet strengthening on slender columns with large curvature at the midheight cross section is very small and the expected concrete strength enhancement could not be reached, which results from very low, almost zero, measured values of CFRP sheet strains on the compressed face and a maximum 0.01% on the tensile face of the column

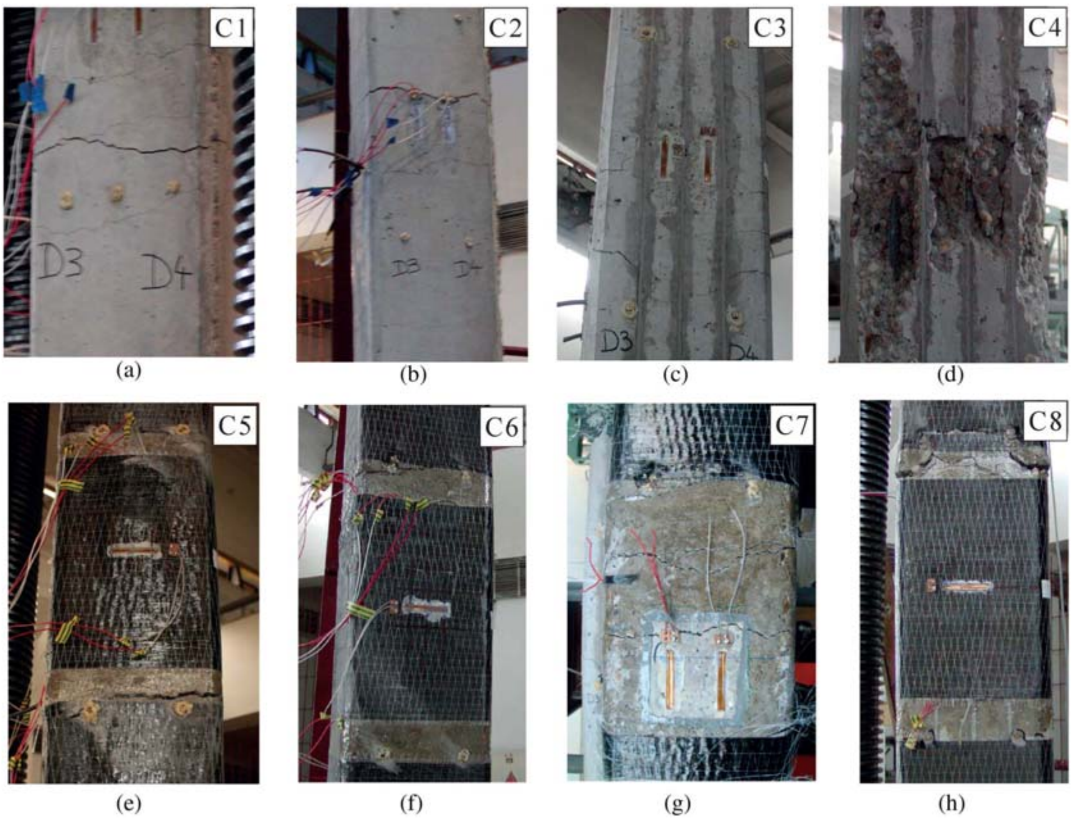

Fig. 8. Columns after failure: (a and b) cracks at the middle of the height of a column on the tensile side of a cross section; (c) tensile cracks near column edges; (d) buckling of steel reinforcing bar and rupture of CFRP strips; (e–g) tensile crack up or down the middle CFRP stirrup with cracks under the sheet; (h) cracks on columns strengthened with NSM CFRP strips and CFRP sheet jacket

J. Compos. Constr. 2013.17:239-248.

Fig. 9. CFRP strips ruptured in failure

cross section. This confirms measurements reported by Tao and Yu (2008).

Analytical Procedure

Along with the experimental investigation, a numerical model was conducted using the program ATENA 3D. More information about computer modeling can be found in the original thesis (Gajdosova 2010). Material properties and static actions were adapted from the full-scale tests. Numerical and experimental procedures yielded identical results.

Theoretical analysis was carried out before column testing with measured material properties according to a number of analytical models found from various sources, which were then modified following the results of the experimental investigation. The models, which primarily corresponded with experimental results, are further recommended for typical use.

In the preliminary part of the analytical procedure, interaction diagrams (IDs) were developed for slender columns (Fig. 10) as

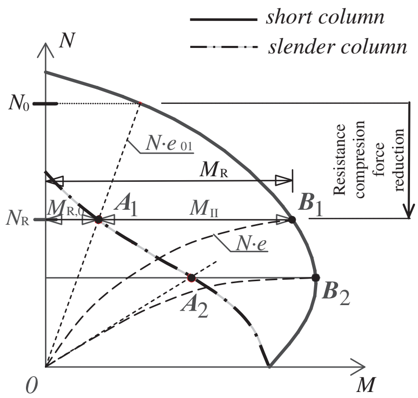

Fig. 10. Interaction diagrams for short and slender columns

the most convenient method for discussing the effects of variables on column resistance. The load-maximum moment curves (at the midheight for columns with hinged supports at both ends), for a given slenderness λ and initial end eccentricity e_{01}, is shown by line 0-B_1. The column fails when this line intersects the ID, at point B_1. At this point, the load and moment at the column ends are given by point A_1. The same relationship holds for line 0-B_2 at end eccentricity e_{02}. This indicates that the interaction diagram for a slender column with a given slenderness λ can be obtained by repeating this process a number of times with different end eccentricities e_{0i}. The maximum load capacity N_R can be determined from the linear relationship between the compression force N and the first order bending moment M_0. Compression force N_R and total bending moment M_R act in the most stressed crosssection. This moment is the sum of bending moments of first ($M_{R,0}$) and second orders ($M_{R,\mathrm{II}}$)

$$M_R = M_{R,0} + M_{R,\mathrm{II}} \cdots \text{[Nm]} \tag{4}$$

The resistance of reinforced concrete cross section, defined by $N_R - M_R$, is calculated as follows from the equilibrium equations:

$$N_R = F_{cc} + \sum F_{si} \cdots \text{[N]} \tag{5}$$

$$M_R = F_{cc} \cdot z_c + \sum (F_{si} \cdot z_{si}) \cdots \text{[Nm]} \tag{6}$$

where F_{cc} = compression force in concrete; z_c = distance of compression force in concrete from gravity center axis of concrete cross section; F_{si} = force in steel reinforcement in row i; and z_{si} = distance of force in row i of steel reinforcement from gravity center axis of concrete cross section.

The interaction diagrams are calculated by assuming a series of strain distributions. Stresses for force calculations are then determined from stress-strain relationships of each material and Eqs. (5) and (6) are quantified. In each point of the section interaction diagram, the real reduced bending stiffness $(EI)_r$ can be calculated and used for determination of curvature, including second-order effects. Following this curvature, a first-order bending moment can be derived to present a slender column interaction diagram.

The second part of the analytical procedure involves the inclusion of the strengthening effects to the column resistance. NSM CFRP strips in the grooves are considered as additional reinforcement near the cross-section surface and the values of their strains are determined based upon concrete strains, depending on their distance from the neutral axis (Fig. 11). From the strain values of the CFRP strips, the stress is determined from a linear stress-strain relationship. The same stress-strain diagram is used both in tension and compression. It is very important to make provision for initial strains in the reinforced concrete section when the CFRP strips are applied. During strengthening the structure is maximally relieved, even though there are some low strains in the concrete and steel reinforcement, and it is necessary for them to be included. The theoretical initial strain values of CFRP strips after unloading ($\varepsilon_{f,un}$) are subtracted. Equilibrium equations are then adjusted as follows:

$$N_R = F_{cc} + \sum F_{si} + \sum F_{fi} \cdots \text{[N]} \tag{7}$$

$$M_R = F_{cc} \cdot z_c + \sum (F_{si} \cdot z_{si}) + \sum (F_{fi} \cdot z_{fi}) \cdots \text{[Nm]} \tag{8}$$

where F_{fi} = force in CFRP strips in row i; and z_{fi} = distance of force in row i of CFRP strips from gravity center axis of concrete cross section.

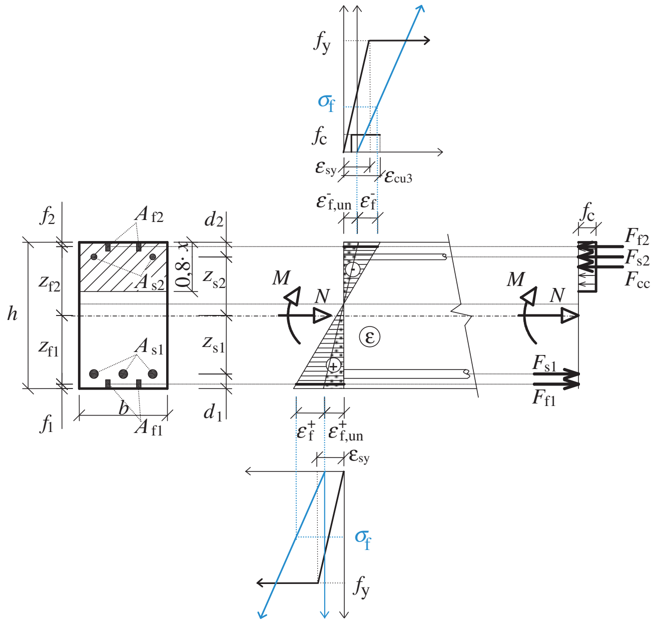

Fig. 11. Forces in cross section strengthened with longitudinal CFRP strips

CFRP sheet confinement is included as an increase in concrete strength and with a modified stress-strain relationship. Lam and Teng's stress-strain model (cited in Hollaway and Teng 2008) primarily correspondents with experimental results. This diagram consists of a parabolic part followed by a linear section ending at a point defined by the confined concrete strength and ultimate strain. These values are calculated in accordance with Teng (cited in Hollaway and Teng 2008)

$$f_{cc} = f_{co} \cdot \left(1 + 3.5 \cdot \frac{f_l}{f_{co}}\right) \cdots [\mathrm{MPa}] \tag{9}$$

$$\varepsilon_{cc} = \varepsilon_{co} \cdot \left(1 + 17.5 \cdot \frac{f_l}{f_{co}}\right) \cdots [-] \quad \text{when } f_l \geq 0.07 \cdot f_{co} \tag{10}$$

$$\varepsilon_{cc} = \varepsilon_{co} \cdot \left(1 + 17.5 \cdot \left(\frac{f_l}{f_{co}}\right)^{1.2}\right) \cdots [-] \quad \text{when } f_l < 0.07 \cdot f_{co} \tag{11}$$

where f_{cc} = confined concrete compressive strength; f_{co} = unconfined concrete compressive strength; f_l = lateral confining pressure; ε_{cc} = confined concrete ultimate strain; and ε_{co} = unconfined concrete ultimate strain.

Confined concrete strength and strain result from the lateral confining pressure provided by the CFRP jacket, which depends on many factors, for which provision must be made. The most important factors are material properties of the CFRP sheet, cross-section shape, radius of rounded edges, and continuous or stirrup-form confinement. Because of the linear stress-strain diagram of CFRP materials, the confining pressure increases continuously with increasing CFRP sheet strains. The confinement effectiveness is highly dependent on these strains.

The final value of the lateral confining pressure is considered as a reduction of the initial value $f_{l,o}$ calculated from geometrical average of pressures in two directions of rectangular cross section

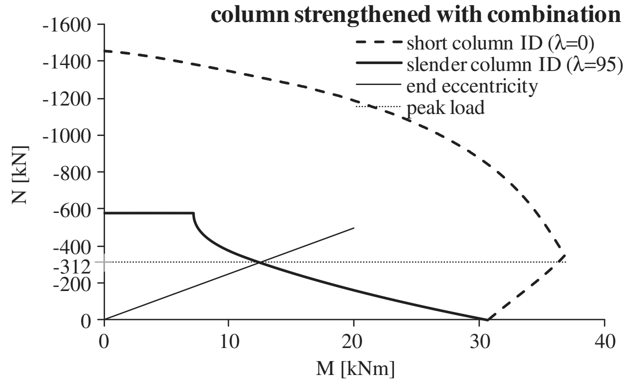

Fig. 12. Interaction diagram of chosen column calculated in accordance with Fig. 10

$$f_l = f_{l,o} \cdot k_e \cdot k_{eh} \cdots [\mathrm{MPa}] \tag{12}$$

where k_e is a factor of confinement effectiveness in a cross section calculated like a ratio of effectively confined cross-section area to the total area of the cross section; and k_{eh} is a factor of confinement effectiveness along column height, making provision for sections with a reduced confinement effect.

Equilibrium equations are the same as for nonstrengthened columns, e.g., Eqs. (5) and (6), but the concrete compression force includes confined concrete compressive strength.

An example of theoretical analysis results for a chosen column is shown in Fig. 12.

Discussion of Results

The measured results of column resistance from the experimental investigation are approximately 8% greater than the theoretical calculations. This is a product of many simplifications in the theoretical analysis. A comparison of theoretical predictions, computer modeling, and experimental tests is shown in Fig. 13, in which only the lower parts of the interaction diagrams (to the peak load of slender column) are displayed.

Given that the behavior and loss of the load-carrying capacity of all the columns were controlled by bending, the columns strengthened with transverse CFRP sheet jacketing in stirrup form yield a response similar to slender nonstrengthened RC columns and it is obvious. In a flexural stress path, longitudinal NSM CFRP strips tend to be more effective. To prevent eventual debonding of CFRP strips in compression and to ensure the stability of the epoxy adhesive, additional CFRP sheet jacketing was provided through the entire length of a column. The synergistic effect of two retrofitting methods results in a slight increase in the enhancement of the column load-carrying capacity in comparison with using only the NSM method.

Effects of Slenderness

On the basis that the theoretical models were confirmed by experimental tests, a theoretical parametric study can be conducted with a variation of arbitrary parameters. For the purpose of the slenderness effects, the verifying calculation summarized in Table 4 was carried out. By changing the column length while retaining the same cross section and reinforcement, slenderness ratios λ of approximately 25, 48, 71, 95, and 118 (lengths from 1,000–5,000 mm) were achieved.

J. Compos. Constr. 2013.17:239-248.

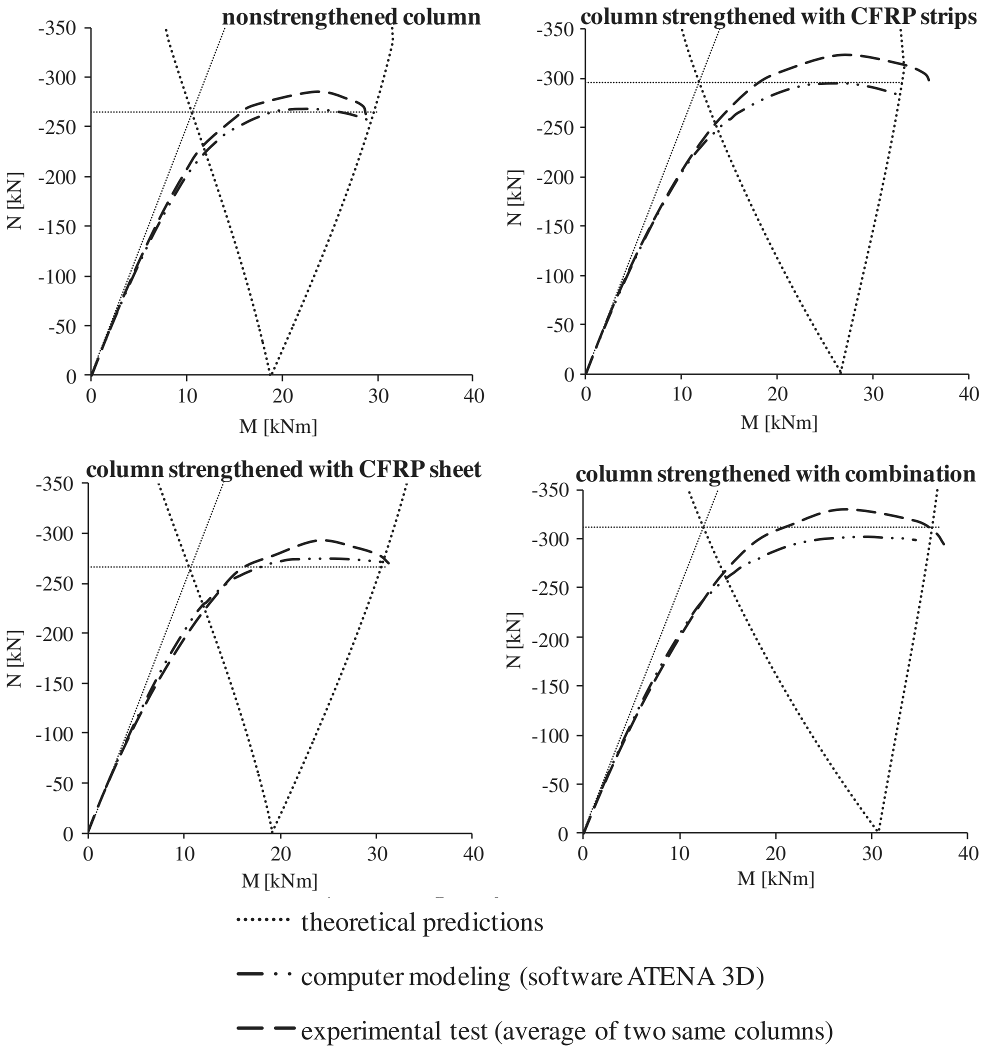

Fig. 13. Comparison of theoretical predictions, computer modeling, and experimental tests

Table 4. Slenderness Effect on Column Resistance in KiloNewtons

Column slenderness	Nonstrengthened column	Column strengthened with NSM CFRP strips	SE	Column strengthened with CFRP sheet	SE	Column strengthened with combination	SE
0	704	713	1	780	11	793	13
25	679	687	1	745	10	762	12
48	594	610	3	638	7	667	12
71	428	460	7	438	2	490	14
95	265	296	12	266	1	312	18
118	137	196	13	174	1	207	20

Note: SE = strength enhancement (%).

The slenderness is calculated as the length to concrete cross-section radius of inertia ratio, whereas the length is considered the length between the hinges.

Resistance of all four columns types decreases in more or less the same proportion with an increase in slenderness. The basic difference is in the increase in resistance for the different strengthening methods; the higher the slenderness, the higher the increase in resistance for columns strengthened with longitudinal NSM CFRP strips and vice-versa with respect to the smaller increase for confined columns.

Effect of Steel Reinforcement Ratio

Another parameter changed for a theoretical parametric study was the longitudinal steel reinforcement ratio. By changing the diameter of steel reinforcement in the range from 6, 8, 10, and 12 mm, the reinforcement ratios 0.0072, 0.0128, 0.0199, and 0.0287 were achieved. With a quadruple increase in reinforcement ratio (from 0.0072–0.0287), the final increase in column load-carrying capacity is reduced from 28 to 8.4%. This observation confirms the conclusions of Barros et al. (2008), that columns

J. Compos. Constr. 2013.17:239-248.

with a smaller conventional steel reinforcement have a larger load-carrying capacity increase than those with a higher reinforcement. The statement applies for both short and slender columns.

Conclusions

Two retrofitting methods, transverse CFRP sheet jacketing and a relatively new method of longitudinal NSM CFRP strips bonded into grooves in concrete cover for enhancing the load-carrying capacity of slender RC columns, were verified in this study. On the basis of the study presented herein, the following conclusions were drawn:

- Strengthening techniques using CFRP materials mounted at or near the column surface can be used to enhance resistance for both short and slender rectangular concrete columns without significant cross section enlargement.
- The effects of strengthening methods are different for short and slender columns as it is dependent on the different predominant type of stress. This can be seen from both experimental investigation and theoretical parametric study.
- Confinement effect of a transverse CFRP sheet is most active in the case of predominant compressive stress, which is assumed for short columns, and for this reason the confinement by a CFRP sheet has no significant effect on the increase of slender column resistance.
- Laminated NSM CFRP strips mounted longitudinally along the column axis act most efficiently in tension, which occurs at predominant bending of slender columns where second-order effects cause an increase in bending moment at the same value of the compressive force. Longitudinal NSM CFRP strips are more effective in slender column flexural resistance enhancement.
- The theoretical parametric study shows the slenderness value of approximately $\lambda = 50–60$ to be the threshold of effectiveness of the two strengthening methods referred in this paper.
- The most effective method to flexural capacity enhancement was experimentally demonstrated by a synergistic effect of NSM CFRP reinforcement ensured by CFRP sheet wrapping.
- Good correlation between experimental investigations, computer modeling, and theoretical modeling results confirms the possibility of short and slender columns strengthening design and verification in accordance with the previously noted analytical method.

Acknowledgments

The research described in this paper was developed within and with the support of research project VEGA No. 1/0306/09, *Application of Probabilistic Methods to Improve the Reliability of Concrete Structures*.

References

Barros, J. A. O., Varma, R. K., Sena-Cruz, J. M., and Azevedo, A. F. M. (2008). "Near surface mounted CFRP strips for the flexural strengthening of RC columns: Experimental and numerical research." *Eng. Struct.*, 30(12), 3412–3425.

Bournas, D. A., and Triantafillou, T. C. (2009). "Flexural strengthening of RC columns with NSM FRP or stainless steel." *ACI Struct. J.*, 106(4), 495–505.

Fitzwilliam, J., and Bisby, L. A. (2010). "Slenderness effects on circular CFRP confined reinforced concrete columns." *J. Compos. Constr.*, 14(3), 280–288.

Gajdosova, K. (2010). "Strengthening of slender reinforced concrete columns with the use of fibre reinforced polymers." Ph.D. thesis, Slovak Univ. of Technology, Bratislava, Slovakia.

Hollaway, L. C., and Teng, J. G. (2008). *Strengthening and rehabilitation of civil infrastructures using fibre-reinforced polymer (FRP) composites*, Woodhead Publishing, Cambridge, UK.

Mirmiran, A., Shahawy, M., and Beitleman, T. (2001). "Slenderness limit for hybrid FRP—Concrete columns." *J. Compos. Constr.*, 5(1), 26–34.

Olivova, K. (2007). "Concrete columns strengthening with carbon fiber strips and sheet." Ph.D. thesis, Slovak Univ. of Technology, Bratislava, Slovakia.

Pan, J. L., Xu, T., and Hu, Z. J. (2007). "Experimental investigation of load carrying capacity of the slender reinforced concrete column wrapped with FRP." *Constr. Build. Mater.*, 21(11), 1991–1996.

Tamuzs, V., Tepfers, R., Zile, E., and Valdmanis, V. (2007). "Stability of round concrete columns confined by composite wrappings." *Mechanics Compos. Mater.*, 43(5), 445–452.

Tao, Z., and Han, L. H. (2007). "Behaviour of fire-exposed concrete-filled steel tubular beam columns repaired with CFRP wraps." *Thin-Walled Struct.*, 45(1), 63–76.

Tao, Z., and Yu, Q. (2008). "Behaviour of CFRP-strengthened slender square RC columns." *Mag. Concrete Res.*, 60(7), 523–533.

Available online at www.sciencedirect.com

ScienceDirect

Procedia Engineering 65 (2013) 94 – 99

Procedia Engineering

www.elsevier.com/locate/procedia

Concrete and Concrete Structures 2013 Conference

Thermal and Strength analysis of foundation slabs, industrial floors and cement covers of road pavements in the early stages

Miroslav Ignačák[a]*, Július Šoltész[a], Ivan Prcúch

Department of Concrete Structures and Bridge, Slovak Technical University of Technology, Bratislava 81368 Radlinského 11, Slovakia

Abstract

Many factors play important role during concreting base slabs, industrial floors and concrete pavements. Often, there is a tendency to design the structure so that the crack does not arise or arise only with the limited crack width. The aim of this article is to present a thermodynamic numerical model. By using this model it is possible to calculate the development of temperature at any time and place of base slab, industrial floor or concrete pavement at the early stage. Then it is possible to investigate the risk of crack creation. The model works on the basis of the final element method and also by appropriate way takes into account the concrete formula, treatment and also climate impacts. Numerically acquired values by the former model are compared to experimental data measured on real buildings. An interesting fact of static task which is investigating cracks on concrete structures, is that an investigating is at an early stage is influenced especially by the composition of the concrete, climate impacts and method of treatment. Based on the former calculations it is possible to optimize the construction process from the point of view already mentioned impacts. Thus, the result can is economically designed structure which satisfies required quality parameters.

Keywords: foundation slabs; industrial floors;concrete pavements; hydration heat; climate impactsIntroduction

1. Introduction

Temperature and its course is the most significant load that influences the stress of a foundation slab in its early stage. In the process of concreting of thick foundation slabs, hydration heat released during the cement hydration

* Miroslav Ignačák. Tel.: 00421907867956.
E-mail address: miroslav.ignacak@gmail.com

1877-7058 © 2013 The Authors. Published by Elsevier Ltd.
Selection and peer-review under responsibility of University of Zilina, Faculty of Civil Engineering, Department of Structures and Bridges
doi:10.1016/j.proeng.2013.09.017

plays an important role. On the contrary, in more subtle constructions the course of temperature is influenced mainly by weather conditions. The aim of this article is to present a thermodynamic numerical model which might be used for complex analysis of the course of temperature at any time and place of the foundation slab in its early stage. The model works on the basis of the finite element method and at the same time appropriately takes into account the concrete composition, its curing and climatic influences. The values calculated numerically by the described model are compared with the data obtained experimentally on a real construction. An interesting part of this task is that in its early stages the static function, which analyses the occurrence of cracks in a concrete construction, is influenced by the composition of concrete, climatic impacts and method of curing.

2. Thermodynamic model TDM

The principle of calculation of the temperature in a concrete construction is based on the recognised differential equation describing a non-stationary thermal field in a general orthotropic body (1).

$$\frac{\partial}{\partial x}\left(\lambda_x \frac{\partial T}{\partial x}\right)+\frac{\partial}{\partial y}\left(\lambda_y \frac{\partial T}{\partial y}\right)+\frac{\partial}{\partial z}\left(\lambda_z \frac{\partial T}{\partial z}\right)+\bar{q}=\rho c \frac{\partial T}{\partial t} \tag{1}$$

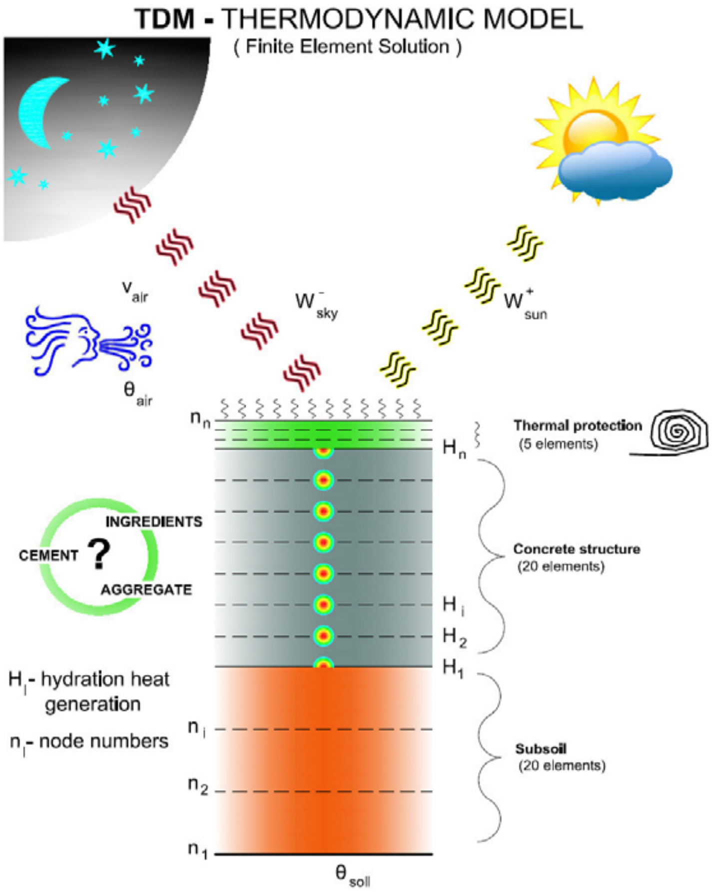

Fig. 1. TDM – thermodynamic model.

For the needs of analysis an algorithm working on the basis of the finite element method was deduced. This algorithm can be easily programmed and enables analysing the course of temperature of a concrete construction at any time and place considering the thickness of the construction. Hence, the algorithm is solving one-dimensional non-stationary thermal field with the internal and external heat resources. The calculation model consists of 45 finite elements (20 soil, 20 concrete, 5 thermal insulation). The complex calculation model is shown in figure 1.

The course of temperature in the early stages of concrete setting is influenced by a number of physical, technological and climatic factors. Their role in the occurrence of cracks changes in dependence on particular conditions. So, it is not possible to determine one factor as the most unfavourable, but at the same time it is not possible to make a general order of factors according to their impact on the course of temperature. The given algorithm solves the problem in a complex way and it is possible to analyse the impact of the parameter itself for a particular construction under particular conditions.

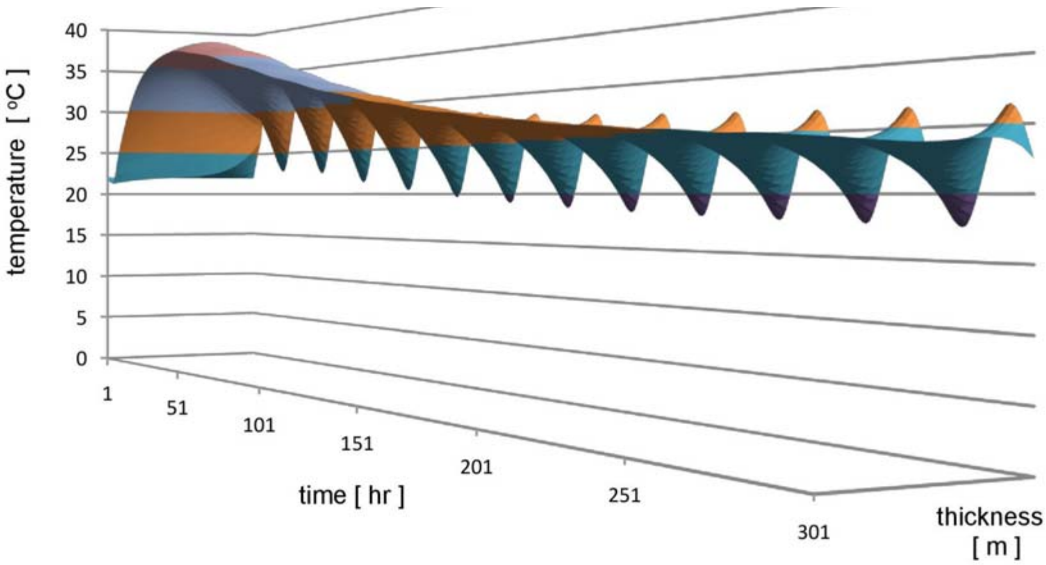

Fig. 2. Course of temperature in the selected foundation slab - thickness 500 mm.

In this case the algorithm on the basis of **finite elements** was programmed in Excel. The time integration itself proceeds by the **step by step** method and the time steps are optional. An optimum choice of the step is 3,600 seconds (1 hour), however, a sufficient accuracy of the calculation can be achieved in the period of the time step of 10,800 seconds (3 hours). In this case the number of calculation steps is 300, but the calculation can be simply extended if necessary. In figure 2 we can see the output showing the course of temperature in the early stage for the selected foundation slab with the thickness of 500 mm under selected conditions and concrete formula.

3. Strength analysis

If the tensile stress exceeds the actual tensile strength of the concrete, cracks appear [1]. In terms of time we distinguish (fig. 3):

early cracks, which occur in the first hours, days after casting the concrete due to concrete cooling, when the maximum temperature from the hydration heat was reached,

late cracks, which occur or get wider after the construction was loaded directly and/or during the first winter after concreting.

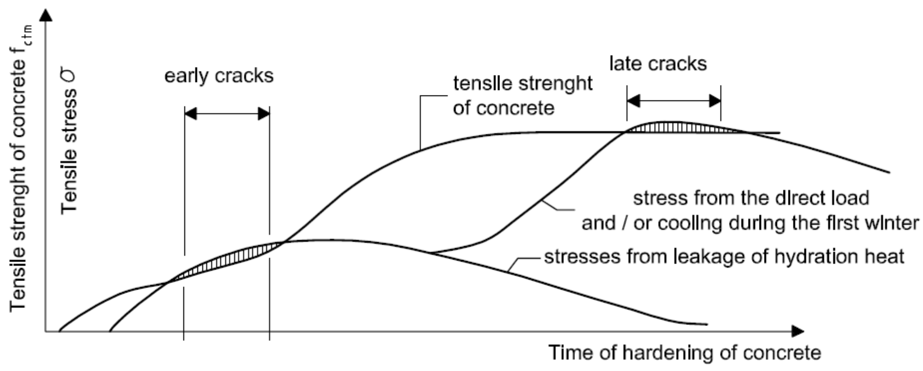

Fig. 3. Schematic illustration of the development of tensile strength of concrete and tensile stress by forced deformation [1].

Primary factors that have impact on tension in the construction in the early stage are the course of temperature, autogenous shrinkage and shrinkage as a result of drying. It is possible to set values of relativede formation by shrinkage according to several formulas; in this case method in accordance with [1] was used. The relative deformation by temperature is adopted from the thermal analysis of the construction shown above.

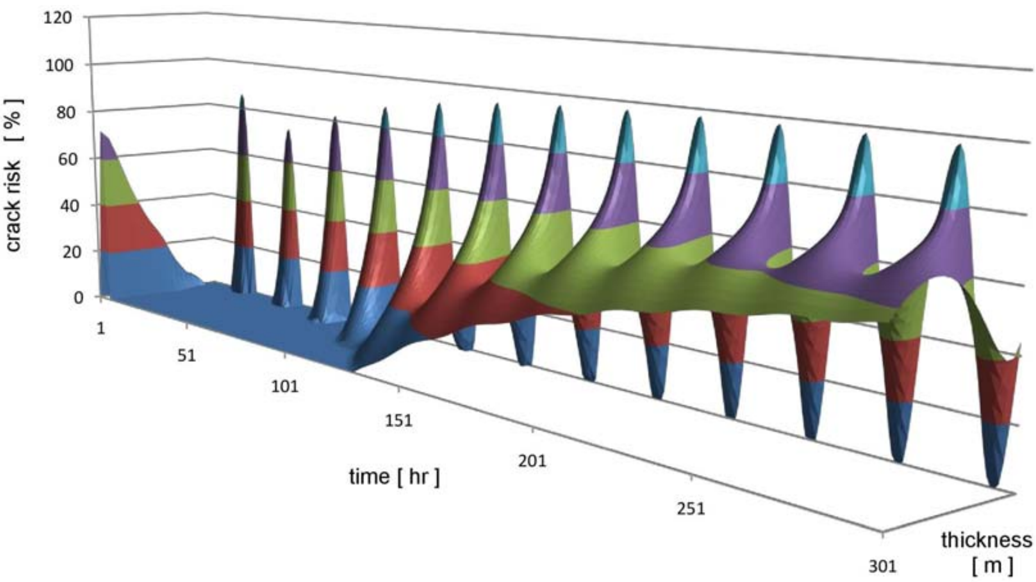

Fig. 4. Risks of occurrence of cracks in the selected foundation slab with a thickness of 500 mm.

In figure 4 we show the result of static analysis of the construction in the early stage of forced deformations. The figure illustrates the risk of occurrence of cracks at any time and level of the concrete construction. At the same time the notion of the risk of occurrence of cracks [%] represents the ratio between the created tensile stress and actual value of tensile strength of concrete (**$\sigma_t/f_{ctm(t)}$**). From a mathematical point of view the strength analysis of the construction in the early stages is relatively complicated and one of the most important inputs for its calculation is an appropriately selected rheological model, realistic load of temperature and shrinkage and also the correct calculation of concrete strength in the time and level of the concrete construction. In this case the load step will last

3,600 seconds (1 hour) and the number of calculation steps is 300, which leads to areshaping matrix of dimension 300 x 300 members for each concrete element. With the aid of Arrhenius' law the tensile strength in time was calculated. It takes into account the real measured course of temperature and the type of utilized cement, which, together with the actual humidity, are the main factors influencing the actual maturity of concrete. Again we do the whole calculation by the step by step method, which enables us to avoid practically impossible integration. All the mentioned parameters are always a function of time and space in the construction (independently for each finite element).

4. Experiment

The goal of the experiment is to measure the course of temperature caused by hydration heat and other factors having impact on the magnitude of the thermal load in the early stage of concrete setting in real concrete constructions. At the same time there was an attempt to measure most factors that can influence the magnitude of the thermal load and the following occurrence of cracks in the early stage. During the concreting and the early stage of concrete setting the course of temperature at any level of the element was monitored and at the same time the weather impacts were measured. The temperatures were measured in the foundation and ceiling slabs (i.e. horizontal slab constructions) to simulate one-dimensional thermal flow.

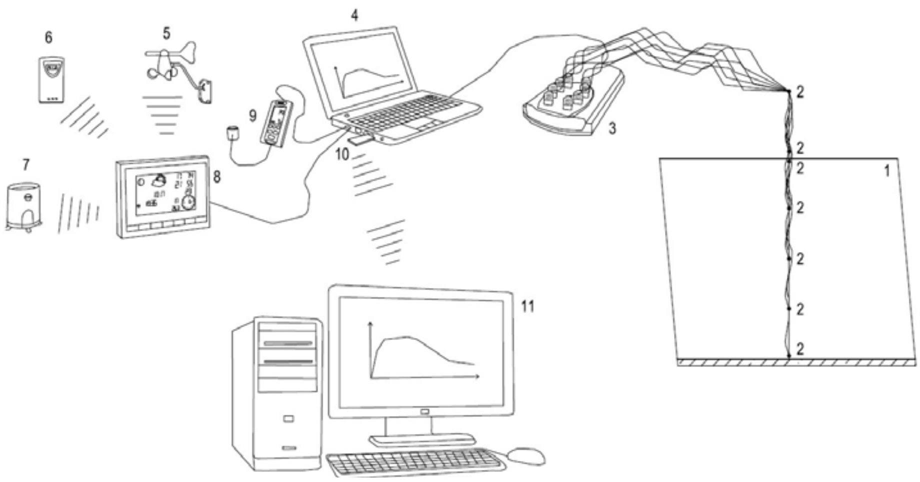

Fig. 5. Schemeofconnection: 1-concreteconstruction, 2-thermal element, 3-data-logger, 4-mini-laptop, 5-anemometer, 6-thermometer+humidity meter, 7-rain gauge, 8-meteo-station, 9-solar-meter, 10-modem, 11- centralcomputer.

The temperature along the height of the element was measured at several levels with the aim to determine the course and development of temperatures as accurately as possible. Thermal elements (type K) and a data-logger (Pico T-08) connected to a computer were used to measure the temperature. The temperatures in individual measured points were automatically read every hour within the period of 5-7 days in dependence on the thickness of the element. Due to this continual measuring and data registering it was possible to measure not only the maximum temperature of the element, but also the course of temperatures at individual levels and time, to verify the above shown numerical model (TDM).

A professional meteorological station TFA-SINUS and solar-meter KIMO SL-200 were used to measure the weather effects, as they have a substantial impact on the course of temperatures in a concrete construction.

5. Conclusion

Compositions of concrete, technological and climatic conditions are the decisive factors that have impact on the course of temperatures in the concrete construction. The results of experimental measurements of the course of temperatures in 5 levels of the element showed a relatively good conformity with the values calculated numerically with the aid of **TDM**. The article presents a possible approach to dimensioning of foundation slabs on which we impose higherstresses from the point of view of marginal state of usability, such as foundation slabs of watertight concrete structures with the strictest criteria (usage class A [1]). It is possible to analyse cement-concrete road decks in a similar way, as well as industrial floors where cracks are undesirable. As it is shown above, we can also analyse other types of constructions, such as walls, floor slabs, etc., if we adjust boundary conditions. In case cracks of limited width are allowed in the mentioned constructions, it is possible to minimise the magnitude of forced relative deformation objectively with the aid of **TDM**.

On the basis of the mentioned calculations it is possible to optimise the process of design and completing the construction in terms of composition of concrete, temperature of fresh concrete, appropriate timing of concreting, curing and thermal protection of the construction, so that the construction is designed economically meeting required qualitative parameters.

Acknowledgements

This article was created with the support of the research project VEGA No.1/0306/09 “Application of probability methods for renovation of the reliability of concrete constructions”.

References

[1] J. Bilčík, P. Čičmanec, I. Halaša, Smernica pre vodonepriepustné konštrukcie „Biele vane“. Bratislava, 2011.

[2] G. Lohmeyer, K. Ebeling, WeisseWannen – Einfach und sichter. VerlagBau+technik, März 2004, 340 p.

[3] DIN 1045-2 TragwerkeausBeton, Stahlbeton und Spannbeton – Teil 2: Beton-Festlegung, Eigenschaften, Herstellung uKonformität, Anwendungsregelnzu DIN EN 206-1, 2005.

[4] V. Červenka, L. Jendele, J. Červenka, Atena program documentation – Atena Theory, Červenka Consulting Ltd, Praha, 2012.

[5] T. Apel, T. Flaig, Simulation and mathematical optimalization of the hydration of concrete for avoiding thermal cracks, Munchen, Germany, 2009, 15 p.

[6] J. Lienhard, Aheat transfer textbook, Cambridge, Massachusetts, 2012, 755 p.

[7] J. Nečas,Vliv vnejš íteploty na napjatost přehrad a jiných betonových masivu, Aplikace matematiky, Institute of mathematics AS CR, 1956, Czech republic 118 p.

Available online at www.sciencedirect.com

ScienceDirect

ELSEVIER

Procedia Engineering 65 (2013) 248 – 253

Procedia Engineering

www.elsevier.com/locate/procedia

Concrete and Concrete Structures 2013 Conference

Effect of Reinforcement Corrosion on Bond Behaviour

Juraj Bilcik[a,*], Ivan Holly [a]

[a] *Slovak University of Technology,Radlinskeho 11, 813 68 Bratislava, Slovakia*

Abstract

One of the major degradation processes of reinforced concrete structures is the corrosion of the steel reinforcement. The main reason associated with the deterioration of reinforced concrete due to reinforcement corrosion is not the reduction in mechanical strength of the reinforcing bar itself, but rather than that the pressure exerted from the expansion of the corrosion products. This may result in damage of the structures due to expansion, cracking and eventually spalling of the concrete cover. In addition to this, the damage of construction may be caused by loss of bond between reinforcement and concrete and loss of reinforcement cross-sectional area. The paper introduces effect of corrosion to bond between reinforcement and concrete.

Keywords: reinforcement corrosion; deterioration models; cracking; spalling; bond reduction;

1. Introduction

Design of concrete structures is currently focused especially on the effects of direct actions. Increasingly the consequences of indirect, accidental and environmental actions are manifesting. Long term exposure to environmental actions (chemical, biological and physical effects of the environment), causes deterioration of concrete and reinforcement. When considering the reliability of structures all types of actions should be taken into account. This holistic approach to the design and verification of structures shall be applied to all constructions,

* Tel.:+421 259 274 546; fax: +421 252 926 213.
E-mail address: juraj.bilcik@stuba.sk.

1877-7058 © 2013 The Authors. Published by Elsevier Ltd.
Selection and peer-review under responsibility of University of Zilina, Faculty of Civil Engineering, Department of Structures and Bridges
doi:10.1016/j.proeng.2013.09.038

especially civil engineering works, because of their large ratio between the area exposed to the surrounding environment and cross-section dimensions as well as longer design life.

One of the most predominant factors responsible for the structural deterioration in concrete structures is identified as a corrosion of reinforcement, which may result in damage of the structures in the form of expansion, cracking and eventually spalling of the concrete cover. In addition to this, the structural damage may be caused by loss of bond between reinforcement and concrete and loss of reinforcement cross-sectional area; sometimes to the extent that the structural failure becomes inevitable [1]. While much research effort has been devoted to researching the causes and mechanisms of reinforcement corrosion, relatively little attention has been devoted to the problem of assessing the residual reliability with respect to cracking and spalling of concrete cover associated with reduction in bond strength. The bond between the reinforcement and the concrete is one of the most essential properties contributing to the successful functioning of the reinforced concrete system.

Nomenclature

α	rib inclination	i_{corr}	corrosion rate
β	rib face angle	$P(t)$	corrosion penetration depth
c	concrete cover	Q_{cr}	critical mass of corrosion products
d	diameter of reinforcing bars	s	bar clear distance
f_b	bond strength	t_{cr}	time to cracking
f_r	relative rib area		

2. Environmental effects

A number of technological parameters have an influence on bond behavior. As for the environmental effects, the most typical are: rust, steel corrosion, high-temperature bond decay and low-temperature bond improvement.

Rusting of concrete reinforcing bars on open storage is a common phenomenon and it is difficult to keep the rebars in as rolled (un rusted) condition at or en route to the construction sites. Further the rebar production technology also has its own characteristic effect on the rebar surface and micro-structure, causing variation in rusting behavior of the product [2]. Initial bar rusting owing to steel exposure to the environment as it cools down from the rolling temperature or to atmospheric conditions consists of a thin coating of iron oxide, which does not impair bond properties, but may even improve bond behavior with respect to newly-rolled bars, see Fig 1.

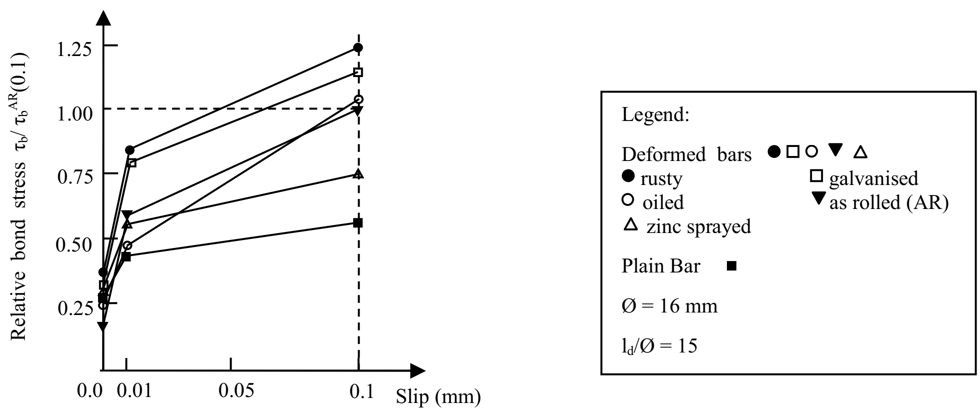

Fig. 1. Effect of various surface conditions on bond stress/slip response in pull-out test [4]

As for the reduction in bar diameter, the value often found in the literature range from 0.008 to 0.04 mm, with a section loss of up to 1 % in the smaller-size bars, compared to the widely-accepted tolerance of 6-10 % in most product standards. In summary, the results show that:

- bond strength is generally helped by the presence of residual rust, possibly up the point where the dimen-sions of the ribs become critical,
- the presence of rust may inhibit further steel corrosion in good concrete,
- the effect of loss of section is too small to be significant, as it is well within the size tolerances [3].

Gases (e.g., oxygen, carbon dioxide) and chloride ions can penetrate concrete, and - once the steel reinforcement is reached – these ions destabilize the film of iron oxide, which protects the bars again corrosion. As a result, an increasing loss of steel cross-sectional area and a weakening of the bar-concrete bond occur, owing to the build-up of the corrosion products at the interface, as well as to cover splitting and spalling [3].

3. Deterioration models

The service life of a reinforced concrete structure is modelled as an initiation and the propagation period of reinforcement corrosion, consequences of reinforcement corrosion and finally serviceability and structural failures, see Fig. 2. Corrosion may be initiated if the concrete around the reinforcement is carbonated and/or if chlorides reach the reinforcement. Depassivation, small reinforcement cross section reduction and cracking represent events related to the serviceability, while excessive loss of steel cross section, spalling and bond reduction represent events related to the structural failures.

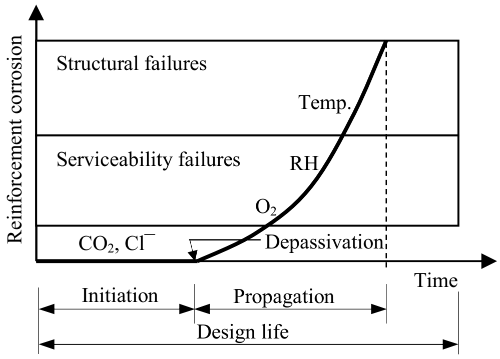

Fig. 2. Deterioration model of service life due to the reinforcement corrosion [5]

3.1. Deterioration model - cracking

It is well known that corrosion of reinforcement results in the transformation of metallic iron to the corrosion products due to the process of oxidation resulting in an increase in volume which, depending on the level of oxidation, may be up to about 6.5 times the original iron volume, see Fig. 3a) [6]. Volume increase associated with the transformation can cause cracking, spalling, and delamination of the concrete (Fig. 3b).

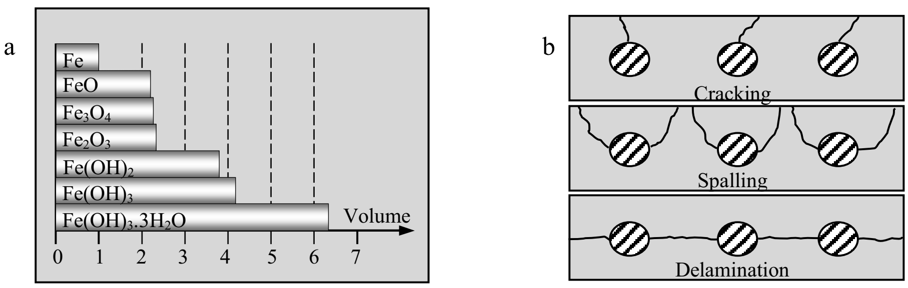

Fig. 3. (a) Oxidation states of iron; (b) representations of visible forms of corrosion [7]

The oxides generated during active corrosion of rebars induce a pressure on the surrounding concrete, wich in most cases leads to cover cracking along the rebar. These longitudinal cracks may affect the load-carrying capacity of the structural elements presenting this distress, and in consequence, may shorten their service life, in addition to opening a path for a quicker arrival of aggressive elements to the reinforcement [6]. Based on field and laboratory data, the empirical equations suggested by Morinaga can be used for predicting the time to cracking. It is assumed that cracking of concrete will first occur when there is a certain quantity of corrosion products forming on the reinforcement. The time for cracking to take place is given by:

$$t_{cr} = \frac{Q_{cr}}{i_{corr}} \quad (1) \qquad Q_{cr} = 0{,}602d\left(1+\frac{2c}{d}\right)^{0{,}85} \quad (2)$$

where Q_{cr} is the critical mass of corrosion products (10^{-4}g/cm^2); c is the cover to the reinforcement (mm); d is the diameter of reinforcing bars (mm); i_{corr} is the corrosion rate (g/day), t_{cr} is the time to cracking (days) [8].

Assuming a generalized corrosion, it may be stated, that for c/d ratios > 2, radius losses of around 50 µm induce crack widths of about 0.05 mm, while for c/d ratios < 2, only attack penetrations of 15-30 µm are necessary. For c/d ratios > 2 crack widths of 0.3 mm appear for radius losses of about 100-200 µm, and of 1 mm for about 300 µm. For larger crack widths, the scatter is very high as the oxides diffuse out of the concrete and the pressure decreases significantly [9].

3.2. Deterioration model - spalling

Du et al. [10] investigated effect of the bar diameter, bar clear distance and concrete cover onto cracking and spalling of concrete beams due to steel corrosion. Fig. 4a) indicate that the bar clear distance dominates the corrosion for the spalling of concrete cover. The radial expansion required for internal penetration increases almost linearly with the ratio s/c of bar clear distance to concrete cover, irrespective of whether the concrete cover was 10 mm, 25 mm or 35 mm. In other words, the smaller is the bar clear distance in term of the ratio s/c, the less is the radial expansion required to cause internal penetration and, therefore, the earlier the spalling of concrete cover would occur.

a

b

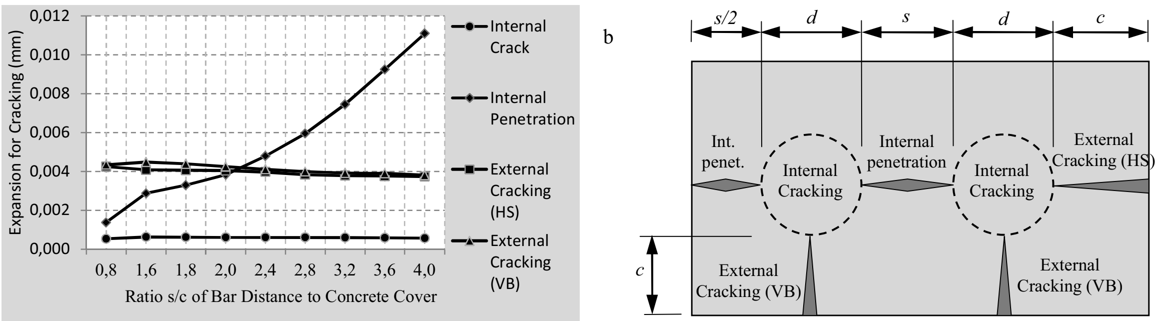

Fig. 4. (a) Effect of bar clear distance on beam cracking for d = 20 mm and c = 25 mm; (b) dominant parameters of concrete beam [10]

Du et al. [10] found, that for the design of a new structure that may suffer from steel corrosion during its service life, in addition to a proper selection of concrete cover to satisfy the requirements in EN1992-1-1, it would be preferable for bar clear distance to be greater than 2.2 times the concrete cover in order that, if corrosion were to occur, corrosion cracks would be seen externally at an early stage of the corrosion process. EN1992-1-1 does not consider the implications for durability of bar spacing and clear distance. The FE analytical results validated against experimental observation, give a very important indicator for the durability design of concrete structures and assessment of existing deteriorated structures. For the assessment and management of existing corroded structures, an engineer should be aware of possible internal penetration where bar clear distance is less than 2.2 times the concrete cover, and bear in mind that an undamaged concrete surface of a structure does not necessarily mean that the structure is in a healthy state without steel corrosion. In summary, the FE analytical results reported in this paper provide engineers with some supplementary information for durability design and assessment of concrete structures.

3.3. Deterioration model - bond reduction

Bond is necessary to anchor reinforcement and to ensure composite interaction between reinforcement and concrete. The reduction in confinement on cracking of the cover will lead to a progressive reduction in bond strength. Magnitudes of the bond strengths reported and the effect of corrosion on those bond strengths differ widely. Despite wide variations in test specimens and in conditioning techniques, the general reported trends are the same in almost all studies, as illustrated in Fig. 3.

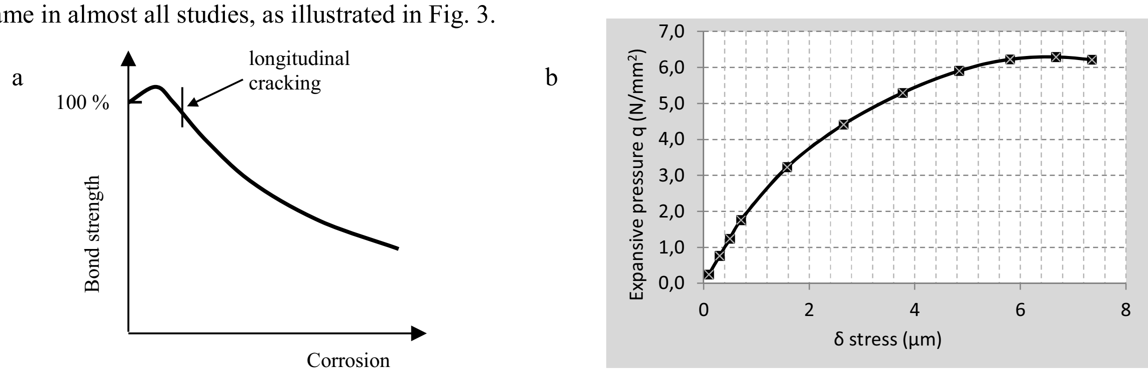

Fig. 5. (a) Variation in bond strength with corrosion [5]; (b) expansive presure on steel-concrete interface due corrosion products [6]

The variation of the bond strength with an initial small increase of bond strength for low level of corrosion followed by an appreciable reduction (even over 50 %), particularly if no confining reinforcement is present; the tendency to a more brittle bond behaviour due to splitting failure and, in several cases, the reduction on bond stiffness [11]. The initial increase has been attributed to the expansive nature of iron oxides, while the subsequent decrease is related to the build-up of a soft layer of loose corrosion products at the bar-concrete interface. However, with further corrosion the bond stress declines consistently until it becomes negligible for about 8.5, 7.5, and 6.5 % corrosion for the 10, 14, and 20 mm bars, respectively. The significant degradation of bar ribs and reduction of cross-sectional area, as well as a heavy layer of corroded material adhering to the concrete at these corrosion levels contribute to the significant decline in bond stress (e.g., loss of mechanical interlocking between ribs and deterioration of concrete, and influence of lubricating effect of flaky corroded material between bars and concrete) [7].

Studies conducted by Auyeeun have confirmed that the loss of bond strength for unconfined reinforcement is much more critical than bar section area loss; that is, a low diameter loss could lead to 80 % bond reduction. Study also showed that confinement provides excellent means to counteract the bond loss.

If the ratio ρ_{tr} of the transverse reinforcement area at anchorage length (considering the reduction due to corrosion) versus the area of the main bars is higher than 0.25 (minimum value established in EC2), the bond strength f_b (in N/mm²) can be predicted as follows [5]:

$$f_b = 4.75 - 4.64P(t) \tag{3}$$

where *P(t)* = corrosion penetration depth (bar radius reduction). This proposal gives bond strength values for each attack penetration, taking account the actual residual stirrup section at the anchorage length.

Chairns [3] developed the emipirical expresion (4). It has been assumed, that only relative rib area is affected by corrosion, and all other parameters are unchanged. Rib face angle and rib inclination have been taken as 45°and 60° respectively. Corrosion is assumed to reduce rib height by amound equal to the thickness of the oxide layer

$$f_b = 1.15 f_r + 0.039\beta + 0.007\alpha \tag{4}$$

where f_b – ultimate bond strength (N/mm^2); f_r - relative rib area (-); β – rib face angle (°); α – rib inclination (°)

Amleh and Ghosh [12] examined the basic influence of corrosion on bond at the steel-concrete interface and the associated split and cracking. The results show that, up to about 5 % mass loss, the bond capacity loss is moderate, at 10 to 15 % mass loss, there is a significant loss in the bond capacity, and at about 20 % mass loss, almost of the bond capacity is lost.

Conclusions.

The exposure environment has been found to have a large influence on the reliability of concrete structures, especially for civil infrastructure, because of their extended service life and great area exposed to the surrounding environment. The paper introduces the effect of different degrees of reinforcement corrosion on the bond degradation. The proposed model can serve as a useful tool for engineers in decision-making regarding the maintenance and repairs of corrosion affected reinforced concrete structures.

Acknowledgements

The financial supports of the Scientific Grant Agency of the Ministry of Education, science, research and sport of the Slovak Republic via Grant No. 1/0784/12 are greatly acknowledged.

References

[1] P.K. Mehta & P.J.M. Monteiro, Concrete Microstructure. Properties and Materials. 1st edit., Indian Concrete Institute, Chennai, 1997.
[2] T. Mehmood, at al., Atmospheric Rusting of Rebars and its Effects on Reinforced Concrete Corrosion. In: CORROSION, NACE International Conference, San Diego Ca, March 22.-27.
[3] fib Bulletin 10: Bond of reinforcement in concrete. August 2000.
[4] E. Morgan, The effect of rust on reinforcement, Concrete (1), 1998, pp. 25-27.
[5] J. Bilcik, I. Holly, Design of concrete structures for durability, 3rd International Symposium on Life-Cycle Civil Engineering, IALCCE 2012; Vienna; Austria; 3-6 October 2012.
[6] X. Zhao, J. Yu, W. Jin, Damage analysis and cracking model of reinforced concrete structures with rebar corrosion, Corrosion Science (53), 2011, pp. 3388–3397.
[7] U.S. Nuclear Regulatory Commission: Primer on Durability of Nuclear Power Plant Reinforced Concrete Structures - A Review of Pertinent Factors, February 2007.
[8] Y. Liu, Modeling the Time-to-Corrosion Cracking of the Cover Concrete in Chloride Contaminated Reinforced Concrete Structures, PhD. thesis, Faculty of the Virginia Polytechnic Institute, State University.
[9] C. Alonso, C. Andrade, J. Rodriguez & J.M. Diez, 1998. Factors controlling cracking of concrete affected by reinforcement corrosion. Materials and Structures, Vol. 31, August-September 1998: pp. 435-441.
[10] Y.G. Du, A.H.C. Chan, L.A. Clark, X.T. Wang, F. Gurkalo, S. Bartos, Finite element analysis of cracking and delamination of concrete beam due to steel corrosion. Engineering Structures (56), 2013, pp. 8–21.
[11] L. Berto, P. Simioni, A. Saetta, Numerical modelling of bond behaviour in RC structures affected by reinforcement corrosion. Engineering Structures Vol. 30, 2008, pp. 1375–1385.
[12] A.T. Joyce, 2012. The effects of steel reinforcement corrosion on the flexural capacity and stiffness of reinforced concrete beams. PhD thesis, Ryerson University, Toronto, Canada.

ELSEVIER

Available online at www.sciencedirect.com
SciVerse ScienceDirect

Procedia Engineering 00 (2013) 000–000

Engineering Procedia
www.elsevier.com/locate/procedia

Concrete and Concrete Structures 2013

The effect of curing conditions (in situ vs. laboratory) on compressive strength development of high strength concrete

Peter Paulík*

Slovak University of Technology, Bratislava, Slovakia

Abstract

During the construction of the bridge near Štrba village, concrete was needed to achieve the cube strength of 35 N/mm^2 after 48 hours to allow the prestressing works. However, the question remained how to practically verify the real strength achieved in the structure after such a short time. Whereas the specimens were cured in accordance with valid standards at 20 °C in water, it was doubtful whether the real strength of the concrete structure, which is hardening at ambient temperatures around 2 °C, corresponds to these measured strengths. It was questionable how to cure the specimens to get as close to the real strengths as possible.

Keywords: concrete, curing conditions, strength development

1. Introduction

Bridge near Štrba village, constructed by the incremental launching technology, reached a length of 600 meters [1]. In 2005 it was the first concrete bridge built by this technology in Slovakia. Using this construction method the bridge is built on one side of the valley and pulled above it by hydraulic jacks. This technology allows a fast construction where one 20 meters long segment of the bridge is completed in 7 days. However, this construction speed places high demands on concrete, especially on its fast strength development. To allow the prestressing works the designer required to reach the compressive strength of 35 N/mm^2, which is quite a common requirement in concrete bridge engineering. But, on the other hand, the construction speed required reaching this strength on construction site in less than 48 hours. To meet both of these requirements, it was necessary to develop a suitable concrete mix. After several trials the final mix proportions, given in Table 1, were found.

* Peter Paulík. Tel.: +421903585663; fax: +421252926213
E-mail address: peter.paulik@stuba.sk

Table 1. Concrete mix proportions

		Weight (kg)
Gravel	- fraction 0/1	100
	- fraction 1/4	730
	- fraction 4/8	180
	- fraction 8/16	700
CEM I 42.5 R		490
Water		149
Super plasticizer admixture		4.8
Air entraining agent		0.5

This concrete formula met the requirements of workability, strength development and also the requirement of frost resistance. Compressive strength of this concrete, measured on standard cubes cured at 20 °C, reached more than 35 N/mm^2 in 48 hours and more than 75 N/mm^2 in 28-days. And although the concrete grade specified in the bridge project was C 35/45, due to the requirement of fast strength development, the final concrete mix met the conditions for classification as a high-strength concrete (according to [5]).
Climatic conditions near Štrba village also required to perform the concrete casting works at temperatures ranging around 2 – 5 °C. Concrete elements cast at these temperatures were covered by thermal curing blanket few hours after the casting.

The compressive strength of concrete was tested on standard cubes with edges of 150 mm, cured in accordance with EN 12390-2 [6]. Since, according to this standard, specimens were stored at 20 °C in water, the question was whether the concrete in real structure, hardening at ambient temperatures around 2 °C, reaches the same strength. Because of the uncertainty of the real strength of the concrete in the structure, project supervisor requested to store the specimens also at ambient temperatures (2-5 °C). These specimens served then as the reference ones and the prestressing works were allowed only if the compressive strength measured on them fulfilled the strength requirements. Even though this conservative solution was safe, it significantly slowed down the construction process (these specimens sometimes needed more than 7 days, instead of 2 days, to reach the prescribed strength). On the other hand, even though these specimens were cured at the same ambient temperatures as the concrete in the structure, specimens had significantly smaller volume than the casted concrete section. Thus the strength of concrete in the structure could reach the prescribed strength faster because of the different heat development in mass concrete [2]. Considering this fact the real strengths of concrete in the structure were uncertain and the conservative solution prescribed by the project supervisor was not acceptable from the speed of construction point of view.

Non-destructive testing of the concrete (Schmidt hammer) was abandoned because of the considerable variations between strengths measured by this non-destructive equipment on construction site and between the strengths measured on cube specimens in laboratory.

The task was to find such curing conditions for the cube specimens, which would ensure, that the strength measured on them after 2 days would represent the real strengths of the concrete in the structure hardening at low ambient temperatures.

2. Experimental investigation

The effect of curing conditions on the strength development of concrete has been described in many scientific papers and monographs [2], [3], [4], [7], [8]. Taking them into consideration it was clear that the curing conditions could significantly affect the strength of concrete not only after 2 days of hardening, but also after 28 days. However, from the bridge construction point of view the early age strengths of the concrete were the most important.

To investigate how the curing conditions affect the strength development of the concrete, in the first phase 45 experimental cube specimens, with the edge of 150 mm, were casted. Specimens were then subsequently divided into 5 groups with different curing regimes (Tab. 2).

Table 2. Curing regimes of the specimens

	Curing conditions	Number of specimens
Series A	cured in water at 20 °C (±1 °C)	9
Series B	sealed and cured at 20 °C (±1 °C)	9
Series C	cured on air at 20 °C (±1 °C)	9
Series D	cured on air at 2 °C (±2 °C), covered	9
Series E	cured on air at 2 °C, (±2 °C), uncovered	9

Compressive strength tests were performed after 2, 7 and 28 days of hardening. The results are shown in Table 3 (each result is the average of 3 measurements).

Table 3. Compressive strength and density of the specimens after 2, 7 and 28 days

	2 days		7 days		28 days	
	density [g/dm^3]	strength [N/mm^2]	density [g/dm^3]	strength [N/mm^2]	density [g/dm^3]	strength [N/mm^2]
Series A	2344	41.8	2358	63.4	2339	81.5
Series B	2337	41.0	2355	58.3	2332	71.8
Series C	2328	39.2	2316	61.4	2317	68.4
Series D	2300	16.1	2344	45.2	2348	66.1
Series E	2308	13.4	2318	40.5	2362	67.3

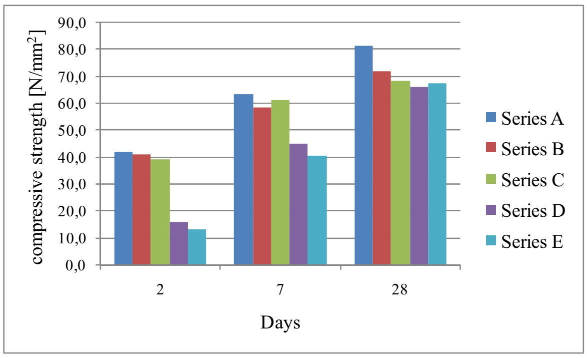

Fig. 1 Measured compressive strengths after 2, 7 and 28 days

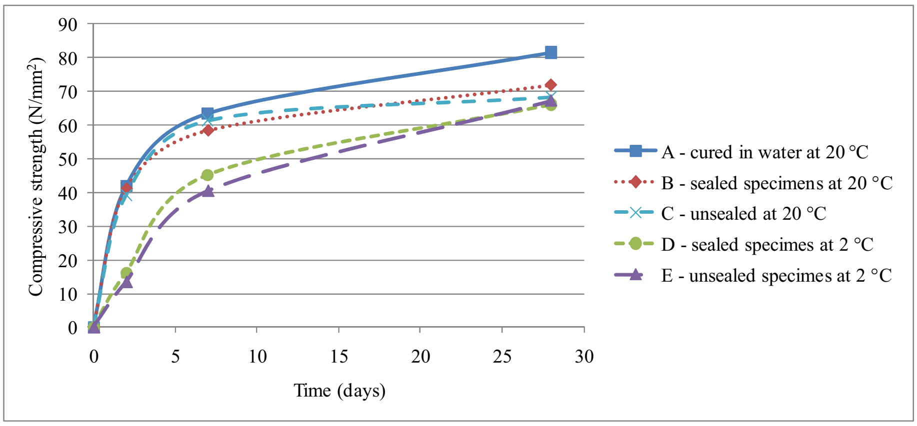

Fig. 2 Compressive strength development of concrete specimens with different curing regimes

The results show that the curing regime has a significant effect on the compressive strength of the specimens especially in early stages of hardening, which were the most important ones. It was clear, that the 2-days compressive strengths of the specimens were most affected by the ambient temperature.

Even though the ambient temperature significantly affected the compressive strengths of the specimens, it was still not clear how much does this temperature affect the compressive strength of the concrete in the structure. Concrete in the casted element has a significantly higher volume than the volume of concrete in the specimen and this could lead to different strengths [2]. One of the reasons is the fact that the initial temperature of the concrete, which was about 10 °C, tends to persist longer in mass concrete (a small specimen tends to cool down relatively quickly to the ambient temperature). Therefore in mass concrete the hydration in the early stages takes place at a higher temperature and progress more rapidly than in the very small volume of the test specimen. Larger volume also produces more heat that accumulates. This internal heat then contributes again to a faster increase in strength of the concrete element when compared with the small specimen cured at the same ambient temperatures [2], [3].

To point out these non-negligible effects of initial temperature and produced hydration heat on strength development, following simple experimental investigation has been performed.

Experimental investigation was focused only on the upper deck of the bridge because it was always casted 2 days later than the rest of the segment and therefore it had less time to harden. Concrete was needed to achieve the prescribed strength in the whole segment and therefore the concrete strength of the upper deck was decisive. For the purpose of the experimental segment the average thickness of the upper deck (320 mm) has been computed from the real thickness, which was ranging from 200 mm to 500 mm (Fig. 3).

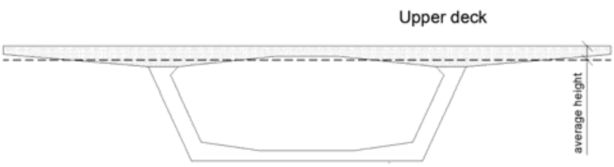

Fig. 3. Scheme of the cross section of the bridge

Fig. 4. Photo of the bridge during the launching process

In the second phase 27 experimental cube specimens, with the edge of 150 mm were casted and they were then subsequently divided into 5 groups with different curing regimes (Tab. 4).

Table 4. Curing regimes of the specimens

	Curing conditions	Number of specimens
Series K	cured in water at 20 °C (±1 °C)	6
Series L	cured on air at 20 °C (±1 °C)	6
Series M	cured on air at 1 °C (±2 °C), uncovered	6
Series N	cured on air at 1 °C (±2 °C), covered	6
Series Z	In concrete segment air temperature 1 °C, (±2 °C)	3

First 24 hours, before demoulding, the specimens of the K-series were stored in laboratory at 20 °C. After demoulding they were stored in water at 20 °C (± 1 °C). Specimens of the L series were stored on air at 20 °C (± 1 °C). They were demoulded after 48 hours. Specimens of the M and N series were stored first 48 hours at ambient temperatures 1 °C (±2 °C, max. at 13:00 = +2 °C, min. at 7:00 = -1 °C). After 48 hours they were demoulded and stored on air at regulated temperature 2 °C (±2 °C). Immediately after casting, specimens of the Z-series were put in the experimental segment, which was stored at ambient temperature 1 °C (±2 °C, max. at 13:00 = +2 °C, min. at 7:00 = -1 °C) for 48 hours (Fig. 5 and 6).

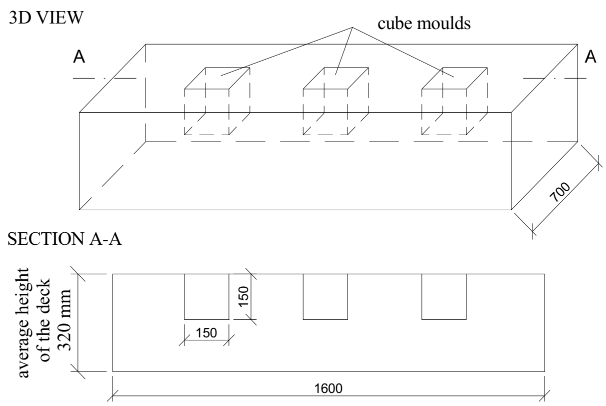

Fig.. 5 Scheme of the expermental segment

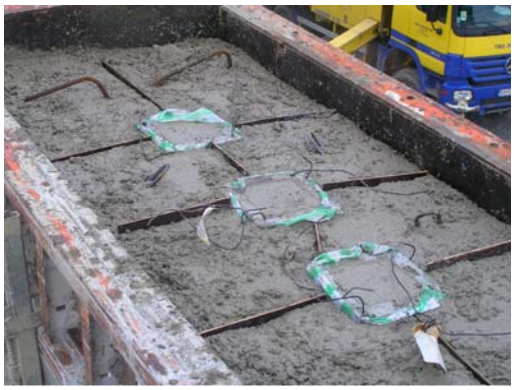

Fig. 6 Experimental segment on construction site

The experimental segment has been 1.6 meters long, 0.7 meters wide and 0.32 meters high. Its height corresponded to the average thickness of the upper deck of the bridge. Cube specimens in plastic moulds were put in their position immediately after the segment has been casted (Fig. 4, and 5). Plastic moulds were provided from the outside by grace and plastic bag to make them easy to pull out from the segment after 48 hours of hardening. Experimental segment and the upper deck were casted at the same time and they were also covered by thermal curing blanket at the same time. Thus their curing regime was almost the same. By this means the experimental cube specimens of the Z series hardened in the mass concrete heated by the ongoing hydration. After 48 hours the plastic moulds were pull out from the segment and the cube specimens were tested. Results were then compared with other specimens hardening at different curing regimes and they were summarized in Table 5 (each result is the average of 3 measurements).

Table 5. Compressive strength and density of the specimens after 2 and 28 days

	2 days		28 days	
	density [g/dm^3]	strength [N/mm^2]	density [g/dm^3]	strength [N/mm^2]
Series K	2325	34.9	2319	77.2
Series L	2297	33.9	2300	72.1
Series M	2307	13.4	2310	63.3
Series N	2302	15.8	2313	64.1
Series Z	2299	31.0	-	-

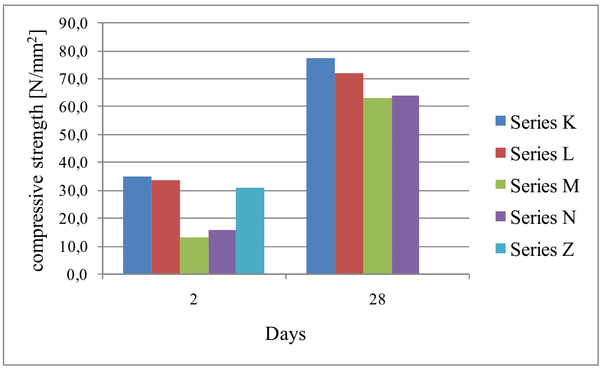

Fig. 7 Measured compressive strengths after 2 and 28 days

From the results shown in Tab. 5 and in Fig. 7 it is clear, that the specimens of the M and N series, cured on ambient temperatures, reached only 40 % of the compressive strength measured on the reference specimens cured in laboratory at 20 °C (K and L series) after 48 hours. The compressive strength measured on the specimens hardening in the experimental segment (Z-series) reached almost 91 % of the strength measured on the reference cubes (K and L series). Specimens of the Z-series had approximately 2 times higher compressive strengths after 48 hours than the specimens of the M and N series.

In this simple manner it was demonstrated that the 48-hour compressive strength of the mass concrete, which is hardening at low ambient temperatures, could not be simply represented by small specimens cured at the same low ambient temperatures. Based on this experimental investigation it was recommended to cure the specimens according to the valid standard requirements [6] and on the basis of their strength to determine the start of prestressing works with a certain safety margin of 5 N/mm^2. Furthermore casting at lower expected temperatures than 1°C has not been allowed.

3. Conclusions

In the paper it was shown that the curing regime of the specimens plays a significant role in the compressive strength development of the high strength concrete, especially in the early age. Differences in compressive strengths were almost 300 % after 48 hours when comparing the specimens cured at 2 °C on air with the specimens cured at 20 °C in water. After 7 and 28 days these differences gradually diminished.

One of the main aims of this experimental investigation was also to eliminate the inappropriate curing of the cube specimens on the construction site during the construction of the bridge near Štrba village. Cube specimens on construction site were cured at low ambient temperatures, left near the casted bridge segment. Construction supervisor and his team believed that this curing of the specimens lead to the best estimation of the real compressive strengths of the concrete in the structure. However, the experimental investigation showed that after 48 hours these specimens reach only approx. 50 % of the compressive strength measured on specimens cured in more realistic regime. Based on this quite simple experiment it was recommended to cure the specimens according to the valid standards despite the low ambient temperatures. The accuracy of this recommendation was later indirectly confirmed. If the real strengths would be as low as they were predicted by inappropriately cured specimens (approx. 50 % of the prescribed strengths) it is highly probable that there would occur failures in the anchorage zone during prestressing works. However no failures were ever recorded and thus the assumptions were indirectly confirmed. Specimens cured at low ambient temperatures before this experimental investigation often reached the prescribed strength only after more than 7 days instead of 2 days. This delay significantly slowed down the whole construction process. Showing that this curing regime does not lead to the real compressive strengths in the structure allowed the works to progress at usual speed, without compromising the safety of the structure. By means of this higher construction speed considerable funds were saved. More detailed study of this problem is recommended in the future, especially if some similar problem arises, because the benefit of accelerated construction could be significant.

References

[1] P. Paulík, M. Búci: Bridge built by the incremental launching technology near Štrba village – field experience from construction, *Inžinierske stavby*, Slovak national report on the third international fib congress and exhibition in Washington D.C., 2010
[2] A. M. Neville: Properties of concrete, 1995
[3] P. C. Aïtcin: High performance concrete, 1998
[4] J. K. Kim, S. Hun Han, Y. Chul Song: Effect of temperature and aging on the mechanical properties of concrete Part I. Experimental results, *Cement and Concrete Research* 32 - 1087–1094, 2002
[5] Technical standard: STN EN 1992-1-1, Design of concrete structures, SÚTN, 2004
[6] Technical standard: STN EN 12390-2, Concrete specimens for strength tests – preparation and curing, SÚTN, 2003
[7] Curing concrete: http://www.ce.memphis.edu/1101/notes/concrete/PCA_manual/Chap12.pdf
[8] Cold weather concreting: http://www.ccaa.com.au/publications/pdf/Cold_Weather.pdf

Appendix A. Curing and testing of the concrete cube specimens – photographs


Fig. 8 and 9 – Curing of the cubes of the A, D and E – series

Fig. 10 – Compression test

Available online at www.sciencedirect.com

SciVerse ScienceDirect

Procedia Engineering 00 (2013) 000–000

Engineering Procedia

www.elsevier.com/locate/procedia

Concrete and Concrete Structures 2013

Long-term losses of prestress in precast members cast from HPC

Jaroslav Halvonik*, Juraj Dolnak, Viktor Borzovič

Slovak University of Technology in Bratislava, Faculty of Civil Engineering, Radlinsk0ho 11, 813 68 Bratislava, Slovakia

Abstract

Paper deals with results of experimental program which is focused on the monitoring of prestress losses in experimental beams cast from normal concrete C40/50 and high performance concrete C70/85. All beams were subjected to the same prestress force initiated by four pre-tensioned strands. Experimental beams were equipped by elastomagnetic sensors which were embedded on the strands for measuring of prestressing forces. Concrete strains were measured by sensitive strain gauges embedded in the beams. Beams were placed outside the facility in order to simulate similar weather conditions as precast girders used for construction of concrete bridges have. Obtained results of measurements were compared to theoretical values predicted by three different rheological models introduced in Eurocode 2 a Model Code 2010.

Keywords: prestressed concrete, prestress losses, creep, shrinkage, precast beams;

1. Introduction

Application of high performance concrete in Slovakia is still limited particularly due to its price compared with a normal concrete. It concentrates mainly on manufacturing of some precast structural elements subjected to high loading level or to the extreme exposure conditions, e.g., containments for nuclear power plant waste.

The largest application of HPC in Slovakia was connected with the construction of motorway bridges composed of prestressed precast beams with reinforced concrete topping (slab-on-girder bridges). However, precast beams were not cast from HPC to employ its excellent properties like high strength or perfect durability here, but for the acceleration of manufacturing processes. Pre-tensioned bridge beams were originally designed from normal concrete C45/55 which allowed prestress transfer 36 hours after beam casting. Using of high performance concrete C55/67 enabled prestress transfer just 18 hours after casting.

* Corresponding author. Tel.: +421- 903- 030 -396; fax: +421- 252- 926 -213.
E-mail address: jaroslav.halvonik@stuba.sk.

In order to initiate an application of HPC for manufacturing of prestressed precast bridge girders in larger scale an experimental program focused on behavior of structural elements cast from normal and high performance concrete subjected to prestressing forces was carried out. Obtained measurements were also used for verification of models for prediction of prestress losses which are introduced in Eurocode 2 and Model Code 2010.

2. Experimental program

2.1. Precast beams

Testing specimens consist of 8 pre-tensioned precast beams. Four beams were cast from normal concrete C40/50 and four other ones from high-performance concrete C70/85, see Fig.1. Beams were subjected to same prestressing force at prestress transfer. Prestressing was initiated by four low-relaxation strands ϕLs12.5 mm/1770 MPa. The length of the beams is 2.5 m in order to ensure full transfer of prestressing force into the beams at mid-span section. Cross-section is rectangle with dimensions of 180×140 mm. The applied force was nearly 500 kN at prestress transfer and compressive stresses in concrete reached 18 MPa, which is the common value in currently used bridge girders. Prestressed transfer was scheduled 5 days after casting.

Fig.1 Prestressed beams at the storage yard

2.2. The other concrete specimens

Together with beams many different specimens were cast for investigation of the relevant material properties of used concrete. Cubes 150×150×150 mm and cylinders 150×300 mm were cast for measuring compressive strength and prisms 100×100×400 mm for measuring Young's modulus of elasticity. In order to determine rheological properties 12 prism specimens were cast having the same cross-section as prestressed beams. Six specimens were used for measuring shrinkage (three for each concrete type) and six specimens for measuring creep.

2.3. Measuring devices

One elastomagnetic sensor PSS16 for monitoring prestressing forces was installed in each beam at mid-span section, see Fig.2. It means each strand was equipped by 2 sensors. Strain gauges type EDS-20V-E were used in four beams at mid-span for monitoring concrete strains. Other four strain gauges were installed in the specimens used for measuring concrete rheology.

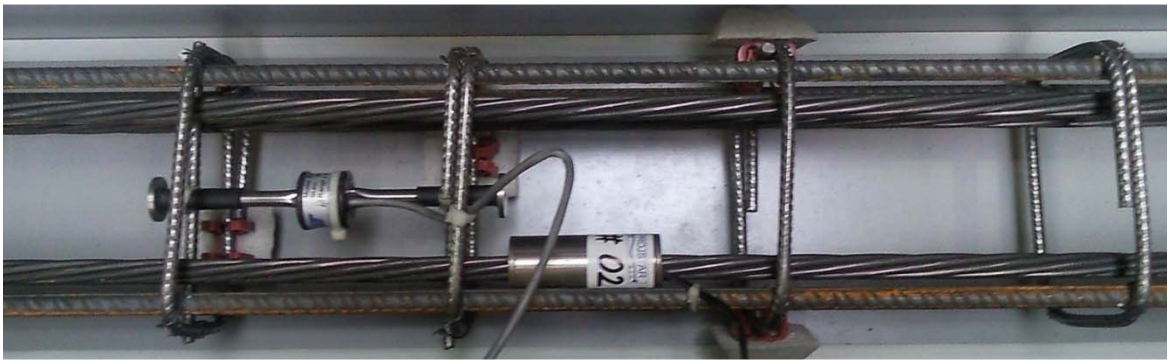

Fig.2 Elastomagnetic sensor and strain gauge embedded in a beam

Concrete strains were also measured by removable deformeters with a length of the base 400 mm. Each prestressed beam and each specimen for measuring of concrete rheology has four bases.

Ambient weather conditions are being monitored with DTHL HydrologgPro device where relative humidity and temperature of air have been recorded from the time of beam casting till now. Temperature of the concrete is measured by strain gauges embedded in the beams.

3. Results and discussion

3.1. Material properties

The material properties tested for concrete were strength, modulus of elasticity, creep and shrinkage. Cube strength of concrete at time of prestress transfer was 40 MPa for normal concrete and 68 MPa for HPC. Measured properties of concrete at the age of 28 days are summarized in the Table 1. Based on statistical evaluation characteristic cube compressive strength was 52,6 MPa for normal concrete and 86,2 MPa for high strength concrete.

Table 1. Material properties of used concrete

Specimen	C40/50		C70/85	
	Cube strength	Modulus	Cube strength	Modulus
	[MPa]	[GPa]	[MPa]	[GPa]
#1	53,0	31,920	94,5	40,780
#2	53,5	34,827	97,5	39,959
#3	53,0	33,954	89,5	40,032
Average	53,2	33,568	93,8	40,256

3.2. Prestress losses

Changes of prestressing force were measured in each strand by EM sensors since their stressing at prestressing bed until now. Strain gauges embedded in beams enable to measure prestress losses indirectly, based on assumption of deformation compatibility between concrete and prestressing tendon. Development of prestressing force in individual strands measured by EM sensors for both NC and HPC concrete is shown in the Fig.3. NC concrete is indicated by red polyline and HPC by blue polyline. Average prestress losses at time of the latest measurement related to the prestressing forces at time of prestress transfer were 17.9 % in NC and 12.8 % in HPC. The changes of prestress force include immediate losses due to elastic shortening of concrete (8.5% for NC and 6.4% for HPC) and long-term losses due to relaxation of the prestressing steel, creep and shrinkage of concrete (9.4% for NC and 6.4 % for HPC).

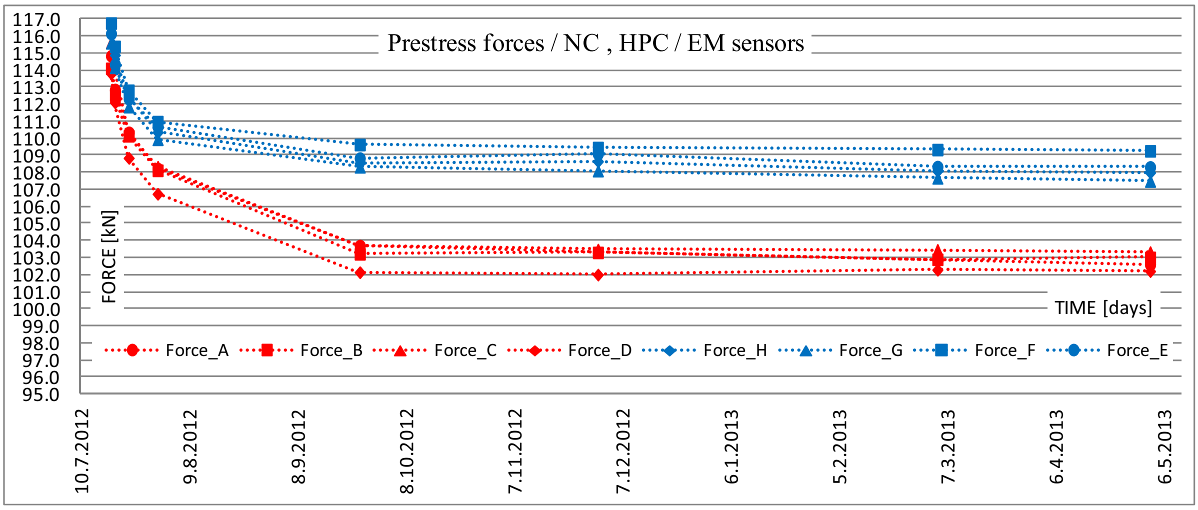

Fig.3 Development of prestressing force in individual strands measured by EM sensors

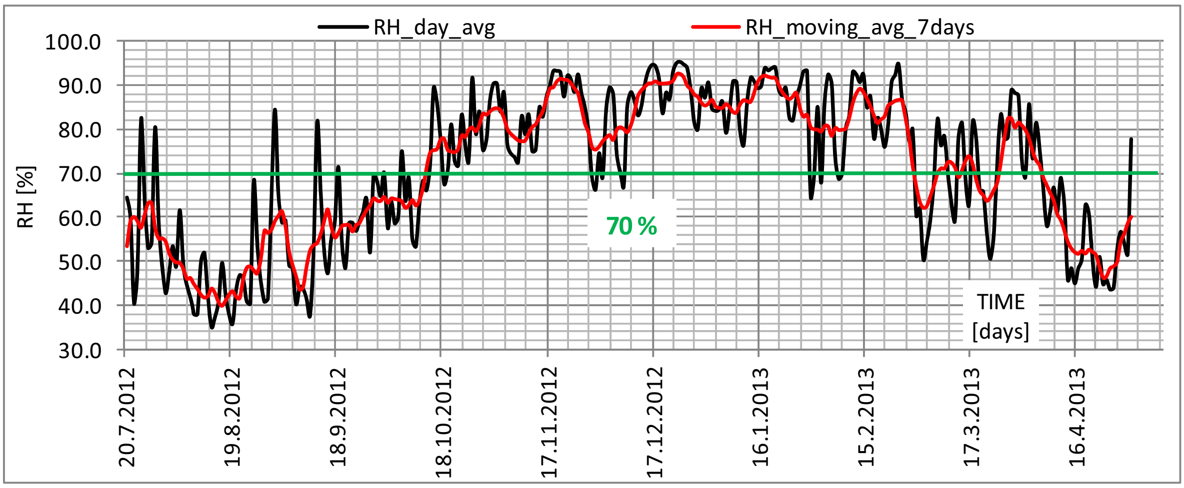

Fig.4 Development of relative humidity of environment at storage yard

Comparison of measured and predicted prestressing forces for NC is shown in the Fig.5 and for HPC in the Fig.6. Three different models for prediction of creep and shrinkage were used in assessment. The first model, indicated by black line, is introduced in EN1992-1-1 Annex “B”, model indicated by blue line in EN1992-2 and the green line represents model from Model Code 2010. All lines also include prestress losses due to relaxation of prestressing steel. Models for prediction of steel relaxation were taken from the same codes. Average relative humidity of 70% was used in the assessment. The value of RH was derived from recording which is shown in the Fig.4.

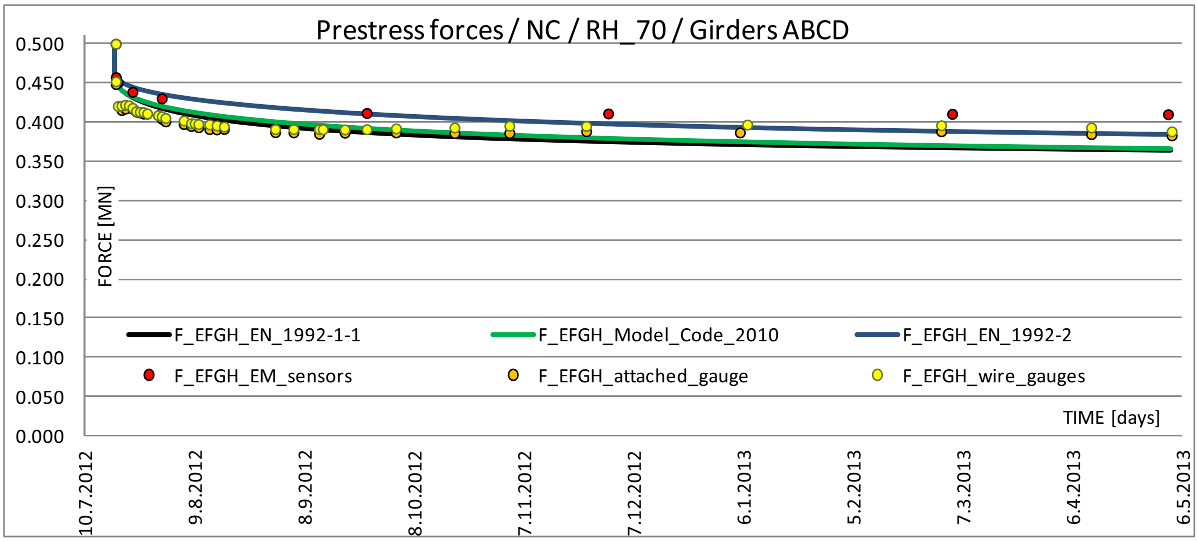

Fig.5 Development of prestressing force in the beams cast from NC

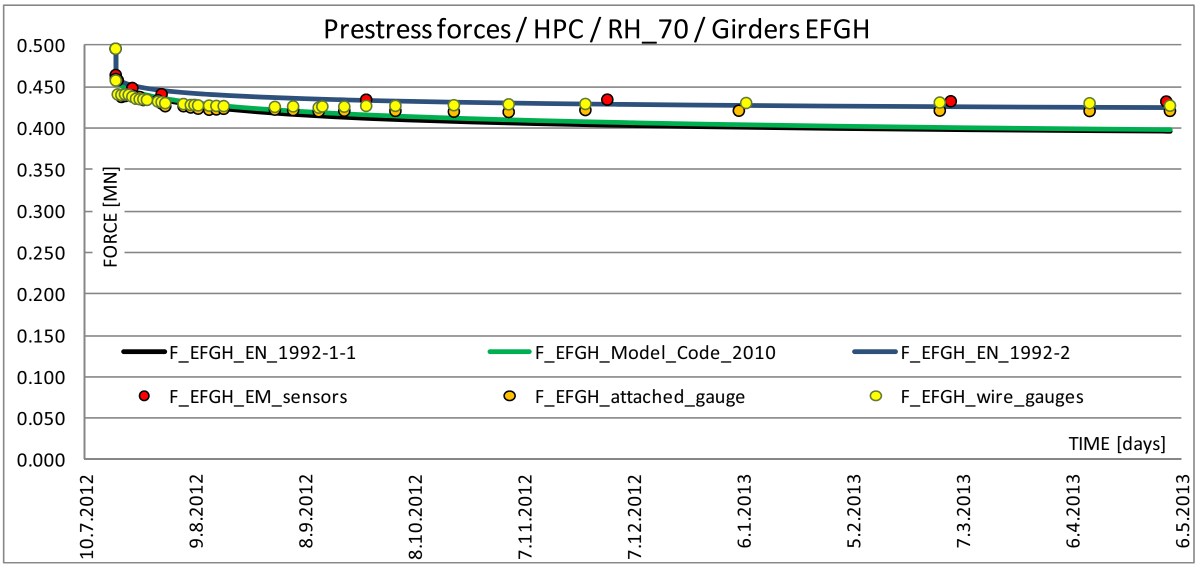

Fig.6 Development of prestressing force in the beams cast from HPC

Colored dots in the Fig.5 and Fig.6 indicate measurements carried out by three different devices. Red dots represent direct measurements of prestressing force by EM sensors, yellow and orange dots were obtained from changes of concrete strains measured by strain gauges.

Comparison indicates quite good prediction of prestress losses. The measured values were higher than predicted ones at the beginning for both types of concrete. Later, it has changed and measurements have approached to the predicted values. The difference at the beginning was caused by low humidity of ambient environment at that time, see Fig.4. The best results agreement was obtained with models for prediction of creep and shrinkage introduced in EN1992-2, blue line. The model was developed for HPC concrete with silica-fume, however it has also been used for prediction of creep and shrinkage for our NC.

4. Conclusions

Measurements confirmed that material properties affecting the prestress losses due to elastic shortening, creep and shrinkage of concrete were much better for HPC compared to the high quality NC. Average prestress losses at time of the latest measurement related to the prestressing force at prestress transfer are 17.9 % in NC and 12.8 % in HPC, it means that the value obtained in HPC represents only 71.5 % of the value in NC.

Testing of the models for prediction of concrete rheology which has significant influence on the precision of prestress losses assessment in structural elements has shown that all three models overestimate prestress losses in the testing beams. The best approximation to measured values was obtained for rheological model introduced in EN 1992-2 (Bridges).

Acknowledgements

Authors gratefully acknowledge Scientific Grant Agency of the Ministry of Education of Slovak Republic and the Slovak Academy of Sciences VEGA No. 1/0690/13 and company Zipp Bratislava Ltd. member of Strabag SE for financing and manufacturing of all testing specimens..

References

[1] Chandoga, M., Halvonik, J., Pritula,A.: (2013), Short and long time deflections of pre and post-tensioned bridge beams, *Proceeding of fib Symposium, Engineering a Concrete Future*, Tel-Aviv, 22-24 April 2013

[2] Moravcik, M., Cavojcova, A.: (2013), Some design aspects of the new precast girder highway bridge, *Proceeding of fib Symposium, Engineering a Concrete Future*, Tel-Aviv, 22-24 April 2013

Available online at www.sciencedirect.com
SciVerse ScienceDirect
Procedia Engineering 00 (2013) 000–000
Engineering Procedia
www.elsevier.com/locate/procedia

Concrete and Concrete Structures 2013

The maximum punching shear resistance of flat slabs

Jaroslav Halvonik*, Ľudovít Fillo

Slovak University of Technology in Bratislava, Faculty of Civil Engineering, Radlinsk0ho 11, 813 68 Bratislava, Slovakia

Abstract

Results of the latest experiments have revealed that the maximum punching resistance defined from crushing of concrete struts at the perimeter of a column in EC2 is an insufficient criterion for limitation of maximum shear forces at the vicinity of columns. Therefore further limitation has been introduced in STN EN 1992-1-1/NA. The paper will deal with the new requirements concerning of maximum punching shear resistance which is based on the k_{max} factor and punching shear resistance without shear reinforcement $v_{Rd,c}$.

Keywords: flat slab, punching, shear resistance,

1. Introduction

Taking into account the latest experimental programs [2], [3], [4] a sub-commission for concrete structures CEN/TC250/SC2 has imposed new limit for the maximum punching resistance of the members with shear reinforcement. Member states should implement this new limit to their National Annexes. This limit and its influence on the design of flat slab thickness are introduced in the contribution.

2. Punching of flat slabs

2.1. Punching phenomenon

Phenomenon of flat slab punching is indicated in Fig.1. There are two possible ways of structural failure due to the punching. The first one is strut diagonal failure (crushing of concrete) at control perimeter of the column u_0. The second one is the tension failure of concrete or transverse reinforcement in area surrounded by the basic

* Corresponding author. Tel.: +421- 903- 030 -396; fax: +421- 252- 926 -213.
E-mail address: jaroslav.halvonik@stuba.sk.

control perimeter u_1. Basic control perimeter should be assumed at distance $2d$ from the face of the supporting member, where d is an effective depth of the slab.

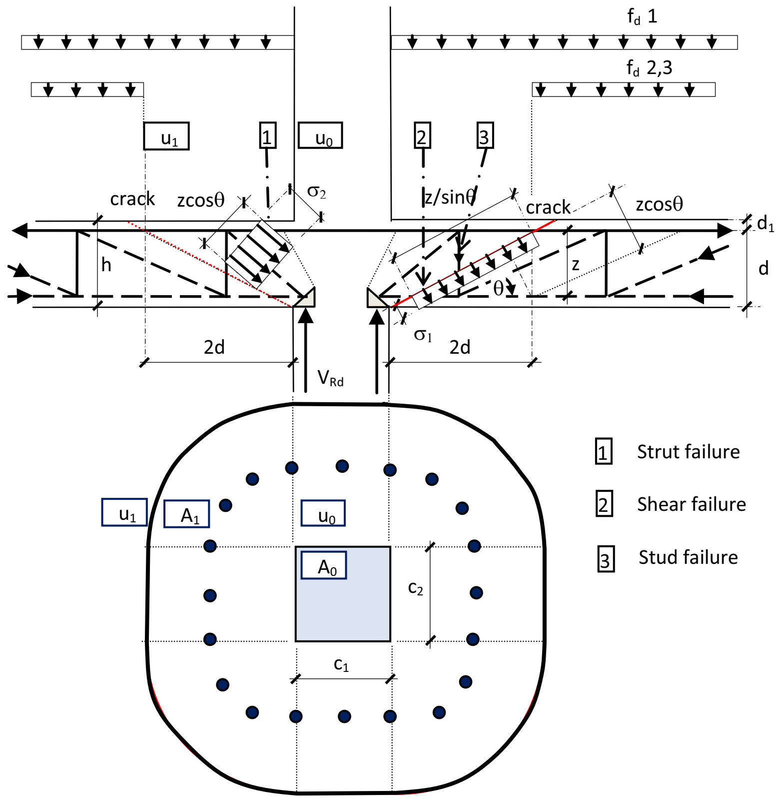

Fig.1 Model of flat slab punching phenomenon
1-crushing of the strut; 2-tension failure at u_1 perimeter; 3-failure of shear reinforcement;

Crushing of the strut at column perimeter is controlled by reduced compressive strength of concrete, see formula (1).

$$v_{\mathrm{Ed,max}} = \frac{\beta V_{\mathrm{Ed}}}{u_0 d} \leq v_{\mathrm{Rd,max}} = 0{,}4\nu f_{\mathrm{cd}} \qquad \nu = 0{,}6.\left[1 - \frac{f_{\mathrm{ck}}}{250}\right] \qquad f_{\mathrm{ck}}\ [MPa] \tag{1}$$

The new limit is based on the punching resistance of a member without shear reinforcement $v_{\mathrm{Rd,c}}$ see formula (2). The maximum punching resistance including effect of shear reinforcement at the basic control perimeter shall be less than value $k_{\mathrm{max}}\, v_{\mathrm{Rd,c}}$, see formula (3). If $v_{\mathrm{Rd,cs}} > k_{\mathrm{max}}\, v_{\mathrm{Rd,c}}$ then v_{Ed} shall be less than $k_{\mathrm{max}}\, v_{\mathrm{Rd,c}}$. The k_{max} value will be introduced in Amendment of EN1992-1-1 and proposed value is 1,5.

$$v_{\mathrm{Rd,c}} = \frac{0{,}18}{\gamma_{\mathrm{C}}} k\left(100\rho_1 f_{\mathrm{ck}}\right)^{1/3} \ \geq\ 0.035 k^{3/2} f_{\mathrm{ck}}^{1/2} \tag{2}$$

$$v_{\mathrm{Rd,cs}} = 0{,}75\, v_{\mathrm{Rd,c}} + 1{,}5\left(\frac{d}{s_{\mathrm{r}}}\right) A_{\mathrm{sw}}\ f_{\mathrm{ywd,ef}} \left(\frac{1}{u_1 d}\right) \leq k_{\mathrm{max}}\ v_{\mathrm{Rd,c}} \tag{3}$$

However the latest experiments have also shown that the k_{max} value depends on many factors. The first most important factor is type of shear reinforcement and particularly conditions for their anchoring [3]. The second important factor is rotation ψ of a slab around the supporting area, see Fig.2. Larger rotation is the reason of lower punching resistance of a slab member [1]. Rotation ψ at supporting area is lower for slabs with higher effective depth because these members need lower rotation in order to develop tensile capacity of the main reinforcement above the support. Therefore for members with higher effective depth the k_{max} value can be increased.

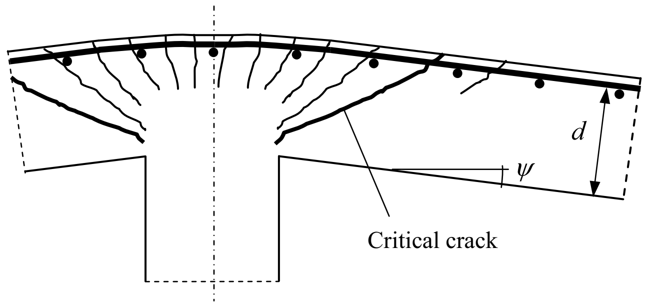

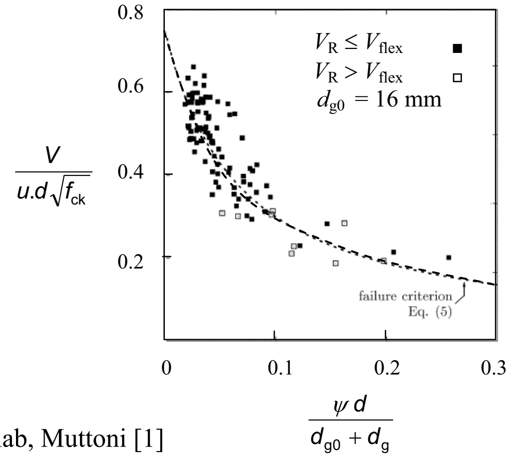

Fig.2 Influence of rotation on punching resistance of a flat slab, Muttoni [1]

The best performance of shear reinforcement system is ensured by double headed studs, see Fig.3a. Studs allow for full development of their tensile capacity just behind the heads. Stirrups overlapping main reinforcement with sufficient development length in compressive face and bent at tension face provide also very good behavior, see Fig.3b. Links and open stirrups see in Fig.3c, have the worst performance from punching resistance point of view.

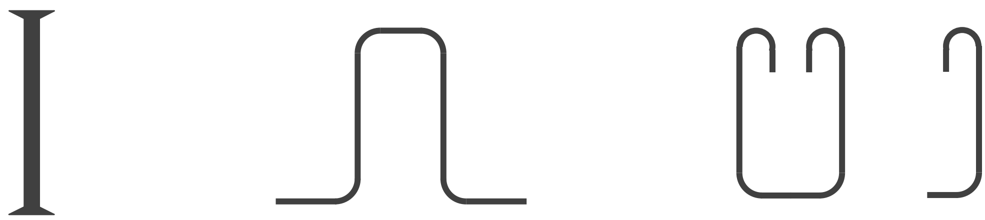

a) Double-headed stud b) Stirrup with bent at tension face c) Stirrup and link with hooks at tension face

Fig.3 Shear reinforcement for punching

These two important factors led us to decision to define k_{max} value in a more refined way. The k_{max} value is 1.9 for slabs reinforced with double headed studs with diameter of heads larger than three times the bar diameter. Double headed studs have to meet also requirements introduced in ETA (European Technical Approval) “Punching Prevention System”. For the other types of shear reinforcement the k_{max} value depends on the effective depth of a slab d. The minimum value is 1.4 if $d \leq 200$ mm and maximum value 1.7 if $d \geq 700$ mm. For intermediate values of d a linear interpolation can be used.

2.2. Design of slab effective depth

Coming from above mentioned limits for maximum punching resistance a slab thickness is possible to determine on the basis of a span length, intensity of load and an amount of main reinforcement. In Fig.3 and 4 are charts for square columns with dimensions 300 and 500 mm respectively and distances of the columns 8 m and concrete class C25/30. Influence of concrete class is compared with chart for concrete C35/45. As it was mentioned above the thickness of a flat slab depends also on main reinforcement. The influence of reinforcement ratio ρ = 0,002; 0,01 a 0,02 on the design of slab effective depth based on punching resistance criteria is shown in the Fig. 2 and 3. The slab thicknesses in Fig.3 – Fig.6 were determined with concrete cover $c = 25$ mm.

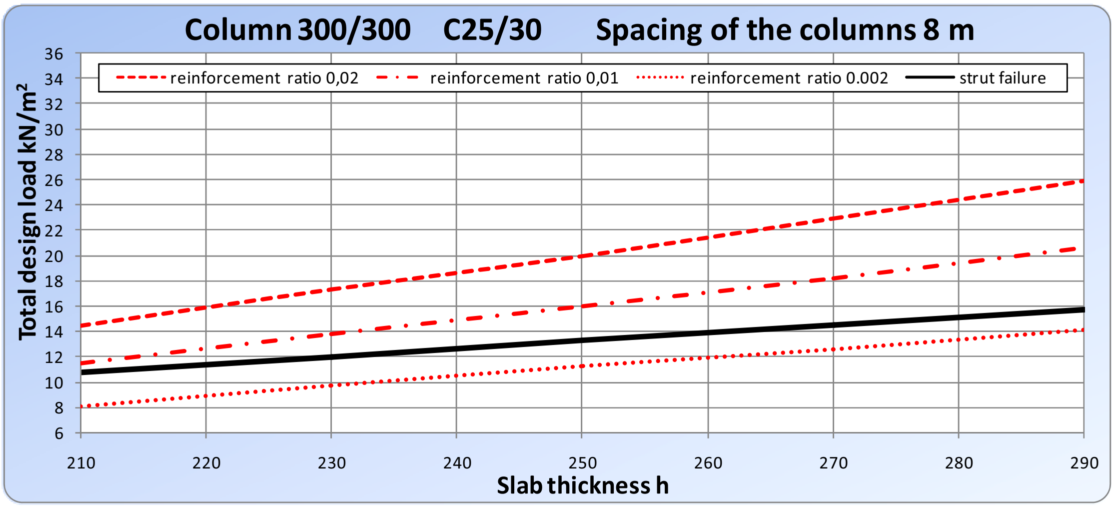

Fig.4 Flat slab depth for column cross-section 300 mm, concrete C25/30 and 8 m span and k_{max} =1,9

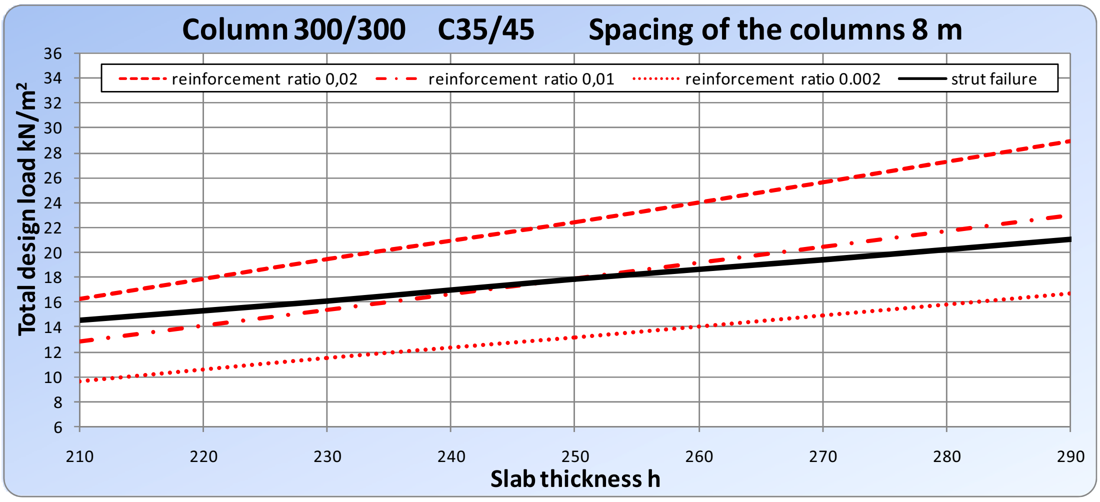

Fig.5 Flat slab depth for column cross-section 300 mm, concrete C35/45 and 8 m span and k_{max} =1,9

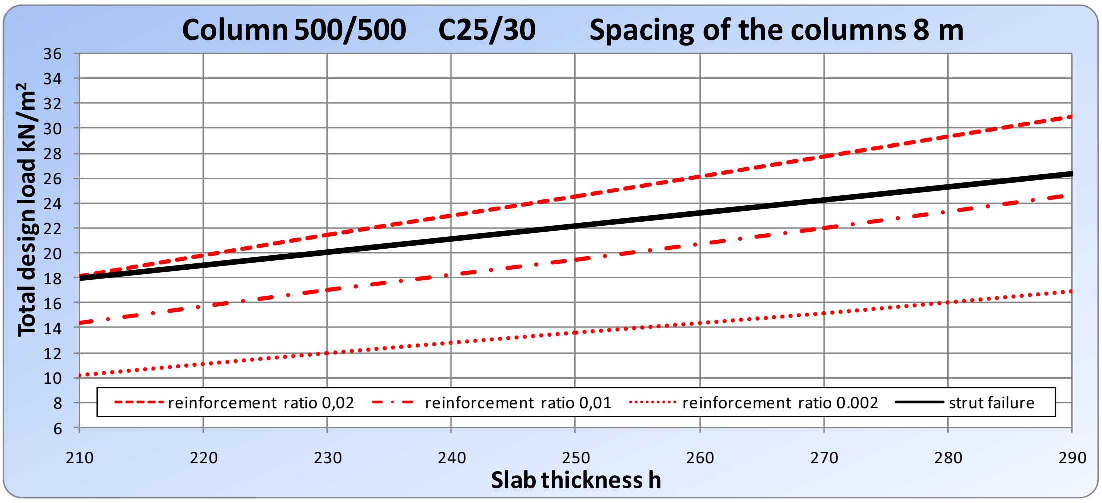

Fig.6 Flat slab depth for column cross-section 500 mm, concrete C25/30 and 8 m span and k_{max} =1,9

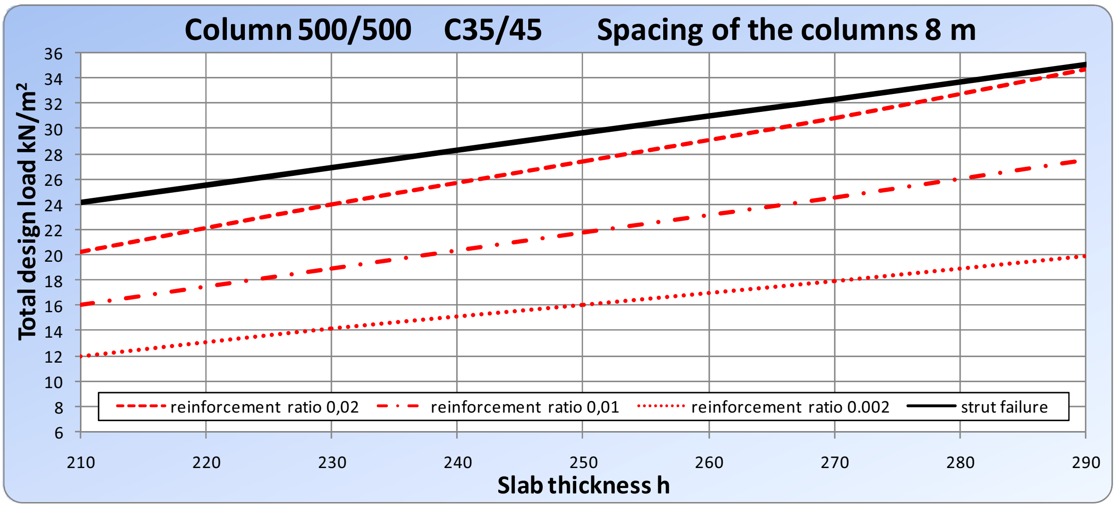

Fig.7 Flat slab depth for column cross-section 500 mm, concrete C35/45 and 8 m span and k_{max} =1,9

3. Conclusions

It is clear from presented charts that the limit based on k_{max} factor will govern minimum effective depth and thus thickness for flat slabs with higher strength class of concrete, lower amount of main reinforcement and for flat slabs supported by columns with larger dimensions. The presented assessments were carried out with k_{max} value of 1,9 where shear reinforcement consists of double headed studs. In a case of different type of shear reinforcement where k_{max} value is approximately 1,5 the new limit will be decisive for design of flat slab thickness at the vicinity of the column nearly for all cases.

Acknowledgements

Authors gratefully acknowledge Scientific Grant Agency of the Ministry of Education of Slovak Republic and the Slovak Academy of Sciences VEGA No. 1/0857/11.

References

[1] Ruiz,M.F.- Muttoni,A. Application of Critical Shear Crack Theory to Punching of RC Slabs with Transverse Reinforcement, ACI Structural Journal V.106 No.4, July – August 2009, pp.485-494

[2] Feix,J.- Hausler,F.- Walkner,R.: Necessary Amendments to the Rules for Punching Design According to EN 1992-1-1, in Proceedings of Workshop “Design of Concrete Structures and Bridges using Eurocodes”, Bratislava 2011, pp.21-27

[3] Hegger,J.- Siburg,C.: Punching – Comparison of Design Rules and Experimental Data, in Proceedings of Workshop “Design of Concrete Structures using EN 1992-1-1”, Prague 2010, pp.113-124

[4] Bujnak,J.- Gavura,S.: On the maximum resistance of slabs reinforced against failure by punching Punching – Comparison of Design Rules and Experimental Data, in Proceedings of Workshop “Design of Concrete Structures using Eurocodes”, Prague 2012, pp.69-75

[5] Regan,P.E.: Shear Reinforcement of Flat Slabs, in Proceedings of International Workshop on Punching Shear Capacity of RC Slabs, TRITA/BKN, Bulletin 57, 2000, pp.97-107

[6] Birkle,G.: Punching of Flat Slabs: The Influence of Slab Thickness and Stud Layout, Department of Civil Engineering, University of Calgary, Calgary, AB, Canada, 2004, 152 pp.

Available online at www.sciencedirect.com
SciVerse ScienceDirect
ELSEVIER
Procedia Engineering 00 (2013) 000–000
Engineering
Procedia
www.elsevier.com/locate/procedia

Concrete and Concrete Structures 2013

Theoretical and experimental studies on composite steel – concrete columns

Andras Lelkes[a], Štefan Gramblička[a]*

[a]*Department of Concrete Structures and Bridges, Faculty of Civil Engineering, Slovak University of Technology, 813 68 Bratislava, Radlinského 11, Slovakia*

Abstract

This paper presents some results of theoretical and experimental analysis of composite steel-concrete (SC) columns, which are completely or partially concrete-encased steel members. In practice, most composite SC columns are relatively slender. In design the second - order effects will usually need to be included. The main topic of the paper is a theoretical analysis of the second - order theory at composite (SC) columns.
According to the results of the experiments, which were made in the Department of Concrete Structures and Bridges, Slovak Technical University of Technology in Bratislava (total of 18 columns were tested in two series), the effects of the second - order theory were analyzed. The experimental results were compared with theoretical from the model developed in the non-linear software Atena 3D.
The evaluation of the results is also shown in comparison with the general design method according to Eurocode 4, Design of composite steel and concrete structures - Part 1.1 : General rules and rules for buildings (EN 1994-1-1).

Keywords: Column, Composite, Second order theory, Non-linear analyses

1. Experimental analysis of composite steel-reinforced concrete columns

At the Department of Concrete Structures and Bridges, Slovak Technical University in Bratislava, there were tested partially encased composite steel-concrete columns. As a steel part, the hot-rolled I - sections HEA 280 and HEA 200 were used. For the longitudinal reinforcement the bars 4ϕ16 or 4ϕ14 were considered (Fig.1,

* András Lelkes. Tel.: +421907300874;
E-mail address: andras.lelkes@stuba.sk.

Tab.1). Total 18 columns with the lengths of 3 m and 4 m were tested. In the tests, the normal compression forces were brought to the columns with the eccentricities from 30 to 80 mm (Tab.1).

Fig. 1 The cross-section of tested composite Sx series columns and failure of the SC column

Table 1 Specimen dimensions and material properties of tested composite steel-concrete columns

Test	Dimensions			Steel section	Eccentricity (mm)	Num.	Material properties			Ref.
	b_c (mm)	h_c (mm)	L (m)	Number and diameter of reinforcement		of columns	f_{cd} (MPa)	f_{sd} (MPa)	f_{yd} (MPa)	
S1-40	200	190	3	HEA200 - 4∅14	40	3	65,45	566,25	305,46	[2]
S2-40	200	190	4	HEA200 - 4∅14	40	3	65,45	566,25	305,46	[2]
Sx1-30	280	270	3	HEA280 - 4∅16	30	3	36,34	569,4	395,8	[1]
Sx1-80	280	270	3	HEA280 - 4∅16	80	3	36,34	569,4	395,8	[1]
Sx2-40	280	270	4	HEA280 - 4∅16	40	3	36,34	569,4	395,8	[1]
Sx2-60	280	270	4	HEA280 - 4∅16	60	3	36,34	569,4	395,8	[1]

2. Analysis of composite steel-concrete columns in software Atena 3D

The results from the non-linear calculation in computational program Athena 3D were compared with the experiments, which was characterized in the previous chapter. With this accurate modeling in Athena 3D is possible to determine the real resistance of members. The width of cracks, deformation and the crushing of concrete and the creep of concrete, respectively, can be considered in the analysis. The program is designed for non-linear analysis of structures and members by using the finite elements method. The arrangement of the models of composite SC column and the detail of the column end are shown in Fig.2. The column was modeled with hinged endings on both sides, just as it was made in the experiments. The exact value of the resistance of the column was determined from the force – deformation diagram. The maximum resistance was reached, when the deformation grows even if there is no load added.

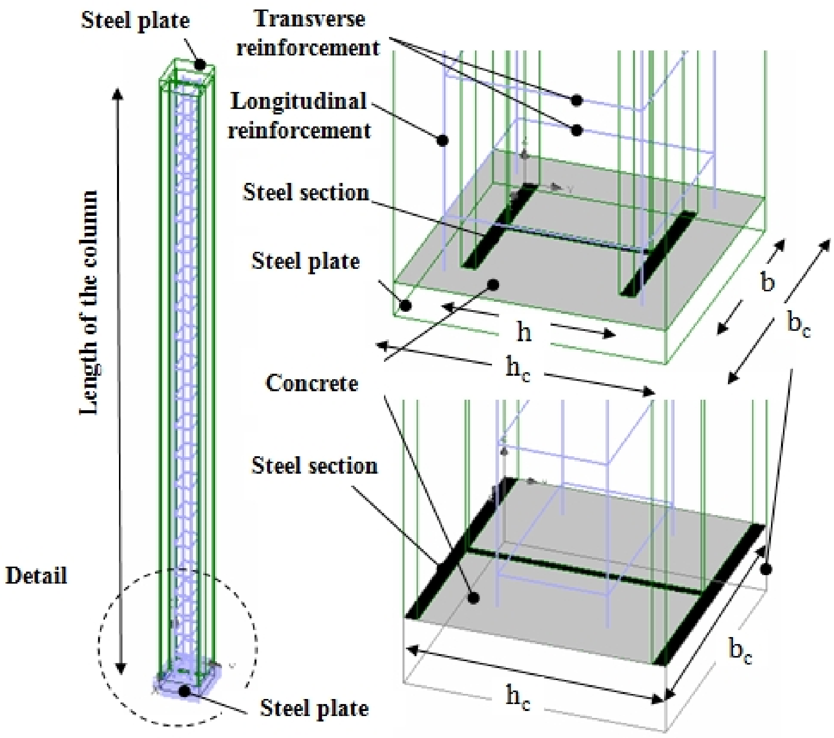

Fig. 2 Model of the composite SC columns in software Atena 3D

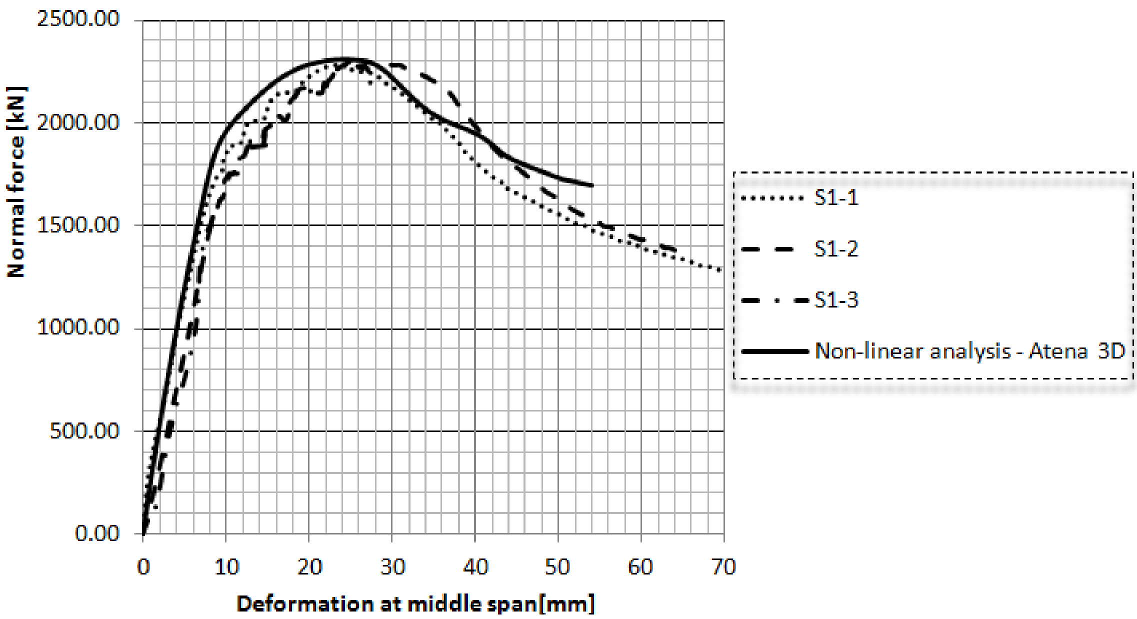

Fig.3 Comparison of the relationships force/deformation of composite S1 series columns - the length of columns is 3 m

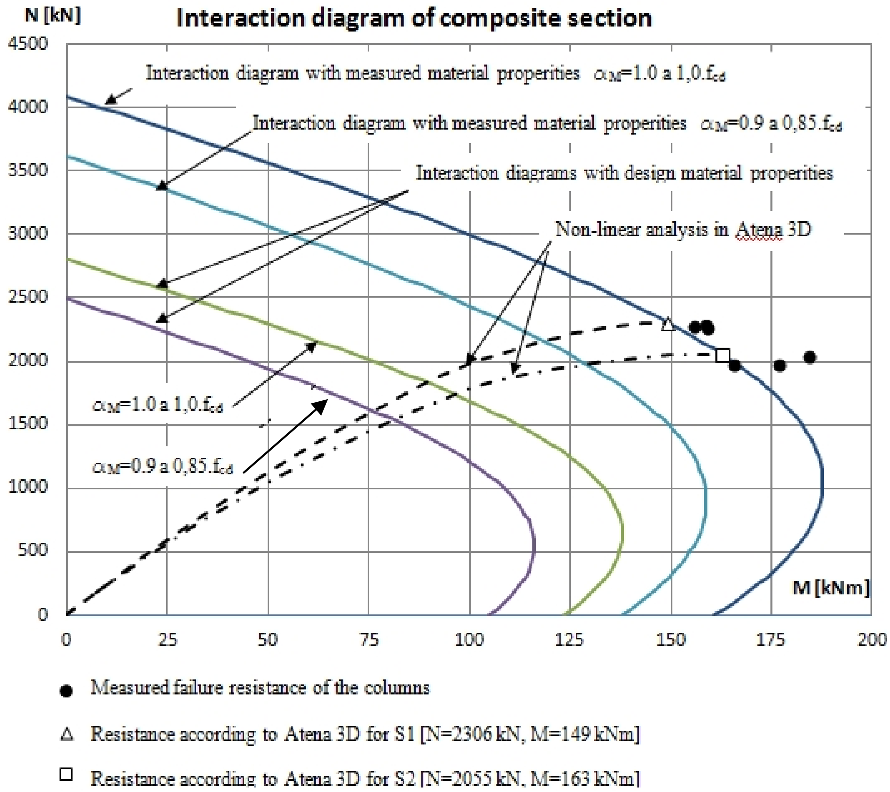

Fig.4 The interaction diagram (in the direction of the web of the cross-section) for the series of experiments S1 and S2 and comparison with the non-linear analysis

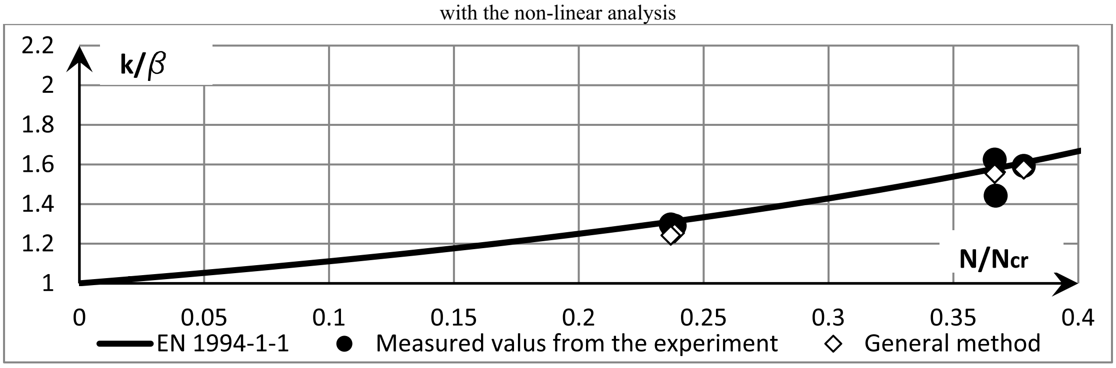

Fig.5 Graphical presentation of the effects of second order theory for the series of experiments S1 and S2

Symbols are according the EN 1994-1-1 [3]:

N_{cr} elastic critical normal force
α_M coefficient related to bending of a composite column
β factor; transformation parameter
k amplification factor for second-order effects

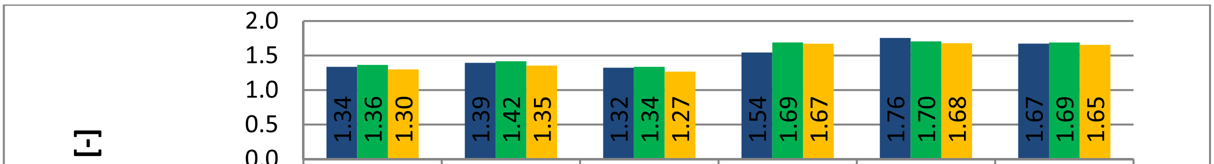

	S1-1	S1-2	S1-3	S2-1	S2-2	S2-3
Measured values	1.336	1.395	1.323	1.544	1.755	1.673
Simplified method	1.364	1.418	1.336	1.690	1.705	1.689
General method	1.300	1.354	1.267	1.671	1.679	1.655

Fig.6 Numerical presentation of the effects of second order theory for the series of experiments S1 and S2

The force – deflection relationship of the composite SC columns of series S1 with the length of 3 m obtained from the nonlinear analysis and the measured deflection are in Fig.3. The experimental obtained resistances of the tested composite SC columns were compared to the calculated resistances from the non-linear analysis. The interaction diagrams were calculated with the design values of the material properties and also real measured values of the material properties (Fig.4). Relationships (force – deflection and interaction diagram) showed a very good match of the non-linear analysis of the ATENA with the experimental measurements.

3. Analysis of the effects of the second order theory

The effect of the second order theory is very important in the design of slender columns. European standards for the design of composite columns give us a simplified relationship to calculate the effects of second order theory. This relationship can be applied only for columns made from concrete class up to C50/60. The steel grades can be from S235 up to S460. The effects of the second order theory can be also calculated by a method according to reference [4], (general method). The main advantage of this method is that it can be applied in case if high-strength concrete is used.

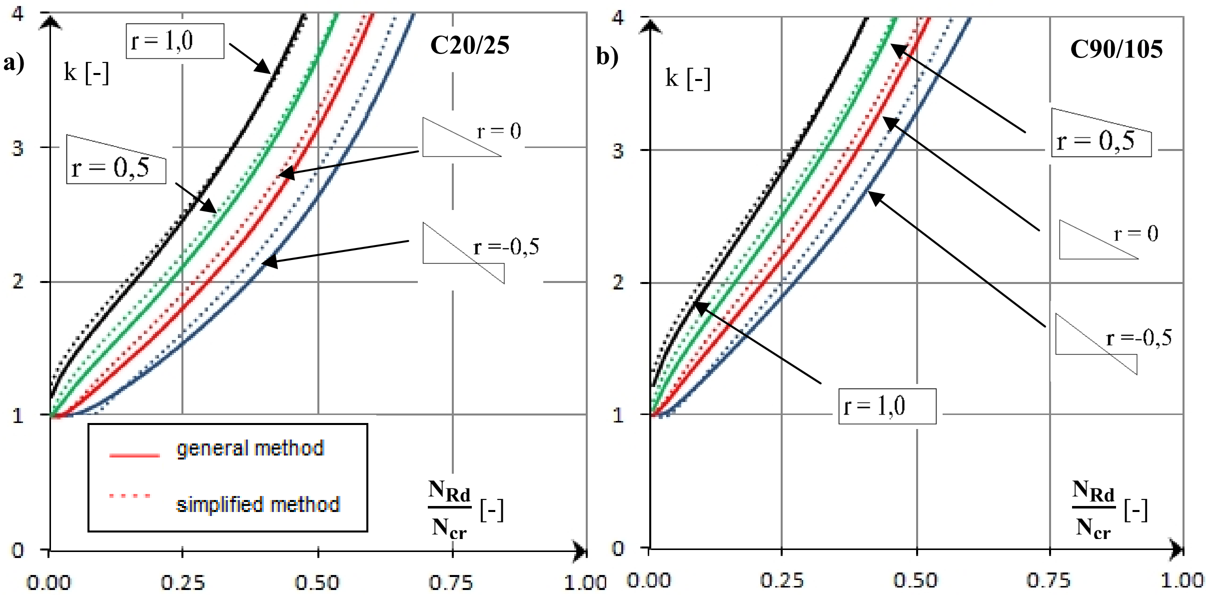

Fig.7 Simplified and general method of second order effects for encased composite SRC section a) with the use of concrete class C20/25, b) with the use of concrete class C90/105

In this chapter we compared the results calculated according to the simplified and the general method. The results obtained from these two methods were compared by the use of factor "k". In case of slender columns, the factor "k" is used to calculate the second order moment by multiplying the first order moment with the factor "k".

$$k = M_{max,II} / M_{max,I} \tag{1}$$

The second order moments were calculated for the fully encased and for the partially encased composite SC columns. In Fig. 7 the results of encased composite SC cross sections of columns are shown. Ratio N_{Ed}/N_{cr} depends on the columns buckling length. Results of the comparison are presented in Fig.7 a) in the case of using the concrete class C20/25 and in Fig. 7 b) when concrete class C90/105 is used. The comparison was made also with the different types of moment distribution.

The results according to the general method show a good agreement with the results calculated according to the simplified method (the difference was 3% in average). We can allege that the simplified method for the second order effects according to the European standards shows results on the safe side in comparison with the general method according to the reference [4]. Moreover it can be also used in cases when high strength concrete (HSC) is used. Experimental analysis of series S1 and S2 also confirmed accuracy of these two methods in case when HSC is used in composite steel-concrete columns (for the experimental analysis was used HSC of strength grade of C60/70). In Fig. 5 and Fig. 6 are presented the comparisons of the measured values of the factor "k" and the calculated values according to the general and the simplified method.

4. Conclusions

The experimental and theoretical analysis of the composite SC columns also with the use of high strength concrete provide the following conclusions:

- a very good match of the resistances and the force-deflection relationship of the of the tested composite SC columns and values calculated in non-linear program ATENA 3D was found,
- the simplified method, which is recommended by the code [3] for calculation of the effects of the second order theory provides the results with a good agreement with the general method according to reference [4]. The small differences were on the safe side. It was also shown a good agreement of the theoretical values of factor "k" with the results from the experimental tests.

Acknowledgements

This contribution was prepared with the financial support of Slovak Grant Agency VEGA 1/0857/11.

References

[1] Valach, P., Design of composite steel concrete columns, Dissertation work, Department of Concrete Structures and Bridges, SvF STU Bratislava (in Slovak), 2005, 187 pp.
[2] Matiaško, S., Design of composite steel and concrete columns with the use of high strength concrete, Dissertation work, Department of concrete structures and bridges, SvF STU Bratislava (in Slovak), 2009, 140 pp.
[3] EN 1994-1-1 Design of composite steel and concrete structures – Part 1.1: General rules and rules for buildings, CEN, Brussels, 2004.
[4] Bergmann, R. – Hanswille, G..: New design method for composite columns including high strength steel. In: Composite Constructions in Steel and Concrete V, ASCE 2006

Available online at www.sciencedirect.com

ScienceDirect

Procedia Engineering 65 (2013) 382 – 386

Procedia Engineering

www.elsevier.com/locate/procedia

Concrete and Concrete Structures 2013 Conference

EUROCODES: Structural Fire Design

Mária Bellová[a]*

[a]Department of Concrete Structures and Bridges, Faculty of Civil Engineering, Slovak Technical University, Radlinského 11, 813 68 Bratislava, Slovakia

Abstract

The European Commission together with European Committee for Standardisation organized and supported on 27-28 November 2012 in Brussels, Belgium – International workshop with worked examples: STRUCTURAL FIRE DESIGN. In the workshop took part 117 participants from 28 countries. Author of this paper was in Brussels the only representative from the Slovak Republic. The workshop sessions presented the **fire resistance assessment** of structures according to the Eurocodes. Each session focused on a specific structural material (steel, steel and concrete composite, concrete, masonry, and timber with the exception of aluminium) and addressed the principles and design methods followed by worked example(s) [1]. Definitions of actions in fire situations were also presented with basic principles and examples at the beginning of the workshop sessions.

The principal objectives of the workshop were to:

- transfer knowledge and information to representatives of key organisations/institutions, industry and technical associations in the Member States of European Committee for Standardisation;
- provide state-of-the-art training material, background information and worked examples to Eurocodes trainers and users;
- facilitate exchange of views, networking and cooperation.

Contribution includes review of background and applications concerning structural fire design of **concrete structures**, presented at the workshop.

Selection and peer-review under responsibility of University of Zilina, Faculty of Civil Engineering, Department of Structures and Bridges

Keywords: Eurocodes – Parts 1-2; structural fire design; fire resistance; basic design methods; worked examples; E – integrity criterion; I – thermal insulation criterion; R – load-bearing criterion; M – mechanical criterion

* Tel.: +421-2-59274-541; fax: ++421-2-52 926 213
E-mail address: maria.bellova@stuba.sk.

1877-7058 © 2013 The Authors. Published by Elsevier Ltd.
Selection and peer-review under responsibility of University of Zilina, Faculty of Civil Engineering, Department of Structures and Bridges
doi:10.1016/j.proeng.2013.09.059

1. Introduction

Parts 1-2 of Eurocodes deal with the design of structures for the **accidental situation of fire exposure.** They only identifie differences from, or supplements to, normal temperature design – **normal temperature** means **20 ˚C.** These parts deal only with **passive methods of fire protection**. Active methods are not covered.

Eurocode 2: Design of **concrete structures** – Part 1-2: General rules – Structural fire design [2-3] however does not cover:

- **structures with prestressing by external tendons,**
- **shell structures.**

The methods given in Part 1-2 of EN 1992 [2-3] are applicable to normal weight concrete up to strength class C90/105 and for lightweight concrete up to strength class LC55/60.

Design safety in the fire situation is important part of structural design of structures**.** One of the components of the design safety in case of fire is **fire resistance** of the structure**.** Fire resistance belongs to the essential requirements to the structures, the same as the requirements to mechanical resistance and stability.

Nomenclature

$t_{\mathrm{fi,req}}$	required time of fire resistance
$t_{\mathrm{fi,d}}$	design value of time of fire classification for a standard fire
$E_{\mathrm{fi,d,t}}$	design effect of actions for the fire situation, including effects of thermal expansions and deformations in determined time t
$R_{\mathrm{fi,d,t}}$	design resistance in the fire situation in time t
θ_{d}	design value of temperature of concrete
$\theta_{\mathrm{d,cr}}$	design value of critical temperature of concrete
a	nominal axis distance of reinforcing or prestressing steel from the nearest exposed surface
E_{d}	design value of the corresponding force or moment for normal temperature, for a fundamental combination of actions
η_{fi}	reduction factor for the design load level for the fire situation, its' suggested value for concrete is 0,7
E 60	member meeting the integrity criterion E for 60 minutes in standard fire exposure
I 60	member meeting the thermal insulation criterion I for 60 minutes in standard fire exposure
R 60	member meeting the load bearing criterion R for 60 minutes in standard fire exposure
M 90	member meeting the mechanical resistance criterion M for 90 minutes in standard fire exposure

The fire terms is it possible to express according to [4] as follows – from the point of view:

- **time** $t_{\mathrm{fi,req}} \leq t_{\mathrm{fi,d}}$ (1)
- **limit load** $E_{\mathrm{fi,d,t}} \leq R_{\mathrm{fi,d,t}}$ (2)
- **temperature** $\theta_{\mathrm{d}} \leq \theta_{\mathrm{d,cr}}$ (3)

2. Fire resistance of concrete members

Concrete – similarly as masonry – disposes of excellent ability to resist to fire exposure (in comparison with other load-bearing materials, like steel and timber). This advantage of concrete is oft used by construction of **fire walls**, which form an obstacle in the event of extending of fire.

Fire wall – wall, separating two spaces (generally two fire compartments or buildings) which is designed for fire resistance and structural stability, including resistance to mechanical impact (criterion M) such that, in the case of fire and failure of the structure on one side of the wall, fire spread beyond the walls avoided (so that a fire wall is designated REI-M or EI-M).

3. Structural fire design of concrete structures

3. 1. Assessment methods

The analysis for the fire situation may be carried out using one of the following design methods:

- detailing according to **recognised design solutions** (**tabulated data or testing),**
- **simplified calculation methods for specific types of members,**
- **advanced calculation methods** for simulating the behaviour of **structural members, parts of the structure or the entire structure.**

- **Tabulated data** – in standard [2-3] are there given recognised design solutions for the **standard fire exposure.** The values given in the tables apply to normal weight concrete (2 000 to 2 600 kg.m^{-3}), made with **siliceous aggregates**. If **calcareous aggregates** or **lightweight aggregates** are used in beams or slabs the minimum dimension of the cross-section may be reduced by 10%.

There are provided tables for fire resistance of 30 minutes to 240 minutes of:
– **concrete slabs: solid, flat** and **ribbed (reinforced and presstresed)** for fire resistance classification **REI,**
– beams simply supported and continuous (reinforced and presstresed) for fire resistance classification **R,**
– walls non load-bearing (EI), load-bearing solid (REI) and fire walls for fire resistance classification **M,**
– columns with rectangular or circular section for fire resistance classification **R.**
In tables are specified **minimum dimensions of cross section** and also the **minimal distances of reinforcement bar from the surface of concrete member** (Fig. 1) by members meeting the load-bearing criterion **R** for determinate time in standard fire exposure.

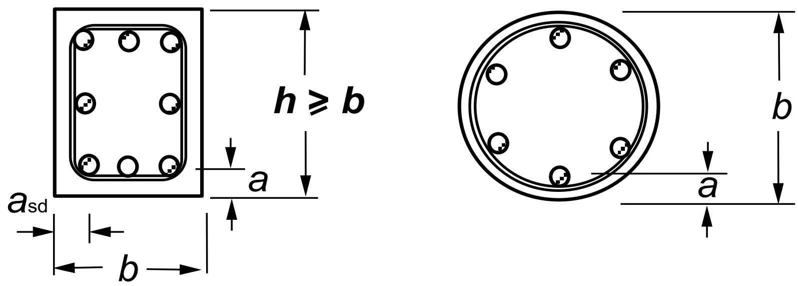

Fig.1. Sections through structural members, showing nominal axis distance *a*.

For fulfilling of criterion **EI** there are in tables provided minimum depths of separating members: walls and slabs.

This method of assessment is simple and fast, but is not general-purpose. It is possible to use the tables only in the case, when special detailing is fulfilled. The values given in tables are conservative. In the table 1 are provided minimum column dimensions and axis distances for columns with rectangular or circular section [5].

Table 1. Minimum column dimensions and axis distances for columns with rectangular or circular section

Standard fire resistance ***R*** [minutes]	Minimum dimensions [mm]: ***b / a*** (rectangular section) ***d / a*** (circular section)			
	Column exposed on one side		Column exposed on more than one side	
30	***b / a***	155/25	***b / a***	200/32
	d / a	155/25	***d / a***	300/27
60	***b / a***	155/25	***b / a***	250/46
	d / a	155/25	***d / a***	350/40
90	***b / a***	155/25	***b / a***	350/53
	d / a	155/25	***d / a***	450/40*
120	***b / a***	175/35	***b / a***	350/57*
	d / a	175/35	***d / a***	450/51*
180	***b / a***	230/55	***b / a***	450/70*
	d / a	230/55	***d / a***	450/70*
240	***b / a***	295/70	***b / a***	-
	d / a	295/70	***d / a***	-

* minimum 8 bars of reinforcement

Notes:

- Tabulated data is given for braced structures only.
- Fire resistance of reinforced and prestressed concrete columns, submitted mainly to compression in braced structures may be considered adequate if the values in Table 1 together with the following rules are applied.
- The validity of the minimum values of the column width $b_{\min}$ and the axis distance of longitudinal reinforcement a given in Table 1 is limited as follows:
  - effective length of the column under fire conditions: $l_{0,\mathrm{fi}} \leq 3$ m
  - amount of reinforcement: $A_s < 0.04\, A_c$

- **Testing the structure** – is very difficult and financially exacting and it is realised in the case of development and verification of new materials, by which is required an increasing of fire resistance. It is really impossible to realize fire tests of a great number of reinforced concrete members (slabs, columns, walls, ...) made from various class of concrete, reinforced with various amount of reinforcement.

- **Simplified cross-section calculation methods** may be used to determine the ultimate loadbearing capacity of a heated cross section and to compare the capacity with the relevant combination of actions. Informative Annex B provides two alternative methods**, B.1 "500°C isotherm method" and B.2 "Zone method" for** calculating the resistance to bending moments and axial forces. Second order effects may be included with both models. Both methods are applicable to structures subjected to a standard fire exposure.
  Method B.1 may be used in conjunction with both **standard and parametric fires.** This simplified calculation method comprises a general reduction of the cross- section size with respect to a heat damaged zone at the concrete surfaces. The thickness of the damaged concrete, a_{500} , is made equal to the average depth of the 500˚C isotherm in the compression zone of the cross-section.
  Method B.2 "Zone method" is recommended for use with small sections and slender columns but is only valid for **standard fires**. The cross-section is divided into a number ($n \geq 3$) of parallel zones of equal thickness (rectangular elements) where the mean temperature and the corresponding mean compressive strength $f_{cd(\theta)}$ and modulus of elasticity (if applicable) of each zone is assessed.

- **Advanced calculation methods** – for simulating the behaviour of structural **member, parts of the structure or the entire structure**.

It shall be verified for the relevant duration of fire exposure

$$E_{\mathrm{fi,d}} \leq R_{\mathrm{fi,d,t}} \tag{4}$$

As a simplification may be the effects of actions obtained from a structural analysis for normal temperature design as:

$$E_{\mathrm{fi,d}} = \eta_{\mathrm{fi}}\, E_{\mathrm{d}} \tag{5}$$

Advanced calculation methods come out from the simulation of **thermal response,** which takes into account development and spreading of the temperature in concrete members and from the simulation of **mechanical response**, which specifies the changes of mechanical properties of concrete exposed to fire.

4. Conclusions

The paper includes review of assessment methods for structural fire design of concrete structures, presented at International workshop with worked examples: STRUCTURAL FIRE DESIGN, which took place on November 2012 in Brussels, Belgium.

It is not now simply to determine fire resistance of concrete member using the Eurocode in comparison with the method used before according to national regulations.

According to [6] and [7] is it in a real fire situation necessary to simulate the temperature development throughout the construction and consequently the reduced material strength, the reduced stiffness of the cross sections and the changed slenderness.

Acknowledgements

This paper was partially supported by grant VEGA 1/0857/11.

References

[1] http://eurocodes.jrc.ec.europa.eu
[2] STN EN 1992-1-2: Eurocode 2 Design of Concrete Structures. Part 1-2: Structural fire design, Bratislava, SÚTN 2007.
[3] STN EN 1992-1-2/NA: Eurocode 2 Design of Concrete Structures. Part 1-2: Structural fire design, National Annex, Bratislava, SÚTN 2008.
[4] M. Čabrák, Structural fire design of masonry structures – STN EN 1996-1-2 (part of lecture at course), Trenčín, 2012.
[5] M. Bellová, " Fire resistance of concrete structures according to Eurocode", 16th Conference on structural analysis. Piešťany, SR 2011.
[6] M. Kofler, D. Maierhofer, "Practical Design of Concrete Columns with Regard to Fire Resistance", Third International Workshop. Vienna, Austria, 2012.
[7] M. Cvetkovska, T. Koce, L. Ljupco, "Axial restraint effects on fire resistance of statically indeterminate RC beams", Journal of Structural Fire Engineering, ISSN 2040 - 2317. Volume 4, No. 1 (2013), pp. 47-58.

Available online at www.sciencedirect.com
SciVerse ScienceDirect
ELSEVIER
Procedia Engineering 00 (2013) 000–000
Engineering Procedia
www.elsevier.com/locate/procedia

Concrete and Concrete Structures 2013

Reliability of Asymmetrically Reinforced Columns

Ľudovít Fillo*, Marek Čuhák, Tamás Porubský

Slovak University of Technology in Bratislava, Faculty of Civil Engineering, Radlinsk0ho 11, 813 68 Bratislava, Slovakia

Abstract

The criterion of reliability - compulsory minimal eccentricity was verified by axially loaded columns which were unsymmetrical reinforced. By design of concrete columns a condition of min eccentricity (e_{min}= h/30 resp. 20 mm) has to be fulfilled to decrease the column resistance defined by normal force N_{Rd}. This condition was supposed to increase a level of reliability of axially loaded columns but it should be substituted by restriction of normal force as it was in previous Slovak and British code. In a case of unsymmetrical cross-section or section reinforced with asymmetrical reinforcement, this requirement is not accurate as in some cases the application of the condition 6.1(4) STN EN 1992-1-1 leads to decrease of the design reliability. Results of theoretical and experimental analysis are content of our contribution.

Keywords: axially loaded concrete columns; reliability; min eccentricity;

1. Introduction

One of the conditions for the ultimate limit state design of cross-sections subjected to bending moments with axial force is the condition in clause 6.1(4) [1]. For cross-sections loaded by the compression axial force it is necessary to assume the minimum eccentricity e_0 = h/30 but not less than 20 mm, where h is the depth of the section. This condition was supposed to increase a level of reliability of axially loaded columns. In a case of asymmetrical cross-section or section reinforced with asymmetrical reinforcement, this requirement leads to a decrease in the reliability of design. In this case looks more general restriction of normal force as it was in previous Slovak STN [2] and British code BS [3](Fig.3). The aim of this presented paper was to analyze the condition and present results of theoretical, numerical and experimental analysis of reinforced concrete columns with cross-sections asymmetrically reinforced.

* Tel.: +421- 903- 403 -553; fax: +421- 252- 926 -213.
E-mail address: Ludovít.fillo@stuba.sk..

2. Reliability of columns subjected to axial force

2.1. Theoretical analysis

Effect of the condition for reduction of max resistance, represented by axial force and defined in [1] clause 6.1 (4), is graphically presented on a reinforced concrete cross-section in Fig.1. This condition is suitable for symmetrical cross-sections, which are reinforced with symmetrical reinforcement. There are other examples of max resistance definition by different codes, previous valid in Czechoslovakia STN [2] and Great Britain BS [3]. After definition in STN [2] the max resistance of axially loaded column was represented by force

$$N_{\mathrm{Rd\,maxSTN}} = \left[\left(A_{\mathrm{s1}} + A_{\mathrm{s2}}\right)R_{\mathrm{scd}} + 0.8 * b * h * R_{\mathrm{bd}}\right]\gamma_{\mathrm{u}} \tag{1}$$

where

$R_{\mathrm{scd}} = \dfrac{R_{\mathrm{sn}}}{\gamma_{\mathrm{m}}}$ R_{sn}- characteristic yield strength

γ_{m} =1.09 - steel coefficient of reliability

$R_{\mathrm{bd}} = \dfrac{R_{\mathrm{ck}}}{\gamma_{\mathrm{b}}}$ R_{ck} – characteristic cube strength (150 mm)

γ_{b} =1.5 - concrete coefficient of reliability

$\gamma_{\mathrm{u}} = 1 - \dfrac{20}{h+50}$ “global” coefficient of reliability

For a possibility to compare these codes in the same figure with different safety factors it was necessary to harmonize the load side of the safety conditions ULS. A comparison ratio, dead versus live load, was supposed 1(50:50). This corresponds to the average coefficient of reliability STN [2] γ_{STN} = 1.2 (γ_G=1.1 and γ_Q=1.3). For EN [1] γ_{EN} = 1.452 (γ_G=1.35 and γ_Q=1.5). Than level of STN [2] resisting force was to increase about γ_{EN}/γ_{STN}=1.19.

After BS [3] 3.8.4.3 the max resistance of axially loaded column was represented by force.

$$N_{\mathrm{Rd\,maxBS}} = 0.75\left(A_{\mathrm{s1}} + A_{\mathrm{s2}}\right)f_{\mathrm{yk}} + 0.4 * b * h * R_{\mathrm{ck}} \quad \text{where} \tag{2}$$

R_{ck} *– characteristic concrete strength*

The similar process was done by the comparison EN [1] versus BS [3]. The comparison ratio, dead versus live load, was also supposed 1(50:50). This corresponds to the average coefficient of reliability BS [3] γ_{BS} = 1.5 (γ_G=1.4 and γ_Q=1.6). For EN [1] γ_{EN} = 1.452 (γ_G=1.35 and γ_Q=1.5). Than level of BS [3] resisting force was to decrease about γ_{EN}/γ_{BS}=0.95.

In a case of an asymmetrical cross-section or a section reinforced with asymmetrical reinforcement, this requirement [1] clause 6.1 (4) was not correct. In some cases the application of this condition leads to decrease in reliability of design. Interaction diagram (Fig.2) illustrates the possible ambiguity by definition of max resistance by min eccentricity. Therefore the previous restriction of the max resistance by the max axial force, as it was presented above in the codes STN [2] and BS [3], could help to avoid the ambiguity presented in Fig. 2 and 3.

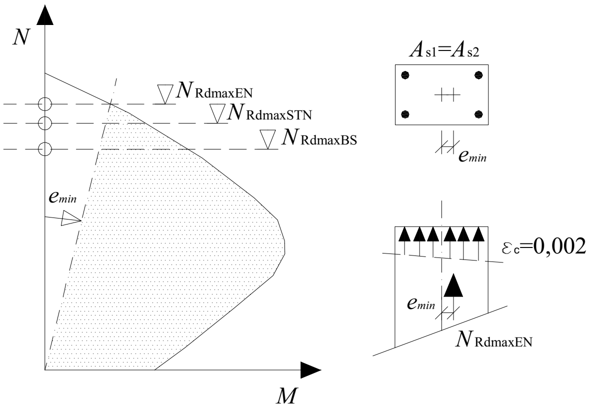

Fig.1 Symmetrical cross-section with symmetrical reinforcement

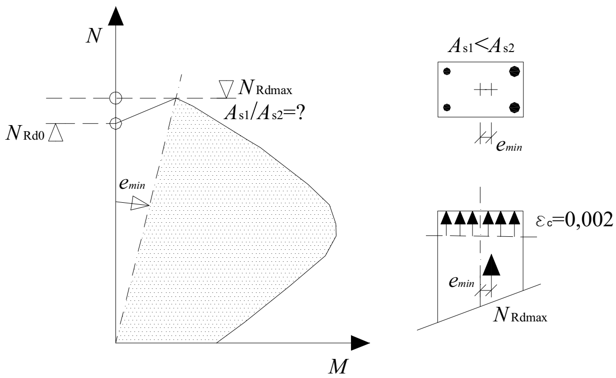

Fig.2 Symmetrical cross-section with asymmetrical reinforcement

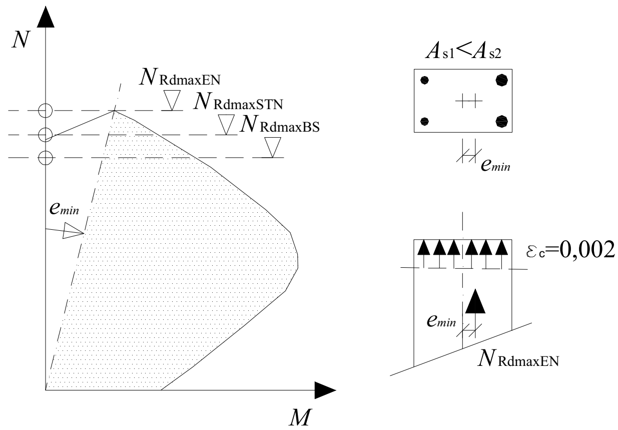

Fig.3 Symmetrical cross-section with asymmetrical reinforcement

2.2. Numerical and experimental analysis

The explanation of the EN 1992-1-1 clause 6.1(4), which application could lead to decrease of the design reliability was one of the reasons for experimental tests of columns made of the concrete normal C 40/50 and HPC 70/85 respectively. These columns with asymmetrically reinforced cross-sections (4ϕ20 versus 2ϕ10 - Fig.4) were verified experimentally and numerically. The columns 1500 mm long with a cross-section 220 mm x 160 mm (b x h) were tested on a press equipment with the max compressing force 6 MN. Columns were subjected to axial force acting on eccentricity 10 mm in the both directions. The results of the experimental tests are compared with theoretical and numerical analysis on diagrams N-y (Fig.7), where the normal force resistances of experimental tests is decreased between 2 to 6 %. This phenomena was probably caused by the support conditions, the application of force which caused the change of critical cross-section with crushing of

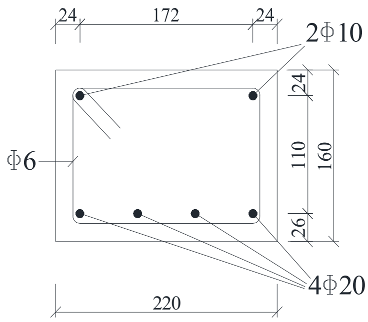

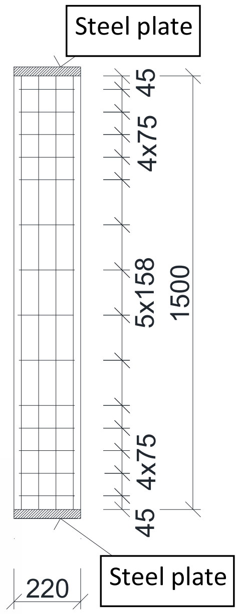

Fig.4 Characteristic of column with cross-section and asymmetrical reinforcement

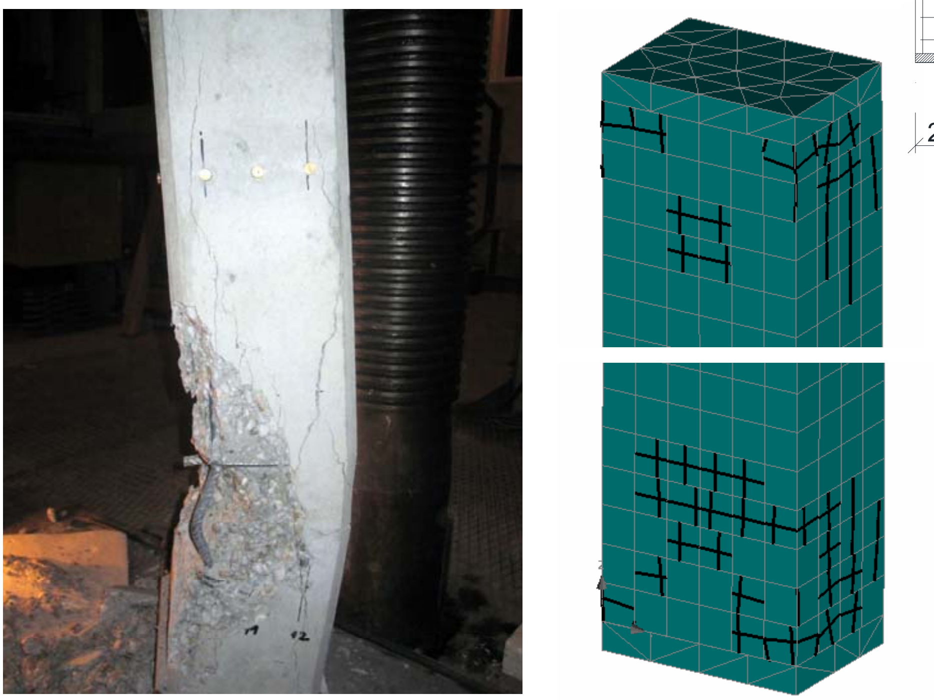

Fig.5 Comparison of experimental and numerical mode of failure

compressed concrete near the supports (Fig.4 and 5). The columns were subjected to eccentrically acting force through steel plate which was not directly connected to reinforcing bars. By the numerical analysis it was not possible to simulate a concrete layer between the steel plate and reinforcing bars. On Fig.5 there are also results of numerical analysis with cracks in support regions. On Fig.6 there is a part of interaction diagram with a path of force by both eccentricities 10 mm on the left and right hand side of the vertical axis for normal force. The theoretical, numerical and experimental results for both eccentricities are in the Table on Fig.6.

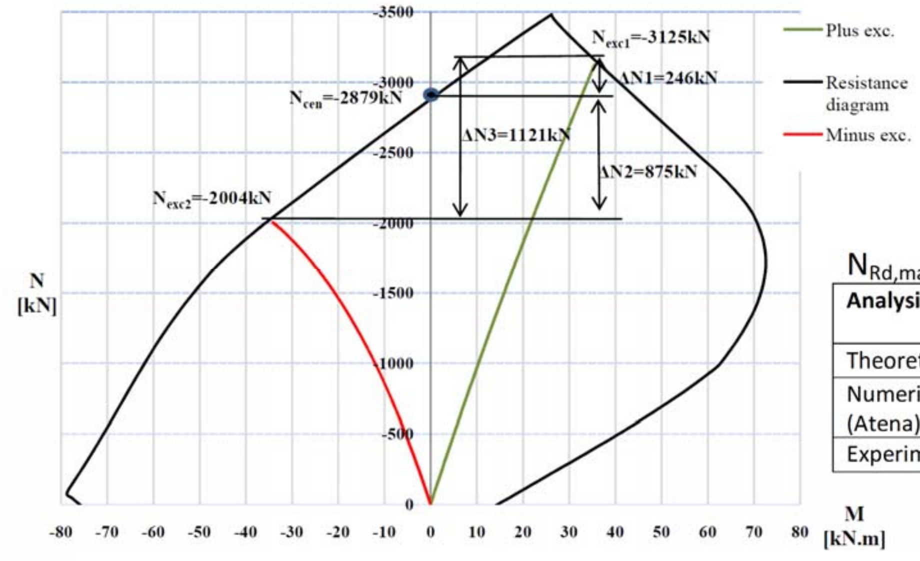

$N_{Rd,max}$ [kN]

Analysis	Minus eccentricity	Plus eccentricity
Theoretical	2074	2935
Numerical (Atena)	2048	3000
Experimental	2020	2780

Fig.6 Interaction diagram for cross-section with asymmetrical reinforcement and comparison of results

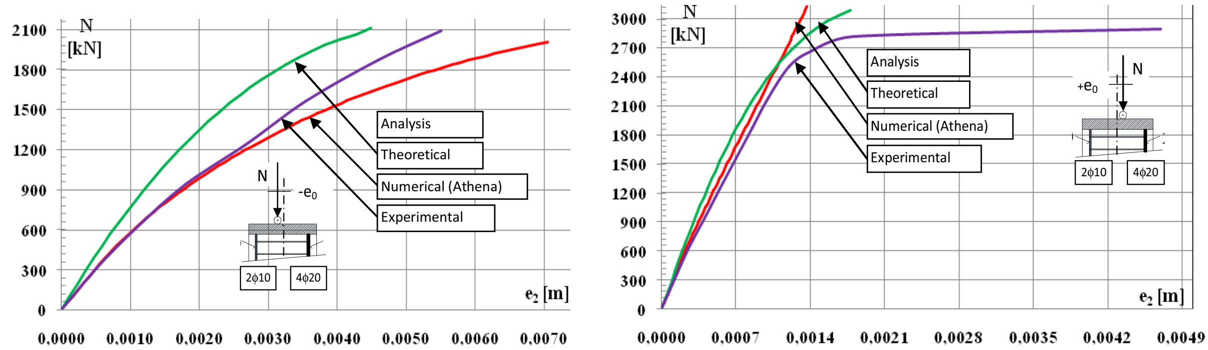

Fig.7 Comparison of results for minus and plus eccentricity

3. Conclusions

The paper deals with the reliability of columns predominantly subjected to axial force. The condition in clause 6.1(4) [1] brings the compulsory, minimum eccentricity e_0 = h/30 but not less than 20 mm, to design of columns subjected to axial force with the aim to increase a level of reliability. In the case of asymmetrical cross-section or section reinforced with asymmetrical reinforcement, this requirement leads to a decrease of design reliability. In this case restrictions of normal force in previous Slovak STN [2] and British code BS [3] look more general. The aim of this presented paper was to analyze this condition and present results of theoretical, numerical and experimental analysis of reinforced concrete columns with cross-sections asymmetrically reinforced.

Recommended is the modification of the clause 6.1(4) [1] to erase the possible mistakes and presented ambiguities. A proposal can be applied with definition of max level of axial force resistance and can be valid for cross-sections design in general, even for the biaxial bending with axial force. This proposal takes into account the increased level of reliability in cases the materials are utilized to the full plastic value. The application of such proposal is even more important for reinforcing steel with the characteristic yield strength less than 460 MPa.

Acknowledgements

Authors gratefully acknowledge Scientific Grant Agency of the Ministry of Education of Slovak Republic and the Slovak Academy of Sciences VEGA No. 1/0857/11 and also ZIPP Slovakia for help by generation of experimental samples - reinforced concrete columns.

References

[1] EN 1992-1-1: 2006 Design of concrete structures. CEN Brussels 2004. 225pp.
[2] STN 73 1201:1986 Design of concrete structures. Praha 1986. 282 pp.
[3] BS 8110-1:1997 Structural use of concrete. BSI 30 NOV 2005. 159 pp.
[4] S.L. Burtscher, G. Rinnhofer, V. Benko, J. Kollegger, Experiments of HPC Spun concrete columns to failure. (In German). Bauingenieur, Band 78, April 2003, p. 187-193.
[5] V. BENKO, Non-linear design of reinforced concrete members. (In German) In.: Innovationen im Betonbau 27. ortbildungsveranstaltung, Österreichische Vereinigung für Beton- und Bautechnik Heft 47/November 2001, p. 9-12.
[6] B. Westerberg, Second order effects in slender concrete structures. Stockholm: KTH, 2002. 98 pp.
[7] FIP Recomendation: Practical Design of Structural Concrete. fib (CEB-FIP) 1999. 113 pp.
[8] J. Bilčík, Ľ. Fillo, V. Benko, J. Halvoník, Concrete structures. Design after EN1992-1-1. Bratislava 2008, 374pp (in Slovak).

Design of Concrete High-rise Buildings

Ivan Harvan[1] Iyad Abrahoim[2]

Abstract:
Computation analysis of high-rise buildings. Tube on the perimeter of the building bound to inner constructions. Reduction of the high-rise buildings' horizontal deflection. Effective shapes of buildings. Reduction of the outer horizontal dynamic effects.
The article contains overview of optimal construction systems of concrete high-rise buildings and superstructures, depending on the amount of levels, static action, history of development and brief description of the highest concrete structures realized worldwide.

1. General definition of the problematic of tube load-bearing system computation analysis

Perimeter tube can take over all of the horizontal loads and it can be strengthened by means of diagonal bonds of certain configuration (see fig. 1 d, e). Calculations related to the tube can be performed with various degrees of mathematical complexity and preciseness. For the *preliminary confirmation of efficient horizontal rigidity of the tube*, we can use a modified cantilever model with cross-section replacing the actual tube (we use average thickness of the perimeter wall, taking windows into account). *Detailed analysis* utilizes 3D models in computer programs based on the finite elements method. While modeling the whole load-bearing construction of a building, which consists of various reinforced concrete elements (slabs, vertical walls and columns, perimeter tube formed by vertical, horizontal and sometimes diagonal construction members), we use framed models and 2D finite elements.

The problem of detailed theoretical *analysis of a high-rise building by a program* in the computer can be the assignment of global stiffness matrix of the load-bearing construction and the solution of a huge system of linear equations with adequate real-time precision (there are at least 6 deformations in every node of the finite elements grid). The second phase of program analysis of the high-rise construction or superstructure includes automatic *reinforcement design* in all of its load-bearing elements in accordance with the clarified standards. In case we consider all the freeness degrees of the finite elements in the FEM nodes, we can obtain generally co-operating inner forces in the sections of elements (in three orthogonal planes of space, there are bending moments, torsion moments and lateral forces acting vertically on the axis or centre-plane, normal and shear forces acting in the direction of the axis or centre-plane), and so it is necessary to take this fact into account when designing the reinforcement in the examined elements. The basis of the correct design of load-bearing construction is in the equality of work of the inner forces and the outer load. Neglecting one of the inner forces when designing the reinforcement of a load-bearing construction member can lead to lower reliability of load transfer by the whole load-bearing construction.

As an example, we can use a computer modeling of joint of a multi-span monolithic ceiling slab with its supports by means of FEM. We usually do not consider the torsion stiffness of edge beam (as thought the support between the slab and the beam was a hinge joint). Be doing this we get zero bending moments in the supports of the slab in the orthogonal direction to the edge beam's axis (in the real stiff junction, these moments have negative amounts due to the torsion capacity of the edge beam, which means that we allow cracks on the upper surface of the slab and gradual development of a hinge support). This means increase in the values of moments in the centre of the slab (and increased required area of reinforcement in the span of the slab) and the edge beam withstands only a mildly

[1] Ivan Harvan, Doc. Ing. PhD., Stavebná fakulta STU v Bratislave, Radlinského 11, 813 68 Bratislava
tel. 02 - 59274 557 E-mail: ivan.harvan@stuba.sk
[2] Iyad Abrahoim, Ing. PhD., Stavebná fakulta STU v Bratislave, Radlinského 11, 813 68 Bratislava
tel. 02 - 59274 551 E-mail: iyad.abrahoim@stuba.sk

increase vertical longitudal bending (longitudal reinforcement design) and shear without torsion moments (lateral reinforcement design). It is, of course, necessary to secure such concept modifications of static action of construction elements by suitable reinforcement arrangement. In the described example of the outer support design, it is required that half of the lower reinforcement of the slab is bent towards the upper surface in one sixth of the span and anchored over the face of the beam (minimum length is the design anchor length l_{bd}). In case the model considers the real stiff joint of the slab with the edge beam, we obtain more actual basis for the edge span and span reinforcement designing (represented by the values of bending moments acting vertically against the edge beam), but torsion moments occur on the edge beam as well. The impact of such moments on the longitudal and lateral reinforcement in the beam must be *considered interactively in the course of reinforcement design* according to the standards as vertical bending moments, lateral forces and torsion moments.

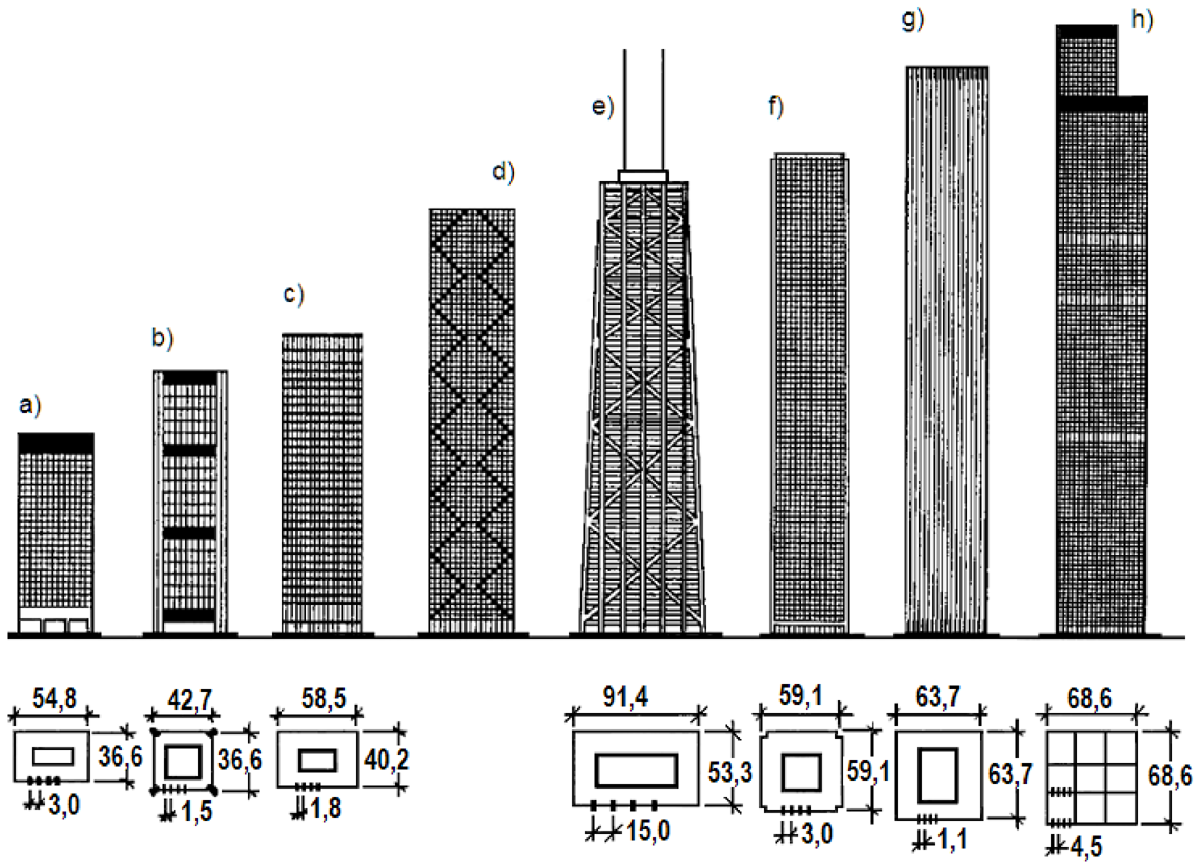

Fig. 1 High-rise constructions based on the perimeter tube enhanced by inner stiffening core, an inner tube. Division of the tube into multiple sections (h)

The above stated example of simplified modeling of co-operating load-bearing construction members (the slab and the edge beam) becomes more complex when applied to a 3D model of a building in case we use fully-fledged junctions on all the load-bearing elements of the construction to the nodes of FEM grid in the direction of all the freeness degrees. This leads to occurrence of additional bending moments and lateral forces on the edge beam apart from normal forces, and the occurrence of membrane forces and shear forces in the slab, acting in the direction of its centre-plane.

It is necessary to realize that we ignore the tensile strength of concrete in the examined section when designing the reinforcement and the designing itself thus becomes non-linear. There is no way we can apply the superposition of the results of individual reinforcement design of each element in the final amount and arrangement of the reinforcement in the examined element. In the process of design itself, it is crucial to *consider all the inner forces in the course of reinforcement design* individually in all load combinations. Such designing methodology can be theoretically demanding in many cases of multiple forces acting at the same time. For example, the critical compressive normal force can act on a column which also withstands bending moments of considerable values in two orthogonal directions.

This strain can be combined with two additional orthogonal lateral forces and a torsion moment in the examined section. Furthermore, it is necessary to take into account the effects of random eccentricities and deflection of a subtle element in case we analyze compressed construction members.

For this reason it is convenient to ignore some of the additional inner forces in theoretical calculation of some load-bearing members, based on the fact that ignoring the results in a mild increase of other inner forces crucial to the reinforcement design. In such speculations, it is necessary to realize, that construction arrangement of the reinforcement must consider the possibility of occurrence of additional inner forces. The design of reinforcement in a column supporting a beamless slab inside a building can be used as an example of such simplified solution. In the computation 3D model of a high-rise building, we can approximate a hinge joint of the ends of the column with the upper and lower ceiling slab, with freeness for horizontal torsion moments. The bending and torsion moments and the lateral forces will then equal to zero, which means that we base the reinforcement design on the compressive normal force together with the effects of designed imperfection and the effects of the 2nd grade moments. Such simplification leads to mild increase in the values of bending moments in the slab mainly due to variable location of the utility loads and, at the same time, to ignoring the bending stiffness of columns when analyzing the horizontal stiffness of the high-rise building against the horizontal loads. In other words, the columns do not take any fraction of the horizontal loads, as these are taken over by the stiffening walls, cores or the perimeter tube. This simplification of the column analysis is much closer to monolithic joints to the ceiling slabs, thus making the slabs thicker and the sections of columns more subtle.

2. Perimeter tube

• Tube in the shape of a spatial grid without diagonal elements

This type of tube is based on the perimeter walls consisting of densely arranged columns with parapet beams stiffly joined, orthogonal to each other. The tube withstands the whole horizontal load without utilizing the inner elements. The inner columns only act to withstand the vertical load and are not consequential in the horizontal stiffness of the building (fig. 2a). Horizontally stiff slabs stabilize the shape of the tube in each level and they transfer the horizontal loads to the densely latticed walls of the tube. The load-bearing construction of a high-rise building can also include concrete communication cores with wall thickness up to 200 mm (fig. 1), with the less important horizontal stiffness of such elements sometimes being ignored in comparison to the considerable horizontal stiffness of the perimeter tube.

A tube in the shape of a grid without multi-level diagonals (fig. 1a, b, c, f, g, h) is a logical evolution of the constriction scheme of a traditional skeletal building. Such scheme is characterized by increased horizontal stiffness even against torsion of the construction, but meets the requirements related to creating open spaces in each level. The grid of columns in the perimeter walls is very dense, but it can be fully accepted in terms of application of window glazing. The above described tube construction is efficient for buildings up to 60 storey high.

It would be ideal in relation to the calculations, if the tube walls weakened by windows acted as one single unit against pure bending cause by horizontal load. In that case, all the columns in the grid would act analogically as longitudal threads of a plate girder, with the strain being linear and limited by axial compression or tension. This limitation of column strain is illustrated by dashed line in the fig. 2b.

However, the actual acting of the tube section is influenced by two schemes of the building's deformation – the deformation of a cantilever girder and the deformations of the framed perimeter system. The sides of the tube parallel with the direction of the wind try to act as independent multi-span frames of certain stiffness of the short perimeter girders. This stiffness is the result of their bending and lateral shear deformations, which manifest as *deplanation impacts* in the side walls of the perimeter tube. The perimeter columns and girders themselves only withstand simple bending. The impact of deplanations of the tube's section under the effect of horizontal load manifests in the non-linear allocation of the axial loads among the columns of the tube, which acts as a perimeter shell construction. Consequently, the corner columns bear greater axial strain N_1 than the internal columns with the smallest force N_2 in the centre (full-lined illustration of column strain in the fig. 2b). Moreover, the spatial shape of the building is similar to a bent cantilever girder with the proportion

H/B > 4:1, while the importance of vertical shear deformations in the tube walls increases with the proportion H/B < 4:1. Their influence is consequential in resolving the static effectiveness of the perimeter tube. To put it simply, we can say that the deplanations of the tube's section increase with lower proportion of H/B to the building's width.

počet podlaží	H/B	N_2/N_1
30	2,4	4,92
56	4,4	3,18
84	6,6	2,34

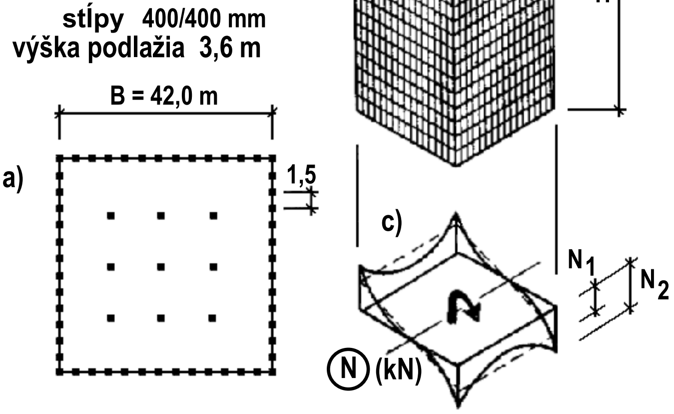

Fig. 2 Square tube formed from a grid of columns and thick parapet girders around the perimeter of the building without diagonal elements (fig. 1) and its vertical membrane strain caused by horizontal load

• Tube in the shape of a spatial grid with diagonal elements

Flexibility of the edge beams is the most important defect of tubes in the shape of spatial grid without diagonal elements. Their bearing capacity against the effects of horizontal load can be considerably increased by placing additional diagonal bonds into the perimeter tube (fig. 4 constructions 1, 2, 4 in [3] and fig. 1 d, e). In that case, the vertical shear strain caused by horizontal loads is not borne by the edge beams, but it is transferred directly into the diagonals which bear axial forces. Lowering the shear deformations in the tube's walls leads to the load-bearing construction's horizontal deformation being more statically effective and it becomes similar to the deformation of a bent cantilever girder.

N case of concrete buildings with multi-storey diagonal elements (fig. 1d,e), it is possible to increase the horizontal distance among the columns of the perimeter tube and so lower the impact of deplanations in comparison with the tube without diagonal elements. Axial compressive strains in the diagonals help us efficiently eliminate tensile stresses caused by the horizontal forces. Consequently, due to the application of diagonal elements, the construction becomes noticeably stiffer and statically effective even for very high concrete buildings with the height up to approximately 90 levels. Concrete diagonal construction members are placed in front of the façade itself, or they can be simply formed by filling the diagonally arranged windows with load-bearing wall members in the full height of the storey. In this way they become an important and noticeable architectural element of the building's façade.

The application of diagonal elements in the perimeter tube of a high-rise building is a highly effective solution for transferring the horizontal load, but it is a lot less effective when considering the vertical load transfer than the vertical columns. Furthermore, the considerable amount of more complex and more time-consuming bonds of diagonal elements, together with difficult window arrangement in the façade, make the solution consisting of grid tubes with diagonal elements usually less acceptable.

3. Perimeter tube bond to inner constructions

The perimeter grid tube can be strengthened b an internal complex of vertical diagonal elements, usually stiffening walls or cores. Some of the principles of construction arrangement of bonds with the inner load-bearing members will be stated in the following part.

• **Perimeter tube with parallel stiffening walls**
Horizontal stiffness of the perimeter tube can be increased by incorporating the inner stiffening walls into the overall load-bearing construction of a high-rise building. We can imagine the walls of the perimeter tube acting as flanges, thus being a part of a composite section of a vertical girder system, with the stiffening walls acting as the wall of the girder's section. The strains in the perimeter tube consist of the amount of vertical axial forces in each of the columns, with the unpleasant deformation caused by vertical shear (i.e. deplanation, fig. 2) being reduced to minimum.

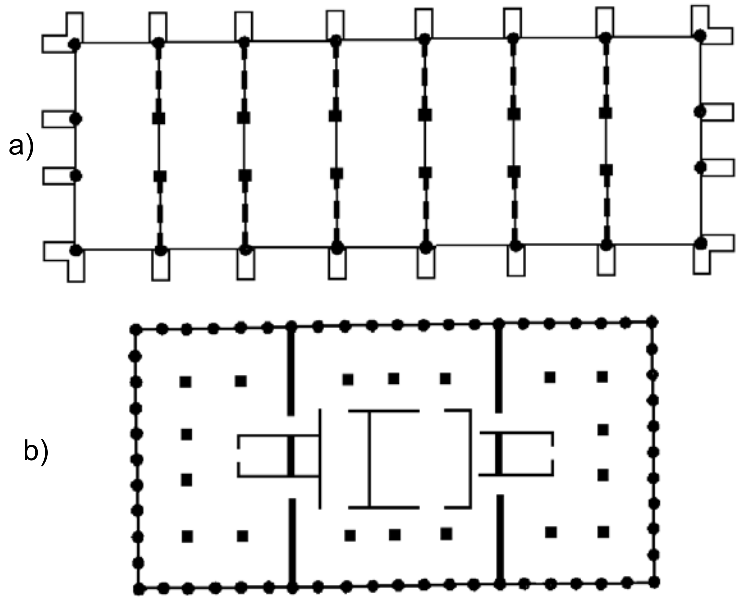

Fig. 3 Perimeter tubes co-operating with the lateral stiffening walls. a) wider distances between the bulk perimeter columns with huge support from the walls, b) smaller distances between subtle columns with only two internal walls

The examples in fig. 3a, b provide sufficient documentation of two possible concepts of bonds between the perimeter tube and the inner stiffening walls: wide distances between the perimeter columns strengthened by walls, and small distances between the perimeter columns with only two stiffening walls.

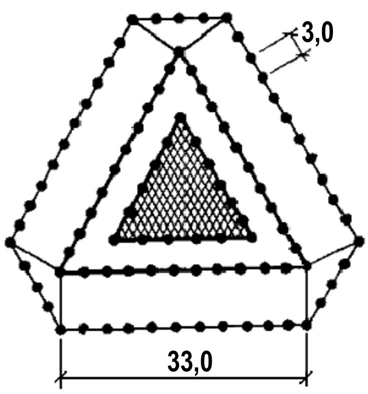

Fig. 4 Perimeter tube of a high-rise building co-operating with two additional inner tubes. The inner tube also serves as the core of the building.

• **Perimeter tube with central stiffening core**
Horizontal stiffness of a perimeter tube can be enhanced by the application of an inner stiffening core mechanism into the overall load-bearing construction of a high-rise building (fig. 1 a – g). The stiffening core bears not only the corresponding vertical load, but a part of the horizontal load of the high-rise building as well. The slabs bind the perimeter tube to the inner stiffening core in such a way, that both construction members act as a single unit against the horizontal load. Co-operation of the perimeter tube with the inner stiffening core manifests when we check the resulting shape of horizontal deflection of a high-rise building. As the deflection shapes are different for the core and the tube, the stiffening core tears away from the tube in the upper part of the building and pulls towards it in the lower part. The perimeter tube thus bears greater portion of the horizontal load in the upper levels, while the stiffening core bears greater portion of the horizontal load in the lower part.

While following the above-described principles, we can look at the load-bearing system of a 60-storey administration building in Tokyo, where the designers applied three tubes illustrated in the fig. 4. Within the load-bearing construction, the wind loads were considered as being borne solely by the perimeter tube, but all the tubes are connected by floor slabs and they act against the seismic load, which is a very important factor in engineering design in Japan.

• **Modified shape of the perimeter tube**
Utilization of tube load-bearing systems is most efficient in buildings which are circular or almost square in their floor-plan shape. With special modifications of the building's shape, it is necessary to adhere to certain exceptional precautions to secure the co-operation of the whole load-bearing construction of the high-rise building. These precautions can be demonstrated on the following example.

Grid tube strengthened by stiff frames. Hexagonal shape of a 40-storey administration building in the fig. 5 made the designers change the principles of perimeter tube system solution. Sharp angles in the hexagon cause increased concentration of vertical shear forces in the tube, thus making effective utilization of tube load-bearing system more complicated. By incorporating additional stiff frames in the lateral direction, we can bind the perimeter walls of the tube together via the interior. In this case, the walls in the triangles were stiffened by frames and together with columns they form additional inner tubes in the forefronts of the building, providing ways to enhance the tube construction's static effectiveness by more equal distribution of the axial strain among the columns on the perimeter of the building

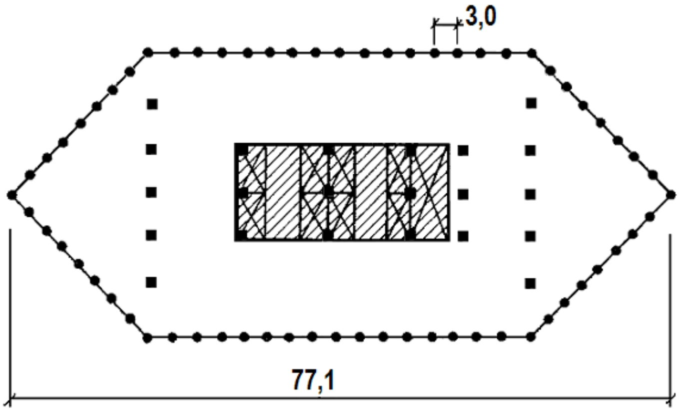

Fig. 5 Hexagonal shape of the perimeter tube strengthened by stiff frames

• **Tube with multiple sections**
One of the main trends of tube constructions' development leads to the application of multi-sectional systems, thus forming multiple division of space inside the tube into single modules (fig. 1 h). Such arrangement of the load-bearing construction is suitable even for very high buildings with up to 100 levels.

Horizontal stiffness of perimeter grid tubes is increased by orthogonal inner walls formed by denser grid of columns (fig. 6), which are joined by stiff header joist. This creates a unified tube divided into multi-sectional modules. The sections themselves can bear the loads individually, they can be bound together into optional shapes and they can be formed in any height level. This means we can apply the multi-sectional tube in the lower part of the building, where the bending moments and shear effects of horizontal loads have higher values. We can skip the stiffening walls between the tube sections gradually as we go higher, with the system slowly evolving into unstiffened perimeter tube in the last 60 to 80 levels. Another advantage of the multi-sectional tube construction system is the possibility of creating bigger open spaces for the interiors. The inner intersection walls act against the shear effects exactly as the walls of a cantilever girder with composite cross-section and they lower the vertical chamfer, i.e. the deplanation. Apart from this, the inner walls placed in the orthogonal direction to the direction of the wind provide additional bending capacity against the effects of horizontal loads (the bending inertia enhances the 2. member of the Steiner's formula, i.e. the area of a section multiplied by quarter of its distance from the central axis of the building's floor-plan section).

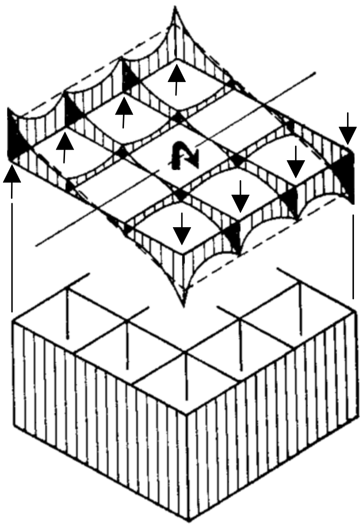

Fig. 6 Increase in the bending capacity of perimeter tube by means of its division into multi-sectional modules. Vertical strain in the tube under the action of horizontal load is influenced by the deplanation of its cross-section (compare to the fig. 2)

The actual acting of such system is characterized by the distribution of vertical axial strains within the multi-sectional tube in the fig.6. The walls between sections, being parallel with the direction of wind, take part of the horizontal shear and contribute to the concentration of vertical strain in places where the orthogonally oriented walls intersect, with the character of bending effects being different for each of the inner sections. It is important to emphasize the differences of vertical strain in the section in comparison with undivided perimeter tube (when there are no internal walls) in the fig. 2. Vertical walls of a multi-sectional tube help to distribute vertical axial strain equally, but the impact of longitudal chamfer caused by vertical shear (deplanation of its section) is still important. Nonetheless, the deviations from the dashed-line curve of the vertical strain in the ideal vertical cantilever girder are not that important.

4. Design of high-rise buildings regarding the limitation of their horizontal deflection

The effects of wind and seismicity have become consequential factors in the trend of high-rise buildings' design these days. When using materials of high strength, we also decrease the measurements of load-bearing construction members and the building's weight, which leads to high slenderness of high-rise buildings and their tendency to react to aerodynamic effects.

Recent superstructures are characterized by increased horizontal deflections and oscillation in comparison with heavy high-rise buildings from previous periods. For example, the famous American skyscraper Empire State Building (built in 1931) has the horizontal deflection of only 165 mm ant the oscillation amplitude of 183 mm. Its maximum deflection then equals $165 + 183/2 = 258$ mm with the wind speed of 130 km/hr. Empire State Building was designed as a composite load-bearing system made of steel and concrete (skeletal system with stiffening walls) and its highest floor is 381 m above the terrain level (the tower building is not included). Maximum deflection is then approximately 1/1500 of its height. The total proportion of the building's height to its width is 9,3.

Limitation of dynamic response of high-rise buildings can be achieved by the following methods:
– increasing the horizontal stiffness of the building by using a more effective construction scheme,
– increasing the building's weight (unacceptable),

– selecting the effective shape of the building,
– creating additional forces within the building to balance the outer horizontal dynamic effects..

Last two options will be described in detail in the following two chapters, using specific examples.

4.1 Effective shapes of a building

Multi-storey buildings are usually designed as having the shape of right-angled prisms and they are vulnerable to horizontal displacements. Buildings of other shapes are not that sensitive to horizontal load. Being stiffer due to their geometric shape, these buildings have highly positive technical-economical indexes; respectively, they allow greater height of the building at much lower cost of constructing. Notice some shapes of such buildings.

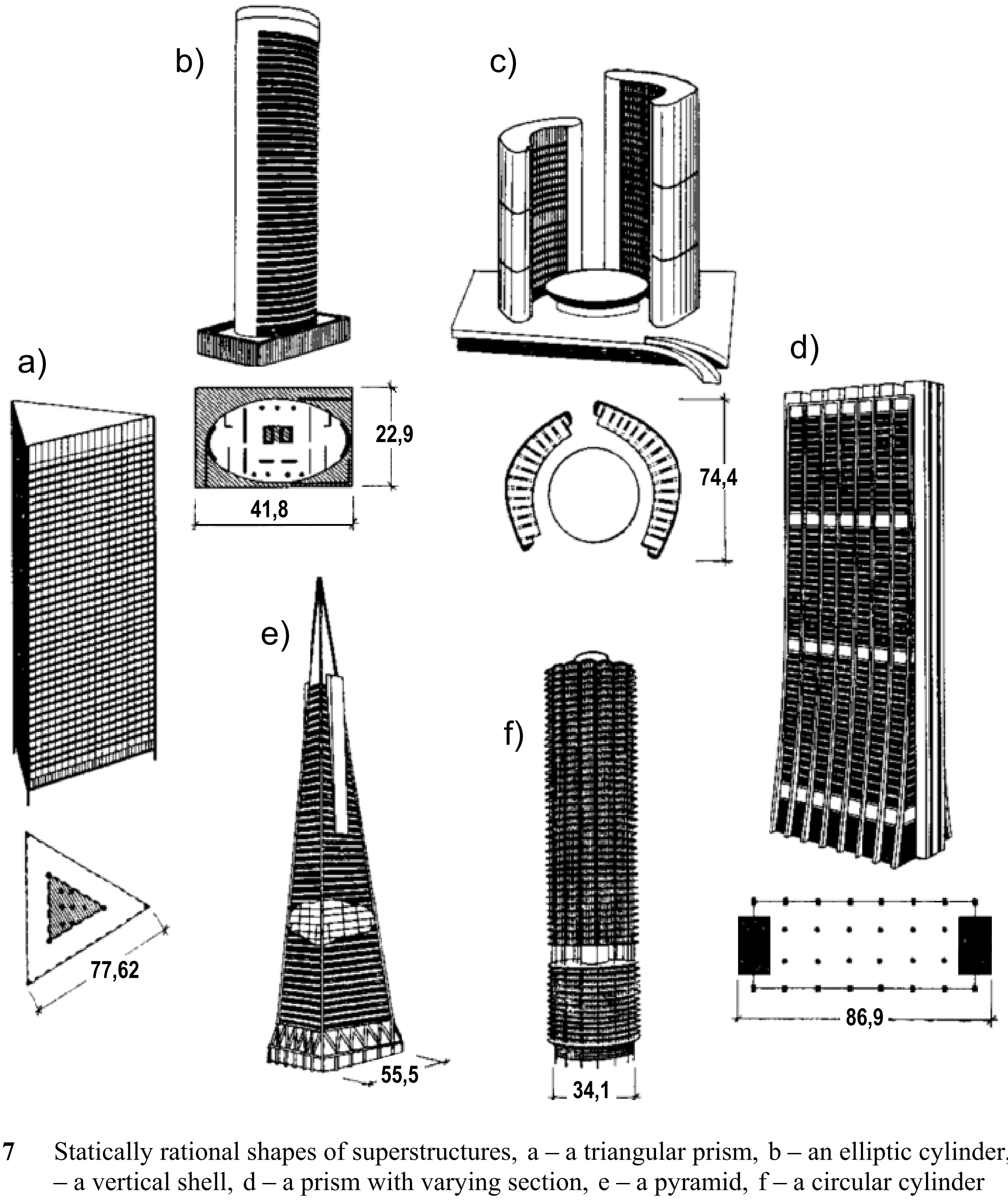

Fig. 7 Statically rational shapes of superstructures, a – a triangular prism, b – an elliptic cylinder, c – a vertical shell, d – a prism with varying section, e – a pyramid, f – a circular cylinder

Stiffness of a building can be greatly enhanced by use of inclined perimeter columns, thus leading to the shape of a walloped pyramid. Horizontal deflection is reduced by 10 to 50%, with the results being most remarkable in high and narrow buildings. FEM calculations by computer have proven that with an inclination of only 8°, the reduction of a 40-storey building's horizontal deflection amounts to 50%.

A complete pyramid of a 50-storey building illustrated in the fig. 7e is a variation of a walloped pyramid. This 260 m high building consists of perimeter frames with stiff bonds, having only four corner columns. Every perimeter frame is A-shaped. The inner vertical columns do not intersect with the inclined perimeter columns. They are divided at the 4,6 m level into intersections with the inclined columns of the lower level. The inner columns only serve to support the ceilings.

Reduction of horizontal deflection of a building can be achieved by narrowing the perimeter cage upwards exactly as the 60-storey building in fig. 7d shows. The inclination of perimeter columns is designed in the lower third of the building's height. The advantages of such a building fully manifest when the building narrows along its full height.

Cylindrical shape of a building provides spatial co-operation of the whole load-bearing construction against the horizontal load (fig. 7f). A typical tower consists of a circle of columns around the perimeter of the building and around the corridor next to the stiffening core. These columns reduce the required measurements of radial girders and they distribute the loads into the foundations. The core bears approximately 70% of horizontal forces. The fenestras in the core are arranged in each level in such a way, that the horizontal stiffness of the core remains intact.

Apart from the advantage of spatial acting of cylinder-shaped building, there is also smaller surface acting against the pressure of wind. In comparison with prismatic buildings, the value of wind pressure is reduced by 20% to 40%, due to the more favorable value of the aerodynamic index which differs considerably from the values used stated for prismatic buildings.

Ellipse-shaped buildings have similar advantages to those of cylindrical ones. The wind load on the building shown in the fig. 7b is reduced by 27%, owing this to the building's elliptic shape. In the demonstrated building, the horizontal loads are transferred by the central stiffening core and the inner and outer load-bearing walls as well. As the system of walls distributes the horizontal load to a great area of the building, the required foundation depth is not that high. With buildings of elliptic shape, the value of wind pressure is reduced by 10% to 30%, due to the more favorable value of the aerodynamic index in comparison with buildings of rectangular type.

Triangular prism is another effective configuration of a high-rise building. Figure 7a shows a 175 m high building, with its perimeter walls being formed by Vierhendel girders (framed girders consisting of stanchions and a beam serving as the upper and lower flange). These one-storey-high girders distribute the vertical load to the corner columns, with the horizontal loads being borne by horizontally stiff ceilings and transferred into the inner core.

The building can be shaped as a crescent or a winding arc to enhance its horizontal stiffness. The static action of an arc against the effects of horizontal load resembles deformation scheme of a shell construction. Fig. 7c shows a building of such system, consisting of two towers in the shape of crescent arc, the towers having 20 levels (78 m) and 27 levels (100 m) and protruding over a common two-storey stage. The load-bearing system of these towers consists of radial beams leading from the inner circle of columns to an outer vertical shell without any windows. The beams' edges are cantilevered, with the length of 2 m, in order to serve as supports for the facade panels inside the arc. Ceiling slabs are placed on the radial beams. Vertical load is borne by the inner columns and ant the cage of the shell. The horizontal load is borne by the vertical shell. Its stiffness is enhanced by cumulative effects of ceilings which serve as bracing ribs.

Crescent shell is an effective shape when the horizontal load acts symmetrically. However, with asymmetric load, it becomes highly irrational. Various torsion strains occur, being balanced by high vertical girder cantilevers at the ends of the towers in the building shown on fig. 7c. The bent shape of the shell, together with short distance between the towers, leads to a considerable increase in the wind pressure. Measurements in an aerodynamic tunnel have shown that the value of air suction on the edges of the building is four times bigger than the engineering standards assumption.

Locating high-rise buildings close to one another is a general problem relating to the trend of their additional realization, with the intense build-up not being predicted. Air flow, air turbulences occurrence, and various difficulties with assuming the wind action on the buildings connected to these phenomenons in ever-changing and unfavorable conditions of high-rise building complexes can make their use as residential buildings much more complicated (higher horizontal deflections and oscillation).

4.2 Limiting the outer horizontal dynamic effects

There are various unconventional ways of limiting the horizontal deflections and oscillation of high-rise buildings. Every one of them relates to the dynamic effects in the first place and rarely considers quasi-permanent reactions of the building against the outer impulses initiated by horizontal effects.

One of the ideas how to limit the horizontal displacements is **incorporating vertical pre-stressed ropes into the load-bearing construction**, which induce deformation of opposite direction (fig. 8). It is not necessary then to enhance the horizontal stiffness by means of increasing the mass of the construction, as can sometimes be required for securing the resistance against maximum wind load once in 100 years. The cables placed close to the perimeter walls are joined to the compactors, which are anchored in the foundations of the building. Sensors in the sections above the ground level evaluate the wind speed and direction. This information is then passed to the electronic control block, which switches the hydraulic compactors to tension some of the cables. Such eccentric pre-stressing evokes bending moments along the building's height, with these having the opposite direction to the moments evoked by the wind. This causes the resulting bending moments to balance and it helps to reduce the horizontal deflections considerably. The value of pre-stress force in the cables and in the pre-stressed part of the building varies according to the speed and direction of the wind.

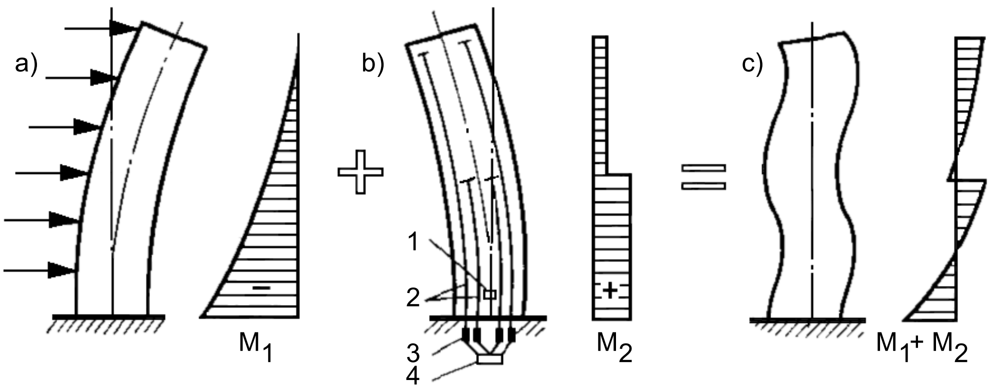

Fig. 8 Limiting the horizontal deflections by means of vertical pre-stressed cables, a) the wind load, b) the effect of tensioning the cables on the left, c) simultaneous effect of pre-stressed left part and the wind load, 1 – wind sensor, 2 – vertical cables, 3 – hydraulic tensioning compactors, 4 – electronic control block

Damping is another principle of reducing the effects of wind on a high-rise building. Exactly as we can use dampers to close doors slowly, we can use **energy absorbers made of vyscoelastic materials** to reduce the deflection and the oscillation amplitude of a building, the absorbers being mechanically joined to some non-bearing construction members. This principle can be realized by, for example, inserting vyscoelastic absorbers between the lower flanges of truss girders and the columns, as can be seen in the fig. 9. The name vyscoelastic material indicates that this kind of material acts elastically (it regains its original shape just like a rubber stripe) and viscidly at the same time (it is forced to creep under the action of compression, like liquid). Vyscoelastic material withstands longitudal shear cut when loaded. It does not accumulate energy like an elastic material, but transforms it into heat which is then distributed to its environment. For this reason the material does not regain its original shape instantly like a spring after removing the load, but this process passes slowly. It can thus lower the oscillation of a building, when dynamic effects of wind impulses or seismicity occur. Instead of acting like that, the building emits heat when the wind load or seismicity expands the absorbers. In civil engineering practice, vyscoelastic material is used in form of clamps, slabs or bodies on the basis of special polymers with special requirements regarding their mass being applied in the course of production.

This principle can also be used in buildings in such a way, that we adjust joints of the horizontally-acting constructions with the secondary vertically-acting framed construction. For example, the complementary ceiling construction, in which the horizontal displacements manifest, can be joined to the columns using vyscoelastic absorbers that will transform the oscillation energy into thermal energy (fig. 9). The impact of absorbers is illustrated in the fig. 10. We can see that an undampened construction has the oscillation period T in case the building itself is not sufficiently dampened (fig. 10a). When using special absorbers, the building deflects as a reaction to the first dynamic impulse, but the backward amplitude is dampened in time much shorter that the period T (fig. 10b), and the building does not start oscillating.

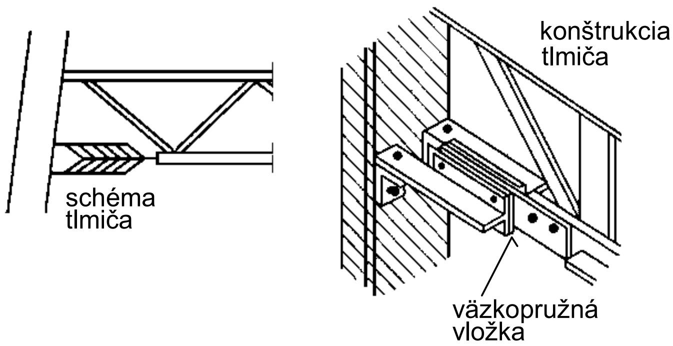

Fig. 9 Vyscoelastic absorber placed in the node of a steel frame (node A in the fig. 10)

Fig. 10 Horizontal oscillation of a high-rise building evoked by dynamic wind effects (only the damping effect of the building itself), a) without the mechanical absorbers, b) with mechanical absorbing system

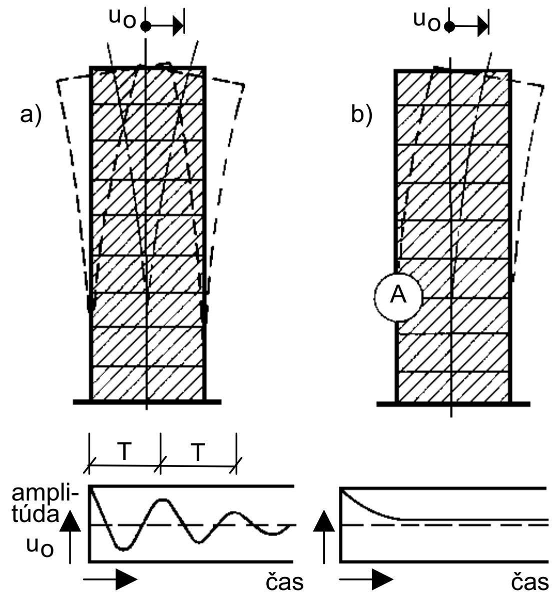

Use of mechanical absorbing system reduces the values of horizontal dynamic load caused by the wind or seismicity. This greatly reduces the possibility of occurrence of parallel dynamic effects generated by random exciting accelerations of different oscillation periods T, as is common with low-dampened oscillations accodring to the fig. 10a.

Another option is filling the thermal division gaps between the ceiling and stiffening core with vyscoelastic absorbers in the form of stripes with required thickness. The proportional deformations in the intercourse of ceiling construction and the stiff core transform the oscillation energy into the energy absorbed by the dampening system.

Another means of absorbing the energy generated by dynamic effects of the horizontal load is **forming inflectable level in the first ground level of a high-rise building**. When adhering to this idea, we assume that the ground level deforms during an earthquake and the upper part of the building acts within the limits of elastic deformations. Stabilizing walls located in the ground level (fig. 11), are designed to withstand loads greater than seismic effects and they can thus damper the displacements in the levels above them.

Many different hypothesis were examined abroad in the past, but their practical realization was incompatible the possibilities of high-rise buildings realization, or they lacked detailed schemes of their actual action. For example, one suggestion was to **use the wind pressure as the source of energy for regulating** more appropriate action of the load-bearing construction by allowing wind to permeate the building's interior in certain places. This field of study is still being examined and new directions for their practical use are being searched for.

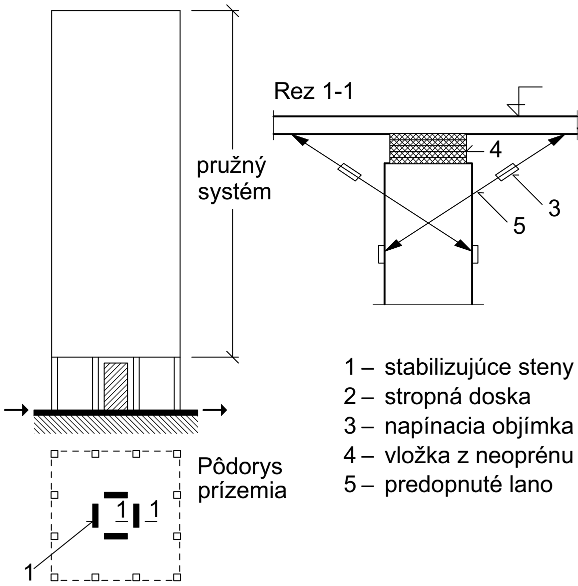

Fig. 11 Principles of checking the degree of damage caused by an earthquake by means of inflectable level which absorbs the oscillation energy

Conclusion

The above described principles of recent high-rise and superstructure design are the reaction to the boxlike forms of modern and post-modern architecture. The load-bearing constructions are usually combined steel and concrete constructions, with concrete becoming the main construction material. When designing and developing new load-bearing systems, we should not ignore the studies of rationality of a construction and its financial demands. Such studies, if they really are complex and include the overall expenses, allow responsible evaluation of a construction with attention paid even to the diminishing natural resources, as well as helping to avoid wasting those resources.

Owing to fast development of concrete constructions, materials technologies and building processes, use of concrete is increasing in the already realized and future buildings world-wide. The ability of concrete to copy the shape of crating is widely used in aesthetic representations of surfaces of constructions. This combines with other required positive characteristics of concrete, e.g. its fire resistance, but well-designed in-situ concrete can absorb the volume changes evoked by temperature, shrinking, plasticization and subsoil movements. The natural stiffness of concrete and its overall safety are important factors. In comparison with steel structures, concrete high-rise buildings are heavier and greater damping effect, which helps to reduce the perception of construction's movements. Heavier constructions are usually more stable in case of load tilting them over. Various studies world-wide state, that use of concrete or composite materials for construction systems of high-rise buildings is very cost-efficient. The amount of time needed for constructing concrete high-rise buildings is equal to the amount of time needed for steel constructions. Even though steel is a great construction material for superstructures due to its strength and ductility, it is expected that many of these buildings in various capitals world-wide are going to be built of concrete.

Resources

[1] HARVAN, I.: Vysoké betónové budovy, navrhovanie podľa spoločných európskych noriem. Vydavateľstvo STU, Bratislava 2010, učebnica, 210 str.
[2] HARVAN, I.: Všeobecné požiadavky na posúdenie účinkov vetra pri návrhu viacpodlažných a vysokých betónových budov podľa EN 1992-1-1. Zborník príspevkov z 15. konferencie Statika stavieb, Piešťany 2010. Spolok statikov Slovenska, Trnava.
[3] HARVAN, I.: Koncepcia návrhu betónových konštrukcií vysokých budov. Zborník príspevkov zo 17. konferencie Statika stavieb, Piešťany 2012. Spolok statikov Slovenska, Trnava.

THE INFLUENCE OF AGGRESSIVE CHEMICAL ENVIRONMENT ON BEHAVIOUR OF HPFRC IN CONDITIONS OF LONG-TERM BENDING PERFORMANCE

Peter Paulík and Igor Hudoba

Department of Concrete Structures and Bridges, Faculty of Civil Engineering,
Slovak University of Technology Bratislava, Slovak Republic

Abstract

The paper is dealing with the research concerning the deterioration process investigation of high performance fibre reinforced concrete (HPFRC) beams in chemical environment. The beams were exposed to long-term bending performance. The influence of degradation process on deformation behaviour of the beams was measured. Long-term deformations process of the beams placed in different environment and final failure capacity was measured and compared. The influence of degradation process on strength parameters by using of standard HPFRC specimens was measured, too. A theoretical model of bended beam degradation process was introduced.

Keywords: High Performance Fibre Reinforced Concrete, Long-term bending performance, Nitrate aggressive environment, Degradation

1 Introduction

Service life of concrete element or structure depends on its ability to resist against aggressive environment. The practical access of solving of this complex problem is by using of standard´s recommendations based on definition of environment aggressivity and concrete class. On the other hand there is a wide spectrum of factors influencing the real service life of concrete elements. Therefore there is an effort of researchers to work out more detailed calculation methods which would be more accurate in determining the service life of the concrete elements or structures
One of the most common ways of degradation of concrete elements is the process of leaching. In this process the hydration products are leached form the hardened cement matrix. Leaching process is caused by deionized water, which can weaken the cross section of the original concrete element and lead to endangering of its load-bearing capacity. In some cases of concrete elements an extreme long service life is required. For instance the box containers used for storing the low and medium radioactive waste have to fulfil the requirement of service life for more than 300 years. Aggressive water in contact with concrete is dissolving the portlandit $Ca(OH)_2$, which solubility is much higher than the solubility of other constituents of the cement matrix. The rate of water aggressivity is dependent on the amount of soluble minerals, or by other words by the water hardness.

2 Modelling of concrete degradation by leaching

For accelerated test of concrete degradation by leaching process the most often used medium is the ammonium nitrate solution (NH_4NO_3). Degradation of concrete in ammonium nitrate solution is very similar to the degradation in deionised water, but much faster. In accordance with the research results [8], in some cases the rate of degradation in ammonium nitrate solution could be about 130-times more than the rate of degradation in deionised water. The result of leaching process caused by NH_4NO_3 is the reduction of the calcium fixed in portlandit $Ca(OH)_2$ and in CSH gel. As the consequence the strength and deformation characteristics of hardened cement matrix are extensively reduced. The relation between the amount of leached calcium and relative concrete compressive strength is presented by different authors e.g. [8]. Measurement results focused on profile determination of solid phase Ca^{++} cations in concrete exposed to NH_4NO_3 published by different authors e.g. [2], [4] confirm, that the zone where the lowering of Ca^{++} cations concentration occur is about 2 mm width. In this layer the strength and deformation characteristics of hardened cement are seriously reduced. For non-loaded concrete element the most suitable degradation model is that, where the process of cross section reduction is determined by the rate of aggressive medium penetration. By comparing many experiment results, where different kinds of concrete and NH_4NO_3 concentration were used, it can be stated, that the rate of NH_4NO_3 penetration into the concrete element (and thus the reduction of its cross section) could be described by simplified diffusion function [3], [5], [7], [8]

$$H = k \cdot \sqrt{t} \tag{1.1}$$

Where H – penetration depth of NH_4NO_3 solution
k – experimentally defined value
t - time

2 Degradation of long-term loaded beams in aggressive environment of NH_4NO_3

Degradation process of loaded concrete elements is different to degradation of non-loaded elements [1], [5]. In accordance with the results presented by Schneider and Chen [5] there exists a boundary, beyond which the degradation process has significantly different course. However the physical background of the degradation of loaded beams has not been described and regression functions were defined empirically. In order to explain this problem it is possible to adopt the following hypothesis: **Alt.1:** When the ultimate relative strain of degraded concrete is higher than the so called basic relative strain caused by the beam load, the process of degradation course will not differ from the degradation course of non-loaded beams. The whole process will follow the diffusion function until the time, when the basic relative strain at the degraded part of concrete will exceed the ultimate relative strain of degraded concrete as the consequence of the reduction of the sound cross section. After reaching this ultimate relative strain of degraded concrete the exponential diffusion function change to linear one. **Alt.2:** When the ultimate relative strain of degraded concrete is smaller than so called basic relative strain, caused by the beam load, a crack will appear after partial degradation of the surface layer of the concrete element. In this case degradation process will not be directed by diffusion function. In this case the reduction of the sound cross section of the concrete beam caused by the degradation process increases the relative strain in degraded surface zone and speeds up the degradation rate. (Fig.1).

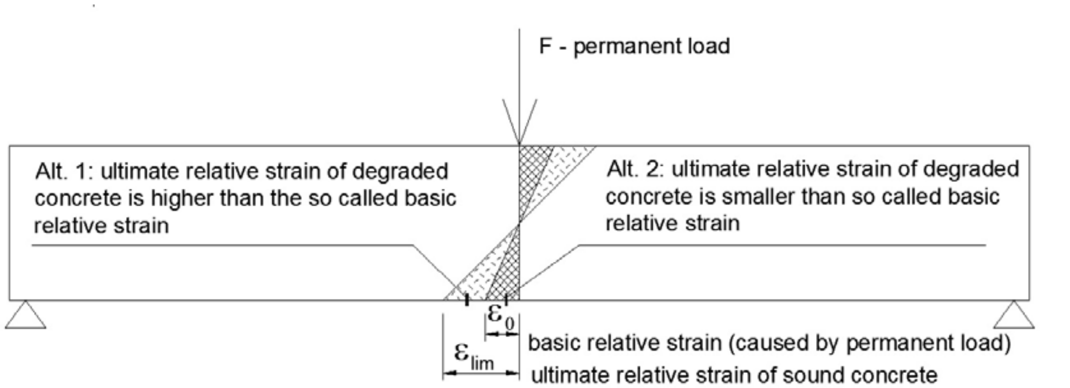

Fig.1 Alternative models of degradation of loaded beam

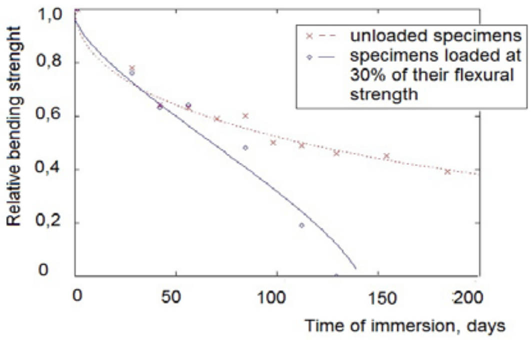

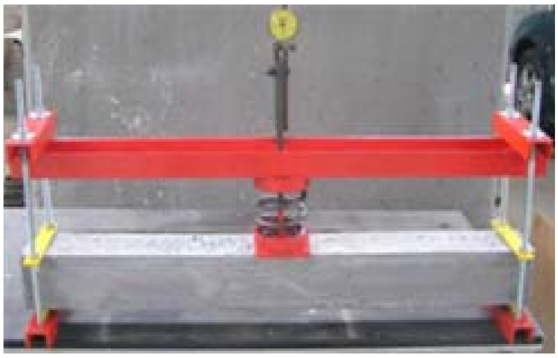

Fig.2 Application of theoretical regression method on test results of Schneider and Chen [5], [10]

Fig.3 HPFRC beams exposed to permanent bending performance by steel springs

Application of this hypothesis on test results of Schneider and Chen [5] shows very good conformity of theoretical solution with test results.

3 Experimental investigation

Experimental research was focused on the investigation of the beam deformations in time. Beams were exposed to a certain level of long-term bending performance and submerged in 5% solution of NH_4NO_3. These beams with dimensions of 105x105x1100 mm were made of HPFRC. For 9 beams long-term bending performance was provided by steel springs (Fig.3). In age of 120 days a part of specimens were submerged in water and the other part in 5% solution of NH_4NO_3. Maximum concrete tensile stress value reached the level of 45% of HPFRC tensile strength by bending. Three beams were submerged into water and 6 beams in 5% solution of NH_4NO_3. During the whole time the deformations (deflections) were measured. Relation between HPFRC beam deformations versus time shows Fig.4. To avoid frequent change of the solution its first renewal was made after 200 days, when its concentration felt bellow 10%. Reduction of aggressive solution concentration after this first renewal is slower, because the diffusion must break a barrier in the form of degraded concrete. Thus all regression functions were applied only on data measured after this first renewal and extrapolated backward in time. If the concentration of aggressive solution would have been kept on constant level from the beginning of the experiment, the increase of deformations in the starting phase would follow the affinitive course to regression curve starting at point 0 (Fig.5).

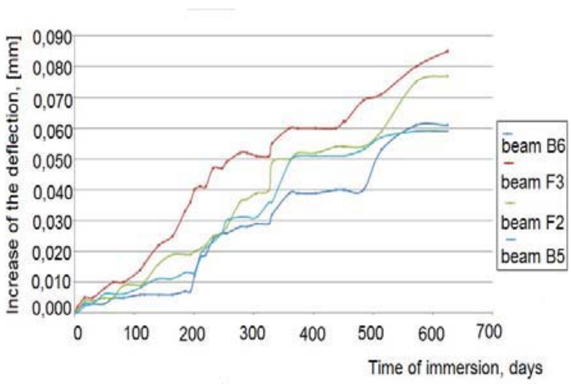

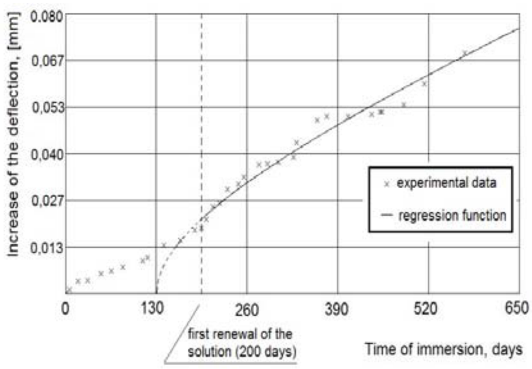

Fig.4 Deformations of HPFRC beams exposed bending performance in NH_4NO_3 environment in time
.

Fig.5 Comparison of theoretical and experimental values of HPFRC beam deformations versus time

When the uniform cross section reduction along the whole beam would be taken in consideration, increasing of deformation will corresponds to a cross section reduction of 6 to 7 mm. Cross section degradation depth tested by phenolphthalein was 9 to 10 mm. Simple diffusion model (1.1) was set up because of the fact, that fibre reinforcement made of anticorrosive amorphous metal fibres was used in the concrete mix. Thus the ultimate relative strain of degraded concrete was believed to be almost equal than the ultimate relative strain of sound concrete. However this hypothesis has not been verified. .

4 Conclusions

The beams made of HPFRC submerged in 5% solution of NH_4NO_3 and exposed to permanent long-term bending performance indicated increasing deformations in time during the whole experiment (650 days). Deformations of beams submerged in water stopped after 5 days. The final deformation of beams submerged in aggressive environment of NH_4NO_3, correspond to a cross section reduction of 6 to 7 mm. Concrete degradation depth indicated by phenolphthalein solution was 8 to 9 mm. This fact indicates the existence of certain residual resistance of degraded zone. Proposed degradation model of stressed concrete element in aggressive environment of NH_4NO_3 solution is considering not only the chemical character of the degradation process, but also the stress state of the concrete element and the material properties of degradated concrete. Theoretical results of degradation models based on the above mentioned hypothesis for concrete elements exposed to simultaneous action of bending moment and aggressive solution of NH4NO3correspondswell with the experimental results of Schneider and Chen [5] and with the result of our research [10] as well. However, further, much more detailed research is needed to confirm these assumptions and the hypothesis on which calculations were made.

References

[1] Schneider U., Chen, S.-W.: Modelling and empirical formulas for chemical corrosion and stress corrosion of cementitious materials, Materials and structures, Vol. 31, 1999

[2] Carde, Ch., Francois, R.: Aging damage model of concrete behaviour during the leaching process, Materials and structures, Vol. 30, 1997

[3] Nguyen, V.H. et al: Chemo-mechanical coupling behaviour of leached concrete, Nuclear Engineering and design 237, 2007

[4] Gérard, B., Bellego, C., Bernard, O.: Simplified modelling of calcium leaching of concrete in various environments, Materials and structures, Vol. 35, 2002

[5] Schneider, U., Chen, S.-W.: Deterioration of high-performance concrete subjected to attack by the combination of ammonium nitrate solution and flexure stress, Cement and concrete research 35, 2005

[6] Banthia, N., Bhargava, A.: Permeability of stressed concrete and role of fiber reinforcement, ACI Materials Journal, Vol. 104, No. 1, 2007

[7] El Saidy, M.I., Abadir, M.F.: Kinetics of dissolution of clinker components in some aggressive solutions, International Journal of Applied Chemistry, 2007

[8] Fagerlund, G.: Leaching of concrete, CONTECVET manual, 2000

[9] Berner, U.R.: Modelling the incongruent dissolution of hydrated cement minerals, Radiochim. Acta 44-45, 1988

[10] Paulík, P.: Contribution to evaluation of concrete elements surface layers, Dissertation, Faculty of Civil Engineering, STU Bratislava, 2011, 107 pages (in Slovak)

.

SHORT AND LONG TIME DEFLECTION OF PRE AND POST-TENSIONED BRIDGE BEAMS

Milan Chandoga, Jaroslav Halvonik, and Andrej Pritula

Faculty of Civil Engineering at SUT, Radlinskeho 13, 813 68 Bratislava, Slovakia (professor, professor, PhD student)

Abstract

Paper deals with monitoring of deformations of two different prestressed precast beams and with analysis of some aspects which influence short and long term deflections of the beams. The first type "T1" is 32,1 m long precast beam prestressed partially by pre-tensioned tendons and later by three post-tensioned tendons. The second type "T2" is pre-tensioned precast beam with length of 29,96m

Keywords: Camber, Bridge girder, Pre-tensioned, Post-tensioned, Strain, Curvature

1 Introduction

Slab-on-girder bridges belong to the very frequent option for construction of long elevated highways in Slovakia. In order to reach required vertical elevation of highways short and long-term deformations of prestressed precast beams play important role in bridge design. It sometimes happens that the theoretical values differ from actual ones and even actual deformations differ from beam to beam. The deflections of prestressed beams are influenced by many factors, some of them are structural but some of them are governed e.g. by concrete technology or by ambient conditions during hardening of concrete.

2 Precast beams type "T1"

Prestressed precast beams had a length of 32,1 m, depth 1,4 m and were used for construction slab-on-girder bridges where continuity over an intermediate support is ensured by RC diaphragm. Therefore prestressing consisted of 18 pre-tensioned low relaxation strands ϕLS15,5/1800 MPa and three post-tensioned polygonal tendons, see Fig.1. Transfer of pre-tensioning strands was scheduled 18 hours after casting and four strand tendons were prestressed one month later.

Fig. 1 Beams type "T1"

2.1 Deformations

Mid-span bending moments due to the first prestressing only slightly exceeded moments due to self-weight of the beams. Therefore predicted cambers were only 9 mm with expected growth up to 11 mm (one month later) and after tendon prestressing cambers should increase up to 35 mm. However actual cambers measured at storage yard were ranging from 1,6 mm to 13,7 mm and fully prestressed from 24 to 39 mm. Some beams which were produced later had instead of camber even sag. To find the reason of camber differences an extensive monitoring was carried out. The monitoring consisted of laboratory testing of materials and in-situ measurements which included measurements of cambers, concrete strains, monitoring of prestressing forces and measurements of curvatures on 1 m long segments with the same cross-section as the beam.

2.2 Monitoring

Three beams were monitored for cambers at the time of prestressing transfer, after setting on the temporary supports at storage yard and after stressing of post-tensioning tendons. The measured cambers ranged from 7,7 to 10,5 mm just after prestress transfer. Beams started to reduce cambers soon and after setting on the temporary supports, one beam had instead of camber small deflection. Development of cambers at mid-span section is in Fig.2. All beams continued in loosing of their cambers and deformation had changed in deflection. Prestressing of post-tensioned tendons lifted beams again approximately by 24 mm. Obtained cambers due to post-tensioning very well coincided with predicted values.

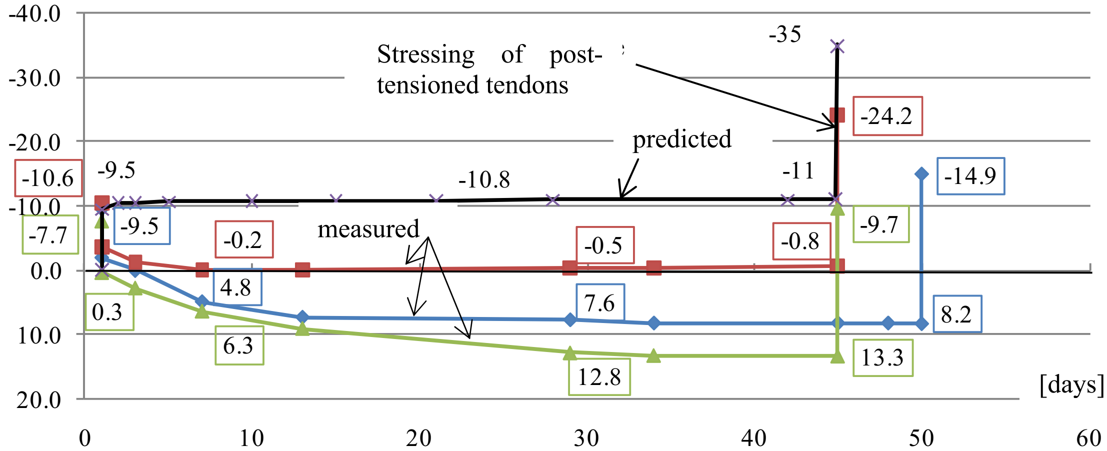

Fig. 2 DSP VP-I04 Development of deformations of monitored beams at mid-span cross-section

Monitoring of prestressing forces was carried-out by elasto-magnetic sensors Projstar PSS20. Sensors were installed on top and bottom strands. Measurements have confirmed prestressing forces used for prediction of beam deformations. Measured values were higher only by 3 % and average prestress losses due to elastic shortening of concrete in the bottom flange were similar with predicted values 6,7 kN to 6,9 kN per strand. The situation was different with losses in the top flange where measured losses were 47% higher than predicted ones.

Excessive elastic losses in the top strands were confirmed by measurements of concrete strains. Strains were measured by strain gages embedded in beams. Each beam was equipped by three gauges, one in the bottom, second 600 mm above bottom surface and the third one 50 mm below the top surface. Measured instant strains (shortly after prestress transfer) in the bottom well coincided with theoretical values, e.g. beam N1 255 vs. 256 microstrains, while measured top strains were much higher than assessed values 306 vs. 212 microstrains. Development of concrete strains in the top flange is in Fig.3.

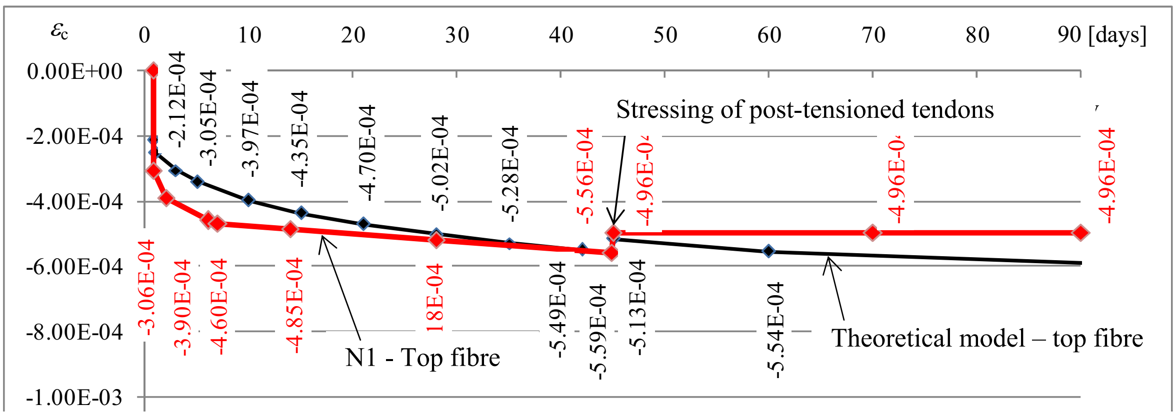

Fig. 3 Development of strains in concrete – the top flange, mid-span section

Developments of concrete strains were also tested on one meter long segments. Three segments were cast together with three beams. Segments had not been prestressed, so only deformation due to the shrinkage and temperature could develop. Each segment was equipped by three strain gauges (top, bottom, mid). Measured strains in the top flange ε_{top} were higher than in the bottom ε_{bottom} in each segment after removal of temperature effects. The largest differences had been developed within one day since casting, see Fig.4. After one day further growing become very slow. Strain differences indicate development of curvature in segments. Differences were ranging from 100 to 150 microstrains and thus curvature from 7,7.10^{-5} m^{-1} to 11,5.10^{-5} m^{-1}. Additional beam deflection obtained by numerical integration of curvature was between 9 and 14 mm. The main reason of the strain differences was uneven shrinkage over the beam depth.

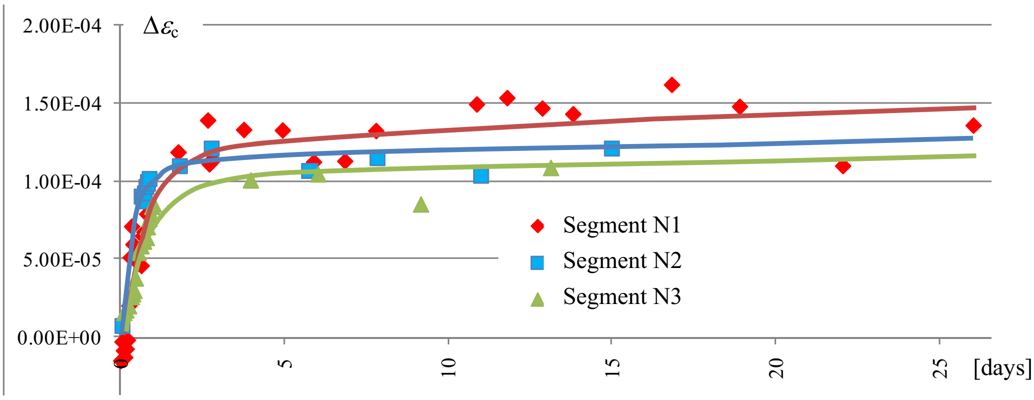

Fig. 4 Development of strain differences $\Delta\varepsilon_c = \varepsilon_{top} - \varepsilon_{bottom}$

2.3 Testing of material properties

All important properties of concrete were tested. Concrete strength, creep, shrinkage and modulus of elasticity were measured. Beams were cast from high-strength concrete C55/67. Concrete placing was divided into two stages. When formwork was half-full, vibrators attached to bottom part of the formwork started compaction. The same procedure was used when formwork was full. Compaction was very intensive and therefore some segregation of aggregates was expected. It was observed that the fine aggregates were concentrating in the top flange with thin layer of water on the surface and larger aggregates have sunk to the bottom. Therefore two sets of samples were prepared. The first one were concrete samples taken from the beam top flange shortly after intensive compaction of concrete and the second one samples made from reference concrete taken from the same batch. Obtained results confirmed different properties of concrete, see Table 1 and Fig.5. A lower modulus of elasticity and density as well as higher shrinkage was observed for concrete taken from the top flange.

Table 1
Comparison of material properties

Three samples	Concrete from top flange			Reference concrete		
	Density	$f_{c,cube}$	E_{cm}	Density	$f_{c,cube}$	E_{cm}
	[kg/m^3]	[MPa]	[GPa]	[kg/m^3]	[MPa]	[MPa]
Mean	2271,3	62,49	25,70	2360,5	64,00	32,83

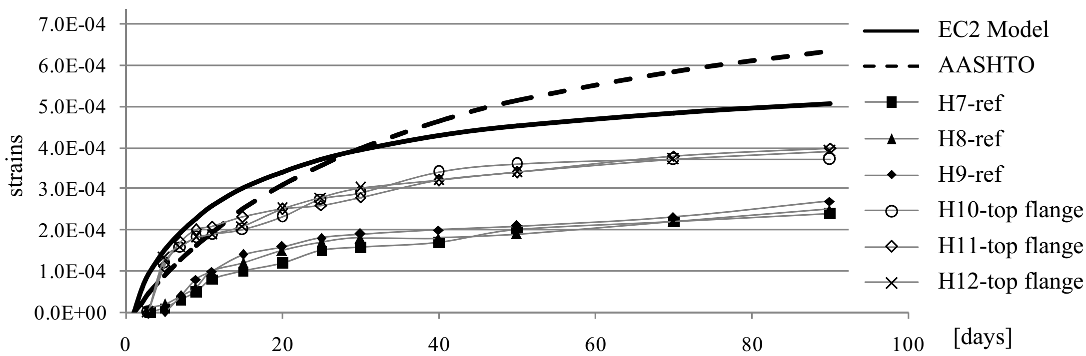

Fig. 5 Shortening of samples due to the free shrinkage

3 Precast beam type„T2“

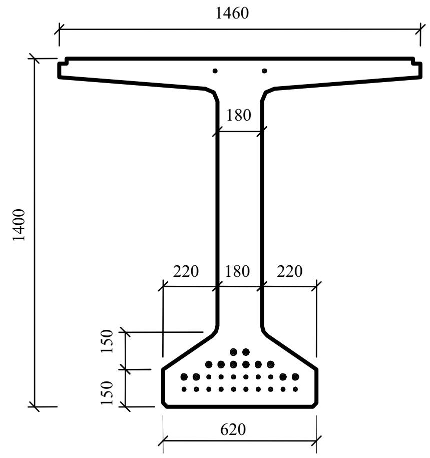

Prestressed precast beams “T2” with a length of 29,96 m were used for construction of a slab-on-girder bridge which consist of simply supported girders. Beams were prestressed only by pre-tensioned tendons, 28 strands ϕLS15,7/1860 MPa in the bottom flange and 2 strands in the top flange. Beams were cast from concrete C45/55.
As previous ones the “T2” beam was monitored for uneven shrinkage along the beam depth. Test was carried out in order to know how the different arrangement of vibrators for concrete compaction influences deformations due to uneven shrinkage. Vibrators were attached to the form in several levels so the intensity of the compaction was lower than in “T1” beams. One segment was cast and obtained maximum strain differences between top and bottom flange were aprox. 70 microstrains, see fig.6. The differences were developed within one day and after five days they had remained constant. Additional deflection calculated from developed curvature was 5 mm. Thanks to the high amount of prestressing resulting in sufficient cambers, more than 50 mm, uneven shrinkage did not influence much the geometry of the beams.

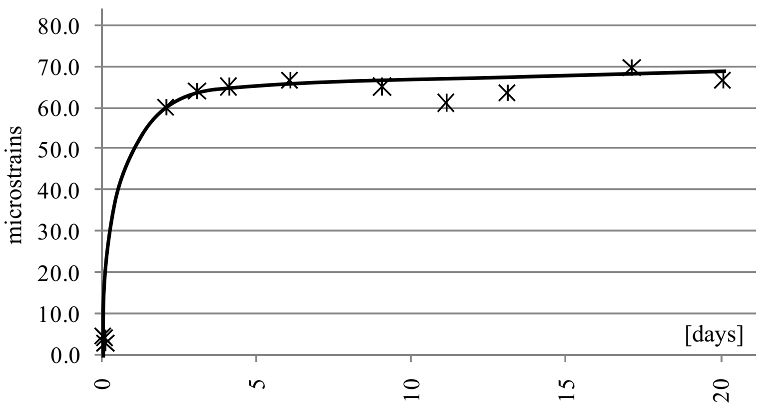

Fig. 6 Development of strain differences $\Delta\varepsilon_c = \varepsilon_{top} - \varepsilon_{bottom}$ beam “T2”

4 Conclusions

More than 200 beams “T1” were checked for camber within the project. An average measured camber of 22 mm was obtained using statistical evaluation while predicted value was 35 mm. We assume that main reason of lower cambers were uneven properties of concrete over the beam depth caused by segregation of aggregates during intensive concrete compaction. Differences were also eyes striking due to the low amount of pre-tensioned prestressing. Much better results were obtained for pre-tensioned beams “T2” where a different way of concrete compaction brought more homogenous concrete in beams and additional deflection 5 mm was negligible compare to the final value of camber.

Acknowledgement

Author gratefully acknowledges Scientific Grant Agency of the Ministry of Education of Slovak Republic and the Slovak Academy of Sciences VEGA No. 1/0857/11 and company Projstar PK Ltd.

References

Chandoga,M., Halvonik,J. (2004), “Interactive Design of Prestressed Precast Beams from HPC” In: Proceeding of Symposium fib, Concrete Structures the Challenge of Creativity. Avignon.

BOND OF STRANDS COATED WITH DIFFERENT ANTICORROSION AGENTS


Ján Laco[1]
Corresponding Author

Viktor Borzovič[1]

[1]**Faculty of Civil Engineering, Slovak University of Technology in Bratislava,** Radlinského 11, 83104 Bratislava, Slovak Republic, www.svf.stuba.sk
Tel: +421 2 59274295, Fax: +421 2 52926213, Email: jan.laco@stuba.sk

Abstract

The time between prestressing tendons and the injection of the ducts in concrete post-tensioned bridges may be several weeks. During this time, it is necessary to protect tendons against weathering and atmospheric humidity. Tendons should be protected with various oil based agents, which can have influence on their bond with a structure.

This paper shows the result from pull-out tests of strands coated with corrosion protection agents. Primary goal is to compare bond stress behaviour at different types of specimens with strand coated and not coated with emulsifiable oil and thixotropic compound.

The paper also deals with the calculation of bond stresses in post tensioned concrete bridges and will try to find out whether a lower bond capacity caused by the use of oil emulsions is sufficient or not.

Keywords: Bond, Post-tensioned concrete, Pull-out test, Strand

1 Introduction

Bond between prestressing unit and concrete or injection grout may be influenced by the use of corrosion protection emulsions. Most of the post-tensioned concrete bridges are designed with the use of prestressing units with bond, where a full connection between reinforcement and concrete is assumed. Main reasons are protection against corrosion of prestressing units, denser distribution of cracks for partial prestress concrete and higher resistance for ultimate limit state.

ISBN 978-80-87158-35-7 (CD)

2 Bond experimental measuring – phase 2

2.1 Specimens and test arrangement description

The evaluation of results of the first phase is presented in [1]. In the second phase of experimental program, two types of corrosion protection agents were tested. The first is emulsifiable oil is prepared from non-aromatic mineral oil soluble with raffinates. The main components are sodium sulfonate, polyvalent alcohols and modified derivatives of fatty acids and antioxidants. It serves as a corrosion and oxidation inhibitor. Density of oil is 904 kg/m3. Concentration by applying was 25%.
The second type of corrosion protection agent is thixotropic compound. It may be used as reliable corrosion protection filling material for various steel elements. It is cold processed, water blocking material based on highly rafined base oil. Also serve as a corrosion and oxidation inhibitor. This compound has zero oil separation in any temperature conditions. Density of compound is 870 kg/m3 and can be applied by cold pumping.
In the experimental program the measuring of the bond on 36 specimens was performed. 12 specimens were dry with uncoated strands, for 12 specimens emulsifiable oil and for 12 thixotropic compound was applied. Specimens were of cylindrical shape with the length of 600 mm and diameter of 165 mm made from concrete and injection grout placed to the plastic tubes. In their centre, strand ø15.7 (0.62“) with characteristic tensile strength of 1860 MPa were placed. The specimen body was made from concrete of mean cube strength 32.1 MPa. In the centre a corrugated steel duct was placed. After reaching 28 day strength of the grout, that means approximately 50 MPa, specimens were tested with device constructed for this purpose.
The test arrangement is shown in Fig. 1. A part of the test arrangement was a calibrated hollow jack. Cylindrical specimen was fixed and the strand was pulled out with the jack. On the specimen there were measured displacements on both ends and also corresponding pulling force.

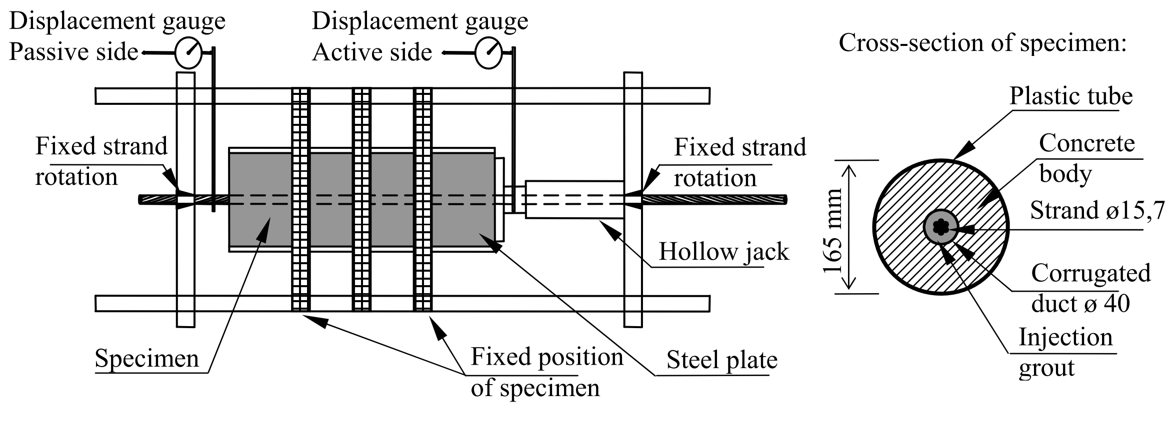

Fig. 1 Test arrangement

2.2 Discussion of results

Typical mode of failure was represented by crushed grout wedge around strand on the active pulling side. Strands were losing their adhesion if coated with anticorrosion emulsifiable oil. Adhesion losing was obviously due to the fact that the strand was possible to screw out from specimen. Therefore strands were prevented against twisting on both ends of the specimen. Results and comparison of maximal bond stress are shown in Fig. 2.

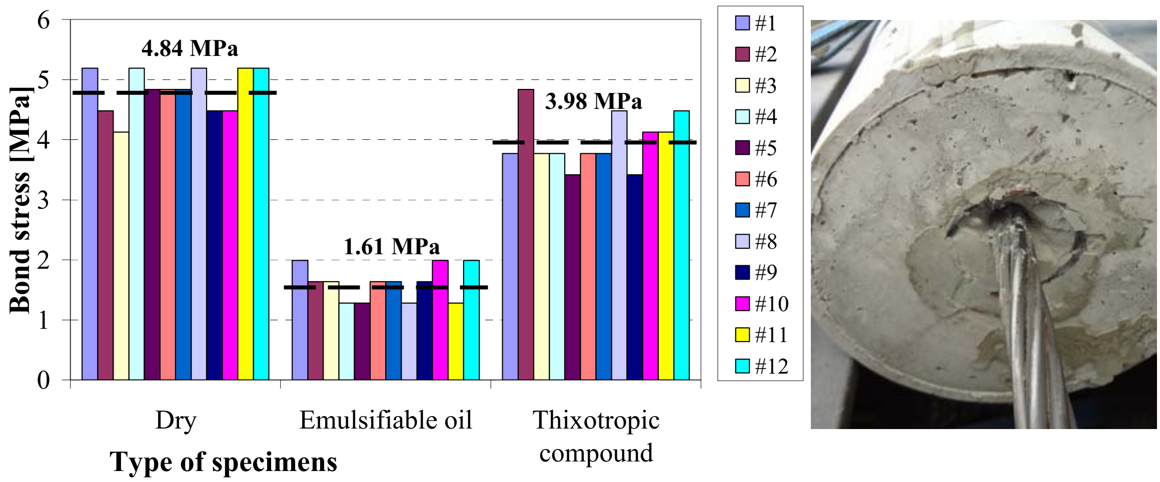

Fig. 2 Maximum bond stress at specimen failure and specimen failure with crushed grout wedge

A failure criterion for bond strength is maximum measured load in a pull-out test on strand. Then constant equivalent bond stress was derived from this force. The equivalent area of interface between strand and grout in specimens is 0.02605 m2. Maximum bond between strand and surrounding grout was reached in dry type specimens without corrosion protection. The strand was pulled out by 126.1 kN in average which is corresponding with constant equivalent bond stress 4.84 MPa. Specimens with strand coated with emulsifiable oil reached average bond stress of 1.61 MPa what is approximately 33 % of dry ones. Specimens with strand coated with thixotropic compound reached average bond stress of 3.98 MPa what is approximately 82 % of dry ones.

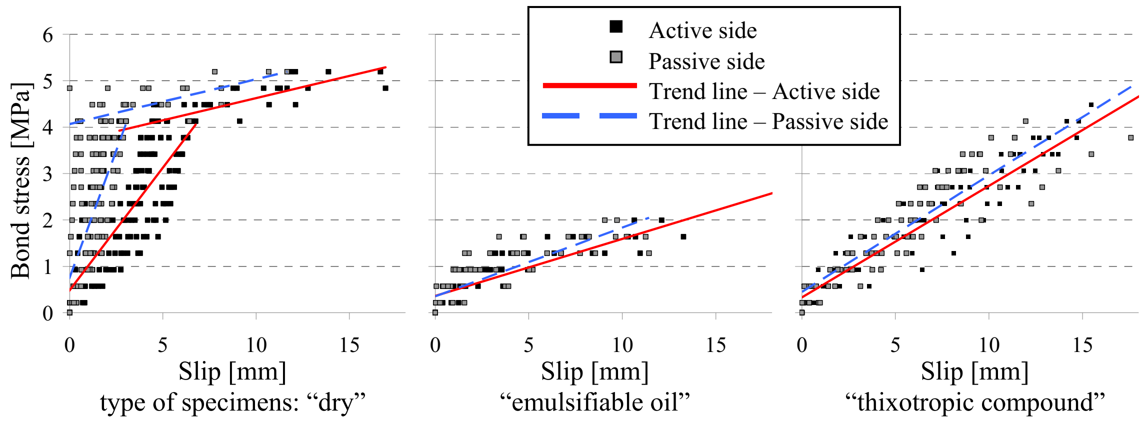

Fig. 3 Bond stress – slip development on active and passive side

Another difference except the bond strength can be observed from Fig. 3, where displacements on active and passive side are presented. Measured displacements were summarized by trend lines for active and passive slips and also for all three types of specimens. Behaviour of dry type specimens may be described as bilinear. After rupture of an adhesion, a friction is activated. This debonding occurs at very small slip. Pulling force

 ISBN 978-80-87158-35-7 (CD)

transmitted before debonding was small and not measurable compared to a force of bond strength. The first part of bilinear trend lines represents a friction due to the radial compressive stress caused by e.g.: irregular shape of strand, varying pitch. After rupture of a friction, a residual bond is provided by mechanical interlock of pulling helical strand. This represents the second part of the trend line. The slope of the second part of trend line compared to the first one is much smaller. Behaviour of specimens with strand coated with corrosion protection may be described as monolinear. Compared to the dry type specimen, the first part of trend line is missing. We consider that friction plays only a minor role in this case.

3 Calculation of bond stress

In post-tensioned concrete bridges, bond stress is relatively low. The next chapter gives a numerical calculation of bond stress between tendons and concrete for a three span continuous bridge. The calculation deals with the analysis of some parameters affecting value of bond stress.

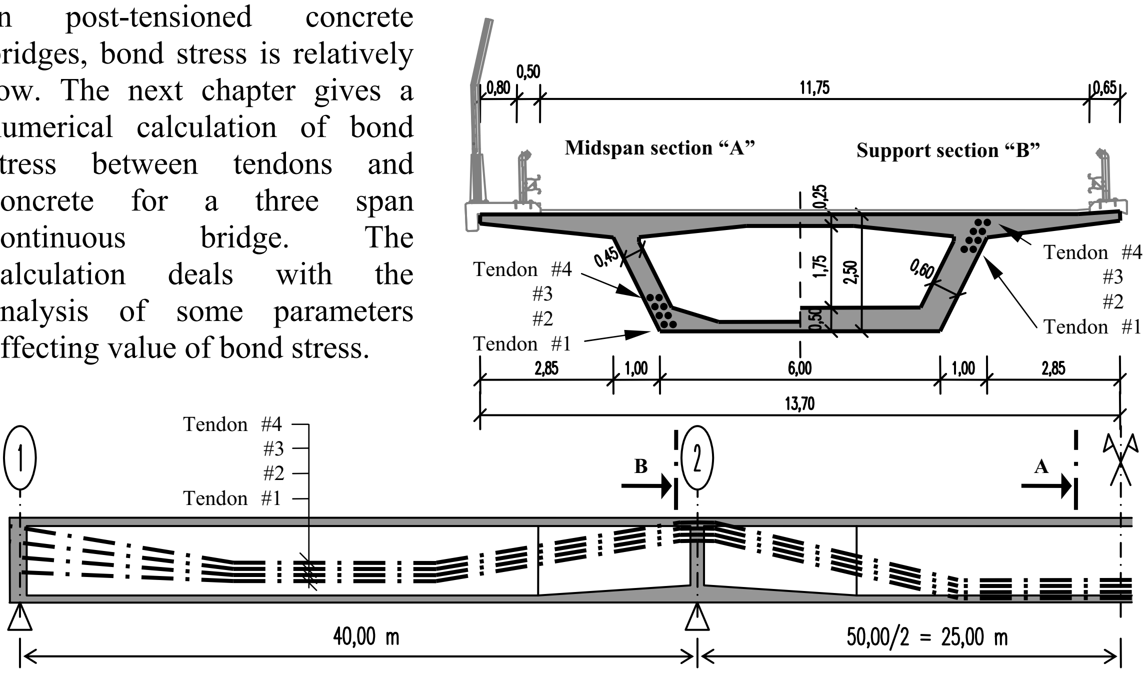

Fig. 4 Cross-section of the bridge and longitudinal section of the bridge, geometry of the tendons

The bond stress is evaluated for three combinations of loads in order to show the bond stress for different level of loading of the structure:

- Frequent load combination (Frq), serviceability limit state (SLS)
- Characteristic load combination (K), serviceability limit state (SLS)
- Design load combination (Ed), ultimate limit state (ULS)

Combinations were made according to European standards. The bond stress at ULS is relevant in deciding, whether the structure acts as bonded or unbonded.

In case of SLS combination, for calculation of shear forces from which the bond stress is derived, it was not considered actions, those started acting before grouting of the tendon ducts (self weight and prestressing). The calculation was made for three alternatives of prestress. Geometry of tendons is the same for all three alternatives. The number of strands in tendon is changing. The first alternative of prestress is provided by 17 strand tendons. For this alternative, decompression is not achieved for frequent load combination. Other alternatives of prestressing are provided by 15 and 13 strand tendons. These alternatives represent a partial level of prestressing 15/17 = 88% and 13/17 = 76% of the first alternative. When normal stress in section does not exceed the value of 2.2 MPa, which is a characteristic tensile strength of concrete C35/45, it was considered to be a cross-section without crack (stage I.). Otherwise, it was considered as a cracked section (stage II.). The results of both normal and bond stress alternative of prestressing by 17 strand tendons are presented in Fig. 5. The first row represents the results for frequent load combination (Frq), the second for characteristic load combination (K) and the third for design load combination (Ed). The first column of each figure represents the envelope of normal stresses for the top and bottom part of the deck, from which the areas, those exceed tensile strength of concrete were taken. Stresses σ_{c_Mmax} were calculated taking into account only envelopes of positive bending moments. Stresses σ_{c_Mmin} were calculated taking into account only envelopes negative bending moments from envelopes for assumed variable actions. The second column shows the development of bond stress for tendons #1 to #4, when sections without a crack were assumed (stage I.). The third column shows the development of bond stress, when cracked sections were assumed for the sections were normal stress exceeds tensile concrete strength (stage I.+II.).

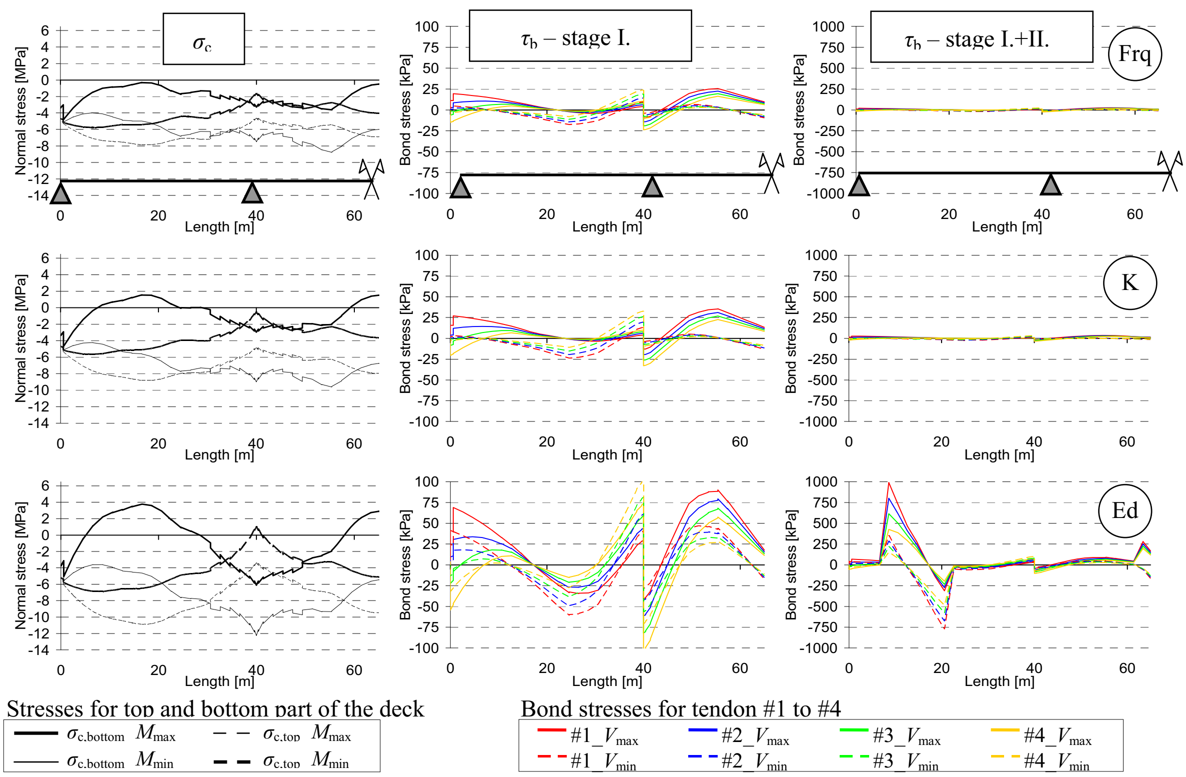

Fig. 5 The charts of normal and bond stresses for alternative of prestress by 17 strand tendons

The results for midspan and inner support section are summarized for all alternatives in the Tab. 1. The bond stress reached a very small value and it was almost the same for all three alternatives of prestressing, when uncracked sections were assumed. It is 20 to 40 kPa for SLS combinations and up to 100 kPa for ULS combinations. When cracks appear, bond stress jump to much higher values. For midspan section, where shear forces do not reach maximum, it is up to 600 kPa for SLS combination. The level of prestress significantly affects the value of bond stress when a cracked section appears. In addition to the increase of the bond stress value, the length of cracked part of the structure also increases.

 ISBN 978-80-87158-35-7 (CD)

Therefore tendons are exposed to higher bond stress. For ULS combinations of load, bond stress reached value of 1 to1.8 MPa at midspan sections. Bond stresses in section over the inner support were maximal up to 3 MPa because of high shear forces.

Tab. 1 Comparison of normal and bond stresses

Tendons	Combination	Midspan Section			Support Section		
		$\sigma_{c,max}$ [MPa]	$\tau_{I.}$ [kPa]	$\tau_{II.}$ [kPa]	$\sigma_{c,max}$ [MPa]	$\tau_{I.}$ [kPa]	$\tau_{II.}$ [kPa]
17-strands (100%)	frequent	-0,3	20	-	-1,59	24	-
	characteristic	1,54	27	-	-0,51	33	-
	design	3,77	69	991	1,06	102	-
15-strands (88%)	frequent	0,88	18	256	-0,44	23	-
	characteristic	2,72	26	344	0,65	31	-
	design	5,09	65	1236	2,35	97	2240
13-strands (76%)	frequent	2,07	17	440	0,72	21	-
	characteristic	3,91	24	613	1,81	29	-
	design	6,41	61	1869	3,63	90	2729

4 Conclusions

The analysis has shown that bond stresses in some sections assessed for ULS load combinations can be quite high. Even the tendons used in real life structures are bundle of strands, that behaviour is different from that of a single strand, the results of pull-out test indicate the level of reduction in bond strength of prestress units coated with corrosion protection.

5 Acknowledgement

Authors gratefully acknowledge Slovak Research and Development Agency, project No. APVV-0442-12. Authors gratefully acknowledge support provided by Doprastav, a.s.

References

[1] Laco, J., Borzovič. V. (2012). *Bond behaviour of prestressing units coated with corrosion protection emulsions,* In *Proceedings of the Czech Cocrete Day 2012*, Hradec Králové, Czech Concrete Society & CBS Servis.

Ing. Ján Laco
✉ Stavebná fakulta, STU Bratislava
Radlinského 11, 831 68 Bratislava
Slovak Republic
☎ +421 2 592 74 295
+421 2 529 26 213
☺ jan.laco@stuba.sk
URL www.svf.stuba.sk

Ing. Viktor Borzovič, PhD.
✉ Stavebná fakulta, STU Bratislava
Radlinského 11, 831 68 Bratislava
Slovak Republic
☎ +421 2 592 74 542
+421 2 529 26 213
☺ viktor.borzovic@stuba.sk
URL www.svf.stuba.sk

SEISMIC CAPACITY UP-GRADE OF PREFABRICATED FIRE STATION BUILDING AT MOCHOVCE NUCLEAR POWER PLANT

			
Július Šoltész[1,2]	**Ján Sedlák[2]**	**Daniel Makovička[3,4]**	**Marek Tengler[5]**

[1]**SvF STU Bratislava**, **Department of Concrete Structures and Bridges**, Radlinského 11, 813 68 Bratislava, Slovak Republic, Tel: +421 (2) 59 274 384, Email: soltesz@svf.stuba.sk

[2]**ISPO spol. s r.o, inžinierske stavby, structural design office**, Bratislava, Konventná 9, Bratislava, Slovak Republic, www.ispo.sk, Tel: +421 908717791, Email: sedlak@ispo.sk,

[3]**D. Makovička – structural and dynamic analysis of structures**, Praha 5, K Jasánkam 895/2, Czek Republic, Tel: +420 235510987, Email: d.makovicka@volny.cz,

[4]**ČVUT v Praze, Kloknerův ústav**,166 08 Praha 6, Šolínova 7, Česká republika, Tel: +420 224353856, Email: daniel.makovicka@klok.cvut.cz

[5]**Rizzo Associates Czech, a. s., civil engineering design and consultancy firm,** Vejprnická 663/56, Plzeň, Česká republika, Tel: +420 377350233, Email: marek-tengler@rizzoassoc.cz

Abstract

The objective of the paper is a description of the static analysis and subsequent design of the seismic up-grade of the civil structure of the fire station building that is monolithically coupled with the civil defense shelter. The shelter herewith forms a basement floor and the foundation structure. The station building is separated by expansion joint of the overhead fire-fighters equipment garage. The building, after its extending an seismic up-grade, shall keep its structural integrity after design basis event or postulated earthquake. The term "structural integrity" means a preservation of functional capability of the building that in a case of a fatal failure of bearing structure system, once, the garage and, as well as, damaging of the adjacent dilatation join separated civil structure - the fire station building.

Keywords: concrete, steel, seismic up-grade, soil-structure interaction, 3D FEM analysis, static model phasing

 ISBN 978-80-87158-35-7 (CD)

1 Introduction

At first sight, a relative simple task has been gradually complicated, namely, of following reasons:

- due to the user of the building and its determined service limitations,
- arrangement of ground lines and structures in near proximity of the building,
- past improper designed and performed seismic up-grades of the building to the value of seismic design value PGAH = 0.1g,
- retrieving of a maximum cost-acceptable option of the solution that meet stipulated nuclear safety requirements.

Fig. 1: The fire station building with garage

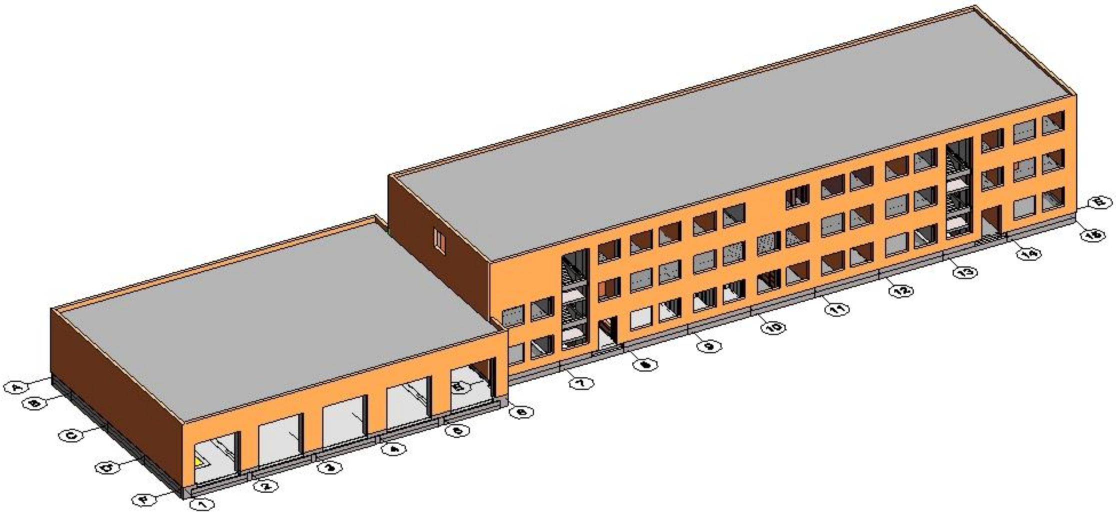

Fig.2 View of garage and the fire station building - CAD model – REVIT

2 Description of the structure, loads and load combinations

The first considered group of load combinations that has been evaluated (loads due to normal operating conditions – PDS - Permanent Design Situation), including permanent and live loads.
The second group of load combinations (design extreme climatological loads – ADS – Accidental Design Situation) represents effect of extreme snow pack and wind. Tornado, airplane crash luckily has not been required to be assumed.
The third group of loads represents the seismic load (EQDS – Earthquake Design Situation) – design basis earthquake with following parameters:

- seismic event recurrent period **10 000 years**;
- peak ground acceleration in horizontal direction PGAH **0.15g**;
- peak ground acceleration in vertical direction PGAV **0.10g**;
- equivalent macro-seismic value of °MSK-64 acc. ISO 6258 **7.5 (8)**.

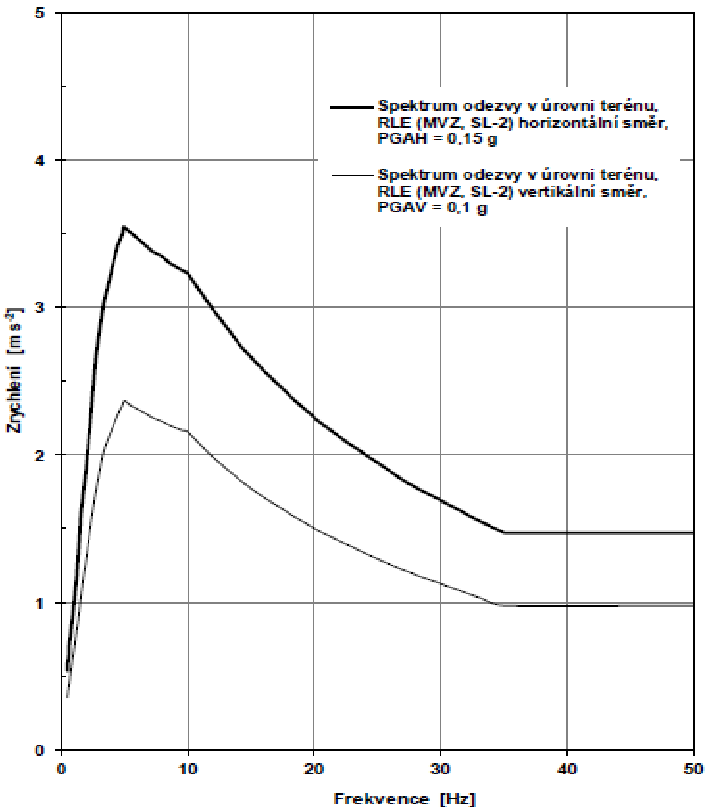

Fig. 3: Design Response Spectra valid for Mochovce NPP

2.1 Description of the structure system and its foundation

The civil structure of the fire station building (FS) is designed as a three-storied building with the plan dimensions 16.60 × 54.80 [m]. There is the civil defense shelter situated

 ISBN 978-80-87158-35-7 (CD)

under the FS in axes 6'-15. To the main building of the FS is attached a one-storied garage for the fire-fighters equipment. The plan dimensions of the garage are 21.60 × 30.60 [m]. The total length of the whole complex is 85.40 m. The civil defense shelter forms a basement for the main building of FS and is placed on a monolithic base foundation slab with the thickness of 800 mm. There is a gravelous sand layer of thickness 0.3 m and a blinding concrete layer of thickness 0.2 m placed under the base slab. Sub soil surroundings partially consist of a clay loam and partially of clayed stone filling. Before basement excavations were realized, the subsoil materials have been consolidated due to the self-weight of the filling, which is 3-8 [m] thick. Main building of FS is designed as a three-storied prefabricated reinforced concrete building of MSRP BA construction type. The building depth is 6 + 3 + 6 [m] in module 9 × 6.0 [m]. Structural height is 3.6 m. Staircase is designed in a half module of precast construction. Columns are rectangular 500 × 500 [mm] cross section, reinforced concrete girder is rectangular 500 × 500 [mm] beam, prestressed ceiling panels of 240 mm height are used in width 590 mm, 740 mm, 950 mm, 1090 mm, 1190 mm, 1550 mm and 1790 mm. Object is braced with stiffening side walls of thk. 140 mm and interior stiffening walls of thk. 240 mm with added reinforcing concrete wall of total thk. 350 mm.

2.2 Sub-soil conditions and soil-structure interaction

Soil-structure interaction (SSI) effects shall be considered for all structures not supported by a rock or rock-like soil foundation material. Subsurface material properties (shear modulus G, damping ratio λ, Poisson's ratio ν and total unit weight γ) shall be determined by field testing or empirical relationships. For impedance function calculations, all mat foundations may be approximated by equivalent rectangular or circular shapes, according to ASCE standard [6]. The equivalent rectangular or circular dimensions shall be computed by equating basemat soil contact area for translational modes of excitation and by equating contact area moments of inertia with respect to the reference axis of rotation for rotational modes of excitation. When the soil below the foundation basemat is relatively uniform to a depth equal to the largest foundation dimension, frequency-independent soil spring and damping constants can be defined in accordance of equations stated in ASCE standard [6]. The method of "equivalent stiffness" verified by check analysis of Dr. Makovička's team and it has been stated that for the resistance of decisive structure elements are calculated results on the safe side; it means that the method, at least for this modeled case, is conservative. Because the time frame, the sub-soils models has not been performed using the 3D solid-elements and an interaction has not been checked in two steps as is recommended in ASCE standard [6].

3 Results

The previous project of design reinforcement did focus to overall strengthening of the building against to seismic event postulated to PGAH = 0.1g. There have been designed new reinforcing walls, anchoring to existing columns, ceilings and to existing walls. But, only anchoring to the existing columns were executed, so the wall does not act as the one element along its height. The analysis procedure of as-built state therefore started with consideration of a real behavior of these walls. It has shown the negative increasing of tensile forces in the columns. Tensile forces that the columns cannot properly transfer with the assumed reinforcement, to be considered in previous reinforcement project (8Φ20), hence are problematic also for existing columns (4Φ20 and 4Φ16). Strengthening in this past project was based on a reduction of tensile forces in columns and an impact evaluation of modifications of the building on the all bearing elements of the structure. The proposed design upgrades can be divided into internal and external modifications of the load-bearing structure. Internal interventions were limited to the minimum due to a continuous duty of the building. It is necessary to revise the strengthened walls, designed in a previous project, to a proposed state – join the reinforcement with horizontal beams. Columns within these walls will be prestressed using prestressing rods. The design prestressing force for columns of first floor is 1600 kN, and for columns of second and third floor is 800 kN. Further reduction of internal forces act on the columns is achieved by outside stiffening towers, which take part of horizontal inertia forces and thus help to achieve the required bearing capacity of columns. The mutual connection of outer stiffening towers and steel-concrete structure is achieved by steel truss on the ceiling of each floor in the longitudinal direction, stiffening towers in the transverse direction is connected directly to the concrete beams. For towers are designed piles foundations. It is necessary to move the underground water lines to new position, because they crossing the area of planned foundations.

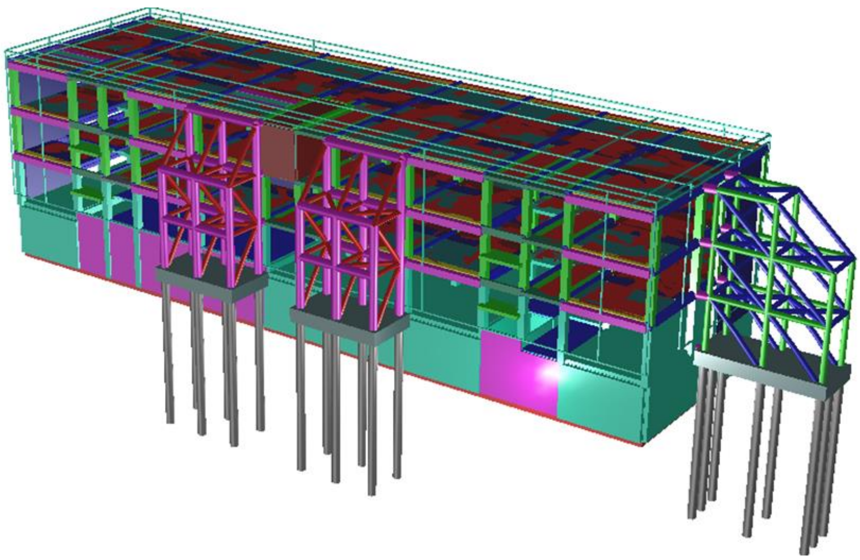

Fig. 4: FEM model of the strengthened structure of FS building

 ISBN 978-80-87158-35-7 (CD)

4 Acknowledgments

The paper was elaborated in support of the research project VEGA č.1/0306/09 "Application of probabilistic methods to renew the reliability of concrete structures". The main author would like to thank his friend, geologist, Dr. Martin Šujan for invaluable consultation on the issue of seismic hazard at Mochovce.

References

[1] Report: PNM34080183 rev.02, Požiadavky na hodnotenie seizmickej odolnosti konštrukcií, systémov a komponentov JE Mochovce 3. a 4. Blok, ENEL-SE, apríl 2009

[2] Rizzo Associates Czech, a. s.: Projektová dokumentace seizmického zodolnění pro objekt jaderné elektrárny Mochovce - Budova požární stanice

[3] STRAP- STRuctural Analysis Programs, ATIR – Tel Aviv, User manual for CAD FEM system STRAP2012

[4] STN EN 1990-1998. „Eurokódy – kompletná sada." SUTN [Slovenský ústav technickej normalizácie]. Bratislava. 2006 - 2012.

[5] Šoltész, J., Binder I., Ecker M.: Rehabilitation of Industrial Structures in the NPP Bohunice in Slovakia Due to Increased Site Seismic Hazard, Proceedings of the 2nd fib Congress, June 5-8, 2006 – Naples, Italy, pp. 652-654, (in English)

[6] Seismic Analysis of Safety- Related Nuclear Structures and Comentary, ASCE 4-98, ISBN 0-7844-0433-X, Reston Virginia, 2000

[7] ŠOLTÉSZ, J., IGNAČÁK, M: Marginal seizmic resistance of concrete shells. In 19. Betonářské dny 2012 : Sborník příspěvků konference. Hradec Králové, 23.-24.11.2012. 2012, s. 99--106. ISBN 978-80-87158-32-6.

Doc. Ing. Július Šoltész, PhD
✉ STU BA (KBKM)
Radlinského 11, 813 68 Bratislava 1
Slovak Republic
☎ Tel: +421 (2) 59 274 384
🗐 +420 244 461 038
☺ soltesz@svf.stuba.sk
URL www.stuba.sk

Ing. Ján Sedlák
✉ ISPO, spol. s r. o.
Slovenská 86, 08001 Prešov
Slovak Republic
☎ +421 517463695
🗐 +421 517463699
☺ sedlak@ispo.sk
URL www.ispo.sk

Doc. Ing. Daniel Makovička, DrSc.
✉ D. Makovička – statika a dynamika…
K Jasánkam 895/2, 15500 Praha 5
Czech Republic
☎ +420 235510987
🗐 +420 235510987
☺ d.makovicka@volny.cz
URL www.makovicka.cz

Ing. Marek Tengler
✉ Vejprnická 56, 31800 Plzeň
Czech Republic
☎ +420 377350233
🗐 +420 377350230
☺ marek.tengler@rizzoassoc.cz
URL www.rizzoassoc.cz

THE EFFECT OF LOAD TYPE ON THE ACTION OF CFRP LAMINATES IN STRENGTHENED CROSS-SECTION


Katarína Gajdošová [1]
Corresponding Author

Jakub Brondoš[1]

[1]**Faculty of Civil Engineering, Slovak University of Technology in Bratislava**, Radlinskeho 11, 813 68 Bratislava, Slovak Republic, www.svf.stuba.sk
Tel: +421 259 274 382, Fax: +421 252 926 213, Email: katarina.gajdosova@stuba.sk

Abstract

Series of experimental verification of strengthened columns and beams showed different capacity utilization of CFRP strips in these cross-sections according to the type of applied load. In strengthened column's cross-section, the strains at rupture of CFRP strips did not reach the values from tension test at static loading. Full use of CFRP materials was demonstrated only under dynamic effects of impact loads. Type of stress has a significant impact on the use of strengthening material.

Keywords: Strengthening, CFRP laminate strips, impact load

1 Introduction

There are the two most widely used forms of fiber reinforced polymers used for strengthening. At first, it is the bonding of strips to the surface or near the surface (NSMR) of structural element and the second one is the sheet (in one or in two directions woven) laminated to the epoxy resin on the site. Method of bonding polymer strips to the surface of structural elements is used for strengthening both the horizontal and vertical structural elements; lamination of sheet in the form of wrapping is applied to columns or shear strengthening of beams. Their applicability and behavior in different combinations of actions are not sufficiently experimentally verified yet. Also due to this fact, a part of the research at the Department of concrete structures and bridges at the Faculty of Civil Engineering of Slovak University of Technology in Bratislava is focused this way.

ISBN 978-80-87158-35-7 (CD)

2 Experimental Investigation

Experimental research on possibilities of CFRP strengthening of concrete structures started at the Department of Concrete Structures and Bridges at the Faculty of Civil Engineering of the Slovak University of Technology in Bratislava in 2006. Short and slender reinforced concrete columns loaded statically and reinforced concrete beams to the dynamic effects of impact load were the subjects of research. The aim was to verify the strengthening efficiency and capacity utilization of CFRP materials for various structural elements and stress ways.

In a series of short columns, 12 specimens (cross-section of 250 x 250 mm, length of 1.5 m) were tested in four groups: non-strengthened reference specimens, specimens strengthened with CFRP strips in grooves, confinement by CFRP sheet and combination of these two methods. Columns were loaded by vertical axial force of a constant value and by a horizontal force the value of witch increased to column failure and changed alternately from tensile to compressive forces. [1]

In second series, 8 full-scale slender columns were tested (cross-section of 150 x 210 mm, length of 4 m). The specimens of this series were divided to same groups like mentioned before. The behavior of specimens at gradually increasing compressive force acting at initial end eccentricity 40 mm was monitored. [2]

In the last series, completed in the first half of 2013, 10 beams were tested (cross-section of 200 x 200 mm, length of 2.2 m) to the impact load simulated by fall of weight of a weight of 118 kg from heights 0.15 to 2.4 m. [3]

In each series of specimens the deflection of element and strains in materials were measured during loading. Based on the measured values, the resistance of specimens and so the strengthening effects were determined. Beyond the determination of the basic increase in resistance it was possible to evaluate the rate of utilization of CFRP materials in reinforced cross-sections.

Fig. 1 Strengthened concrete element of each series

The results of experimental measurements were compared with theoretical and numerical analysis and the good correlation of results can be the basis for parametric study and can lead to determination of the most appropriate models offsetting the effects of strengthening usable in everyday design practice.

ISBN 978-80-87158-35-7 (CD)

3 Measured Results

Results of presented investigation clearly show the difference in the effect of CFRP materials in various structural elements depending on the prevailing way of stress. For columns subjected to static loading, it was found, that the effect of transverse CFRP sheet wrapping is the most significant one in predominantly compressive loading of short columns. In predominantly bending stress of slender columns, a more significant increase in column resistance was achieved by strengthening with CFRP strips. At the dynamic effects of impact load on beams, the greatest effect on increasing in resistance was achieved by adding CFRP strips into grooves.

Tab. 1 Measured resistance for short concrete columns (loaded by vertical axial force 650 kN)

column	*Horizontal force at failure H (kN)*	*Increase in resistance compared to non-strengthened column*
Non-strengthened	84.2	-
Column strengthened by NSMR CFRP laminate strips	91.7	8.9%
Column strengthened by confinement with CFRP sheet	96.1	14.1%
Column strengthened by combination of aforementioned methods	99.2	17.8%

Tab. 2 Measured resistance for slender concrete columns

column	*Compression force at failure N (kN)*	*Increase in resistance compared to non-strengthened column*
Non-strengthened	285.5	-
Column strengthened by NSMR CFRP laminate strips	323.4	13.3%
Column strengthened by confinement with CFRP sheet	292.7	2.5%
Column strengthened by combination of aforementioned methods	329.6	15.4%

Tab. 3 Measured resistance for beams under impact load

Beam	*Maximal relative deflection at weight height 1.2m (mm)*	*Increase in resistance compared to non-strengthened beam*
Non-strengthened	24.95	-
Beam strengthened by NSMR CFRP laminate strips	20.6	21.1%
Beam strengthened by confinement with one layer of CFRP sheet	23.88	4.5%
Beam strengthened by confinement with three layers of CFRP sheet	23.57	5.9%
Beam strengthened by combination of aforementioned methods	19.15	30.3%

 ISBN 978-80-87158-35-7 (CD)

The measured values of CFRP strip strains at rupture were of about 5-times lower than ultimate strains from uniaxial tension test at slender columns and of about 2.5-times lower for short columns under lower levels of compressive loading. On the other hand, during impact loading of strengthened beams, the behavior of NSM CFRP laminate strips was different; the reached CFRP strains at rupture were almost the same as those obtained from tension test.

4 Conclusions

For short columns under predominant compressive stress, confinement effect of a transverse CFRP sheet is most active. Second-order effects at slender columns cause an increase in bending moment at the same value of the compressive force – significant effect on slender columns resistance increase is achieved by NSM CFRP strips. Equally significant effect of CFRP strips was observed even in beams subjected to bending under dynamic effects of impact loads. CFRP sheet confinement had a relatively small effect on the increase in resistance here, but it had a more significant effect on the resistance to crushing of concrete at the impact load.

5 Acknowledgement

The research was developed with the support of research project “Analysis of capacity utilization of CFRP strips in reinforced concrete cross-section” within the Program to support young researchers at Slovak University of Technology in Bratislava and within the research project VEGA No. 1/0784/12 “Holistic design and verification of concrete structures”.

References

[1] OLIVOVÁ, K.: *Strengthening of concrete columns by strips and sheet from carbon fibers* : Dissertation thesis. Bratislava, 2007, 207pp. (in Slovak)
[2] GAJDOŠOVÁ, K.: *Strengthening of slender concrete columns with the use of fiber reinforced polymers* : Dissertation thesis. Bratislava, 2010, 115pp. (in Slovak)
[3] BRONDOŠ, J.: *CFRP materials strengthening of concrete members under impact load* : Dissertation thesis. Bratislava, 2013, 91pp. (in Slovak)

Ing. Katarína Gajdošová, PhD.
✉ Stavebná fakulta STU v Bratislave
Radlinského 11, 813 68 Bratislava
Slovak Republic
☎ +421 259 274 382
🗐 +421 252 926 213
☺ katarina.gajdosova@stuba.sk
URL www.svf.stuba.sk

Ing. Jakub Brondoš, PhD.
✉ Stavebná fakulta STU v Bratislave
Radlinského 11, 813 68 Bratislava
Slovak Republic
☎ +421 259 274 380
🗐 +421 252 926 213
☺ jakub.brondos@stuba.sk
URL www.svf.stuba.sk

VIII. TEACHING

VIII.1 Graduate Study

Obligatory subjects

Bachelor's degree study	Semester	Hours per Week Lectures Seminars	Lecturer
Design of Concrete and Masonry Members	4.	2 – 2	Ľ. Fillo
Design of Concrete Members (Slovak and Englisch)	4.	3 – 2	J. Bilčík
Reinforced Concrete Members	5.	3 – 2	J. Halvoník, V. Benko, Š. Gramblička
Reinforced and Prestressed Members	5.	2 – 2	Ľ. Fillo
Design of Concrete Structures I.	5.	3 – 2	J. Bilčík
Design of Concrete Structures I	6.	2 – 2	I. Hudoba
Reinforced Concrete Structural Systems	6.	2 – 2	I. Harvan, V. Borzovič

Master's degree study	Semester	Hours per Week Lectures Seminars	Lecturer
Masonry Structures of Buildings	1.	2 – 2	M. Čabrák
Design of Concrete Structures II	1.	2 – 2	I. Hudoba
Prestressed Concrete	1.	2 – 2	I. Harvan
Design of Environmental Constructions	1.	2 – 2	J. Bilčík
Design of Concrete Bridges I	2.	2 – 2	J. Halvoník
High – Rise and Span Structures	2.	2 – 2	I. Gramblička, J. Šoltész
Modelling of Civil Engineering Works	2.	2 – 2	J. Šoltész
Design of Composite Structures	3.	2 – 2	Š. Gramblička
Design of Concrete Bridges II	3.	2 – 2	J. Halvoník
Experimental Testing of Concrete Structures	3.	0 – 3	V. Priechodský
Special Problems of Concrete Structures	3.	2 – 2	Ľ. Fillo
Repair of Concrete Constructions	4.	2 – 1	J. Bilčík
Masonry Structures	4.	2 – 1	M. Čabrák
Execution of Concrete Structures	4.	2 – 1	I. Hudoba

Optional Subjects

Bachelor's degree study	Semester	Hours per Week Lectures Seminars	Lecturer
Design of Concrete Structures	8.	2 – 2	I. Harvan

Master's degree study	Semester	Hours per Week Lectures Seminars	Lecturer
Modelling of RC Structural Systems I	1.	2 – 2	I. Harvan
Modelling of RC Structural Systems II	2.	2 – 2	I. Harvan
Modeling of RC 2D Structures	1.	2 - 2	J. Šoltész
Modeling of RC 3D Structures	3.	2 – 2	J. Šoltész

Postgraduate courses

Modelling of Concrete Structures
Experimental Testing of Concrete Structures

IX. THESES

IX.1 Bachelor Theses

ANTAL, M.: Staircase Made of Cast-in-Situ Reinforced Concrete
Supervisor: Hudoba, I.

BEHÚL, L.: Structural Analysis of Cast-in-Situ Concrete Floor Slab of a Parking Garage
Supervisor: Bilčík, J.

BOLJEŠIK, D.: Structural Analysis of a Rectangular Water Tank Cast-in-Situ Concrete Roof Slab
Supervisor: Bilčík, J.

BRANIŠ, T.: Design of a Floor Slab in an Apartment Block
Supervisor: Šoltész, J.

DRINKA, J.: Single-Storey Frame Concrete Structure: Analysis of Columns
Supervisor: Fillo, Ľ.

DRŽÍKOVÁ, D.: Single-Storey Frame Concrete Structure- Analysis of Shear Punching
Supervisor: Fillo, Ľ.

FARKAŠOVÁ, K.: Single-Storey Frame Concrete Structure: Analysis of Punching
Supervisor: Fillo, Ľ.

GABAN, P.: Structural Analysis of Cast-in-Situ Concrete Floor Slab of an Office Building
Supervisor: Bilčík, J.

HACURA, L.: Pedestrian Ramp Made of Cast-in-Situ Reinforced Concrete
Supervisor: Hudoba, I.

HODOROVSKÝ, P.: Design of a Floor Slab in an Apartment Block
Supervisor: Šoltész, J.

KOZÁK, M.: Structural Analysis of a Bottom Plate of PP-2 Type Building
Supervisor: Paulík, P.

LAMPARSKÝ, J.: Reinforced Concrete Slab of Apartment Building
Supervisor: Borzovič, V.

LUTTEROVÁ, P.: Apartment Building: Cast-in-Situ Reinforced Concrete Structure
Supervisor: Gajdošová, K.

MIŽÁK, V.: Slab Floor of an Office Building
Supervisor: Gramblička, Š.

PECNÍK, M.: Reinforced Concrete Slab of an Apartment Building
Supervisor: Brondoš, J.

RICHNAVSKÝ, B.: Design of Floor Structure Using Lattice Girder Slab Panels
Supervisor: Halvoník, J.

ROVŇÁK, P.: Reinforced Concrete Slab of Office Building
Supervisor: Borzovič, V.

SKLADANÝ, P.: Slab Foundation Analysis of Building PP1
Supervisor: Paulík, P.

VÍTEKOVÁ, M.: Design of One-Way Cast-in-Situ RC Floor Slab
Supervisor: Halvoník, J.

IX.2 Graduate Theses

BIRÁS, M.: Supporting Structure of a High-Rise Building of a Residential Complex
Supervisor: Gramblička, Š.

BUGÁŇ, D.: Apartment House: RC Skeleton Structure with Stiffening Walls
Supervisor: Harvan, I.

DOVIČOVIČ, J.: Railway Bridge over the Nosice Retaining Dam
Supervisor: Paulík, P.

FEDORKO, A.: Cast-in-Situ Bridge on the Motorway D1 over the Krpeliansky Channel
Supervisor: Halvoník, J.

GUNÁR, L.: Central Police Office in Bratislava: Multi-Storey RC Skeleton Structure with a Stiffening Core
Supervisor: Harvan, I.

HALMO, M.: Cast-in-Situ Bridge at Road I/11
Supervisor: Halvoník, J.

HANZEL, J.: High-Rise Building of an Office Centre: Cast-in-Situ Reinforced Concrete Structure with Flat Slabs and Stiffening Core
Supervisor: Harvan, I.

HEBANOVÁ, V.: AT Hotel: Cast-in-Situ Reinforced Concrete Structure
Supervisor: Gajdošová, K.

HLINŠŤÁK, K.: SEGUM Shopping Centre: Cast-in-Situ Concrete Structure
Supervisor: Gajdošová, K.

HORVÁTHOVÁ, S.: High-Rise Residential Building: Cast-in-Situ Reinforced Concrete Supporting Structure
Supervisor: Bartók, A.

HRUBÝ, M.: High-Rise Residential Building: Cast-in-Situ Reinforced Concrete Supporting Structure
Supervisor: Bartók, A.

KENDICKÝ, P.: Multifunctional Building: Hanging RC Structure
Supervisor: Benko, V.

KŘEPELA, M.: Design of the Bearing System of a Part of Shopping Centre
Supervisor: Šoltész, J.

KUBALOVÁ, Z.: Production Factory: Precast Concrete Hall
Supervisor: Borzovič, V.

KÚDELA, M.: Bottova Centre: Cast-in-Situ Reinforced Concrete Structure
Supervisor: Gajdošová, K.

KÚSKA, F.: Design of the Bearing System of a Part of Shopping Centre
Supervisor: Šoltész, J.

MACKO, D.: Bridge over the River Váh on the Motorway D1 Built by a Balanced Cantilever Method
Supervisor: Halvoník, J.

MAJTÁNOVÁ, L.: Tatracity: Cast-in-Situ Reinforced Concrete Structure
Supervisor: Borzovič, V.

MATEJKA, J.: Dunajská Multifunctional Building: Cast-in-Situ Reinforced Concrete Structure
Supervisor: Gajdošová, K.

MICHLÍK, M.: Hotel Jasná: Cast-in-Situ Reinforced Concrete Structure
Supervisor: Gajdošová, K.

OLOS, D.: Static and Dynamic Analysis of a High-Rise Building
Supervisor: Šoltész, J.

ONDREJKA, M.: Road Bridge over a Highway
Supervisor: Fillo, Ľ.

OROLÍN, M.: Apartment House in Poprad: Cast-in-Situ Reinforced Concrete Structure
Supervisor: Gajdošová, K.

PAVLAČKA, P.: Blending Silo: Cast-in-Situ RC Structure
Supervisor: Borzovič, V.

PAVLÍKOVÁ, V.: Multifunctional Building: Cast-in-Situ RC Structure
Supervisor: Borzovič, V.

PRÁZNOVSKÝ, M.: Bridge between Čadca and Žilina
Supervisor: Paulík, P.

PRIŠČÁK, T.: Bridge Built by a Balanced Cantilever Method Prestressed with Extradosed Tendons
Supervisor: Halvoník, J.

RAUČINA, J.: Office Building: Cast-in-Situ RC Structure
Supervisor: Borzovič, V.

RUMANČÍK, M.: Hotel: Cast-in-Situ RC Structure
Supervisor: Borzovič, V.

SELECKÁ, A.: Load-Bearing Structure of a High-Rise Office Building Center
Supervisor: Gramblička, Š.

SLOVÁKOVÁ, L.: Chimney of an Incineration Plant
Supervisor: Šoltész, J.

STRUHÁR, M.: Multifunctional Building: Cast-in-Situ RC Structure
Supervisor: Borzovič, V.

ŠTURDÍK, J.: Hotel***- Staré Grunty, Bratislava: Combined Cast-in-Situ RC Structure with a Stiffening Core
Supervisor: Abrahoim, I.

TATALA, D.: Static and Dynamic Analysis of a High-Rise Building
Supervisor: Šoltész, J.

TISOVSKÝ, M.: Load-Bearing Structure of a High-Rise Office Building Center
Supervisor: Gramblička, Š.

TRSŤAN, T.: Hotel A: RC Skeleton Structure with Stiffening Walls
Supervisor: Harvan, I.

IX.3 Stundent's Scientific Conference Theses

BUGÁŇ, D.: Assessment of Crack Width at the Reinforced Concrete Wall

DRINKA, J., VAŠEK, T.: Reliability Reduction of an Unsymmetrical Reinforced Columns and Walls

DRŽÍKOVÁ, D., FARKAŠOVÁ, K.: Modified Rules for Punching of Slabs and Footings

GUNÁR, L.: Reinforcement Requirements for Concrete Structures Located in Seismic Areas

HANZEL, J.: Transition Structure of the 47 Storey Building at the Change of its Support System in the Pedestal

HEBANOVÁ, V.: Effectiveness of the Design of Foundation Structure of the Multistoreyed Building

JURIGA, V.: Columnal Pedestal under Multi-storeyed Building with the Load-Bearing Walls

KENDICKÝ, P.: Analysis of Concrete Columns of Hanging Concrete Building

KOZÁK, M., SKLADANÝ, P.: Soil Models and their Influence on the Structural Analysis of Foundation Slabs

MAJERČÍK, J.: Minimal Depth of Horizontal RC Structural Members

MAJTÁNOVÁ, L.: Railway Bridge Uľanka

MARKOCSY, E., LACO, K.: Theoretical and Actual Extension of Cables by Prestressing and its Influence on the Stress in Cables

MATEJKA, J.: Practical Solution of the Building Foundation by the Use of Water-tight Concrete Structure

MIŠKOVIČ, M.: Optimization of Determination of RC Structural Elements Preliminary Dimensions

PAVLAČKA, P.: Design Optimization of the Blending Silo Structure

PAVLÍKOVÁ, V.: Kopráš Viaduct

TRSŤAN, T.: Approximate Wind and Seismicity Effect Analysis of Multi-Storey Building